Stony Brook University

An *in vivo* Characterization

of Sox2+ Neural Progenitor Cells

A Dissertation Presented

by

Jane Lee

to

The Graduate School

in Partial Fulfillment of the Requirements

for the Degree of

Doctor of Philosophy

in

Neuroscience

Stony Brook University

December 2009

Stony Brook University

The Graduate School

Jane Lee

We, the dissertation committee for the above candidate for the

Degree of Doctor of Philosophy, hereby recommend

acceptance of this dissertation.

Hollis Cline – Dissertation Advisor
Professor, Cell Biology

Grigori Enikolopov – Dissertation Co-Advisor
Associate Professor, Cold Spring Harbor Laboratory

Simon Halegoua – Chairperson of Defense
Professor, Neurobiology and Behavior

Shaoyu Ge
Assistant Professor, Neurobiology and Behavior

Raffaella Sordella
Assistant Professor, Cold Spring Harbor Laboratory

This dissertation is accepted by the Graduate School

Lawrence Martin
Dean of the Graduate School

Abstract of the Dissertation

An in vivo Characterization of Sox2+ Neural Progenitor Cells

by

Jane Lee

Doctor of Philosophy

in

Neuroscience

Stony Brook University

2009

The knowledge and technology to isolate and manipulate stem cells *in vitro* and the demand for medical therapies to treat intractable brain diseases such as Parkinson's Disease have initiated research into understanding the fundamental characteristics of neural stem cells (NSCs) and neural progenitor cells (NPCs) both in the developing and mature brain. The goals of this thesis project were to identify and characterize a specific pool of NPCs, determine if CPG15, a known activity-dependent gene, plays a role in activity-dependent regulatory mechanisms of neurogenesis, and identify other genes that may play an activity-dependent role in NPCs of the developing brain. Using the visually powerful *in vivo* approach of the *Xenopus laevis* model system, this work aims to bridge the gaps between NPC research in *X. laevis* and other model systems as well as between basic biological research and real life medical applications, such as neural stem cell transplantations.

First, I developed the molecular tools necessary for positively identifying a specific population NPCs in *X. laevis* tadpoles using Sox2, a known neural stem cell marker. I took advantage of Sox2 as a hetrodimer transcription factor with Oct3/4 (Oct3) and used the transcriptional binding domain in the FGF4 enhancer (Sox2/Oct3.mFGF4) to successfully promote the expression of a fluorescent reporter in cells endogenously expressing Sox2 and Oct3. I used immunohistochemical labeling for endogenous Sox2 protein to show that the Sox2/Oct3.mFGF4 driven reporter fluorescently labeled cells in the *X. laevis* brain which colocalized with cells endogenously expressing Sox2. Additionally, I used data obtained from the microarray experiments and imaging experiments to show that cells labeled with the fluorescent reporter had known NPC characteristics further demonstrating the high fidelity of the reporter.

Second, I used microarray technology for three purposes. One, characterize the expression signatures of the NPC population of interest in the visual system of *X. laevis* and compare them to differentiated neurons in *X. laevis* and NPCs of other model systems. Next, identify genes involved in activity-dependent signaling cascades in NPCs. Last, identify the signaling cascades involved in the functional knockdown of CPG15 in order to determine the role of CPG15 in activity-dependent regulation of neurogenesis. Pathway analysis of the microarray data of *X. laevis* NPCs resulted in identifying many pathways involved in stem cell biology; comparing NPC microarray data of the rodent model system resulted in the identification of similar pathways suggesting that NPCs in *X. laevis* have similar characteristics as NPCs in rodents. In addition, pathway analysis of microarray data of CPG15 functional knockdown with morpholinos showed activation of many pathways involved in cell death and neurodegeneration suggesting that the functional knockdown of CPG15 in NPCs triggered cell death and neurodegeneration pathways correlating with *in vitro* data. By filtering all the microarray datasets, fifteen candidate genes that may be involved in activity-dependent regulation of neurogenesis were selected for further studies.

Finally, to complement the microarray studies, I used previously established *in vivo* imaging techniques in the albino *X. laevis* visual system as a basis for establishing a new imaging protocol using Kaede, a photo-convertible fluorescent protein, in order to observe the proliferation and differentiation of NPCs *in vivo* at the site of neurogenesis and to screen the microarray-identified candidate genes. The goals of the imaging experiments were to first establish a baseline for observing NPCs *in vivo*, and second, to determine if the functional knockdown of candidate genes including CPG15 with morpholinos would result in a visually identifiable functional output, such as changes in proliferation or differentiation. In doing so, I was able to establish an imaging baseline for NPCs *in vivo* in *X. laevis*, confirm that CPG15 functional knockdown resulted in cell death, and found that functional knockdown of Dio3, a candidate gene, may increase NPC proliferation,. In addition, I took advantage of the visual system of the *X. laevis*, which can be directly influenced by physiologically-relevant sensory stimuli to investigate the role of visual activity in the regulation of neurogenesis. I found that the imaging data correlated with the BrdU experiments performed by Pranav Sharma, a member of the Cline laboratory, using a similar visual stimuli protocol. This *in vivo* study was unique in that it provided a characterization of NPCs in their native state; further investigations using these methods may ultimately lead to a better understanding of which genes are involved in the regulation of neurogenesis and how best to exploit endogenous and transplanted NPC pools in humans using these genes.

Dedicated to
Morgan, Taylor, and the One

Table of Contents

List of Symbols

APBS..... Amphibian Phosphate Buffered Solution
aRNA ..... antisense RNA
BAC ..... Bacterial Artificial Chromosome
BP..... Basal Progenitor
cDNA ..... complementary RNA
CMV ..... Cytomegalovirus Promoter
CNS..... Central Nervous System
CPG15..... Candidate Plasticity Gene 15
EB ..... Elution Buffer (PicoPure)
FGF4 ..... Fibroblast Growth Factor 4
FP ..... Fluorescent Protein
GOI ..... Gene of Intereste
HA..... Homologous Arm
LCM..... Laser Capture Microdissection
mFGF4 ..... minimal FGF4 promoter
mRNA ..... messenger RNA
NE ..... Neural Epithelial
NPC..... Neural Progenitor Cell
NSC..... Neural Stem Celll
PB..... Phosphate Buffer
PFA ..... Paraformaldhyde
PML ..... Promoterless
RG..... Radial Glia
RGC ..... Retinal Ganglion Cell
RT ..... Room Temperature
totRNA..... total RNA
WBE..... Whole Brain Electroporation
ZdSS..... Zero-divalent Steinberg's Solution

List of Figures

List of Tables

Acknowledgments

This thesis work would not have been possible without the support of many people. First, I would like to thank my research advisor Dr. Holly Cline for her guidance on everything from designing and performing research to organizing it into a thesis. She has been incredibly supportive of everything I proposed to do in the laboratory allowing me loose reins to explore my own ideas while at the same time always keeping me on the right track. Her gentle supervision has taught me to solve my own experimental problems and formulate my own scientific ideas; this early education on intellectual independence will no doubt be a great asset in my future research and medical endeavors. I would also like to thank her for providing me a great laboratory environment with a great group of supportive and bright people to share thoughts, exchange ideas, and participate with in making memorable life moments.

For my old lab mates, I would like to thank Emiliano Rial Verde for his initiation into the Cline laboratory during my first year rotation. His enthusiasm for science and everything else had convinced me that this was the lab for me. I also would like to thank Jen Bestman for her knowledge in imaging which carried me through the early years and then again through the later years. In fact, the imaging portion of my thesis would not have been possible without her. I would like to thank Pranav Sharma whose work has influenced many parts of this thesis project and for his great insights in the subject matter. I would like to thank Yeon Lee, a fellow cloning expert, who has helped me construct many of the plasmids used in this thesis project. Also, I would like to thank Kim Bronson for her perfect cryosections and for keeping the lab organized and functional. I think without her help, no one in the lab would have been able to get any work done. Finally, it would not be right not to thank the rest of the Cline crew at Cold Spring Harbor, Rebecca Ewald, Kasandra Burgos, Vatsala Thirumalai, Shu-ling Chiu, Masaki Hiramoto, Lucio Schiaparelli, Jorge Santos Da Silva, Haiyan He, Wanhua Shen, and Chih-Ming Chen for providing the perfect work hard and play hard atmosphere.

For my new lab mates since the Cline laboratory departure from Cold Spring Harbor, I would like to thank everyone at Cold Spring Harbor Laboratories both scientific staff and support staff members. Especially, I would like to thank Grisha Enikolopov for being my co-mentor and the Enikolopov laboratory, June Hee Park, Tatyana Michurina, and Natalia Peunova for moral support. I would like to thank the Sordella laboratory, Matt Camiolo, Trine Lindsted, Zhan Yao, Maria Pineda and of course Raffaella for allowing me to take over the laboratory microscope for my experiments for four months. I would also like to thank the Huang lab, Rae Hum Paik, Anirban Paul, Matthew Lazarus, Scilla Wu, Ying Lin, Xiaoyun Wu, Yu Fu, Keerthi Krishnan, and Hiroki Taniguchi for exchange of both formal scientific conversations and informal banter over morning coffee and lunch. I would like to thank everyone at the animal facility, especially Lisa Bianco, Eileen Earl, and Jared Downing for all the help they have provided in caring for the frog colony left behind for me to take care of all by myself. I would like to thank the CSHL Microarray Core Facility, Chris Johns, Sohail Khan, and Rob Lucito for help with my microarray experiments. I would like to thank the new members of the Cline

laboratory at Scripps including Jenesis Kam who kept me connected to Holly when she could not be reached and Mohan Gudurvalmiki for his vested interest in my project. Finally, I would also like to thank members of DART Neuroscience: Tim Tully for intellectual and financial support and Jerry Lee for his expertise in microarrays.

Secondly, I would like to thank the members of my committee: Drs. Grisha Enikolopov, Simon Halegoua, Shaoyu Ge, and Raffaella Sordella. They have been both critical and supportive of my thesis project. I especially would like to thank them for their thoughtful consideration of my MSTP track and the extraordinary situation I found myself with the Cline laboratory departure to Scripps.

Thirdly, I would like to thank all the members of the Neuroscience department for providing a solid graduate program in neuroscience. I especially would like to thank Diane Godden for keeping me connected with Stony Brook and helping me through the graduate school process. I would like to thank Lonnie Wollmuth for his enthusiastic directorship of the program. I would also like to thank the members of my first year class, Terry Aubele, Tina Chen, Yang Yang, and Yu Fu for providing a fun and supportive first year.

Fourthly, I would like to thank the MSTP program and the Stony Brook School of Medicine for moral and financial support. I would like to thank Mike Frohman for his MSTP directorship and Carron Kaufman for dotting all the i's and crossing all the t's to make the MSTP program run smoothly. I would also like to thank everyone in the MSTP program, especially Adam Schuldt, Prem Premsrirut, and Kasandra Burgos for moral support because we are in it together. Finally, I would like to thank the administrative staff at Stony Brook School of Medicine, especially Peter Williams and Burke Kincaid for guidance through life in medical school and the Medical School Class of 2007, especially Waitz Ngan, Joanne Kong, Susan Shin, Janet Chung, and Ricky Chung for suffering though medical school with me.

Finally, I would like to thank my family. My sister who always reminds me "You are on the road you are on because that is the road that you are supposed to be on." She has been incredibly supportive of my life choices always assuring me that the choices I've made were the correct ones for me no matter what anybody else says. My brother who always looked up to me and in doing so gave me the confidence to do my best. My parents who has raised all three of us right; I hope they are proud of us as we are proud of them. My two daughters, Morgan and Taylor, who inspires me everyday to be all that I can be for I know they are looking up to me. Finally, for my soul mate, I would like to express my deepest gratitude for just being you and keeping things real.

Chapter 1 Introduction

The brain has fascinated philosophers and scientists alike. Aristotle, who valued the muscular multi-chambered heart as the originator of human thought, reason, and emotion, often rejected the value of the brain. Yet his contemporary, Hippocrates, the "Father of Medicine", was entirely in favor of this fragile and deceptively simple looking organ. The Roman physician, Galen, hypothesized through his surgical observations, the brain's function as the master controller of movement. Needless to say, the brain has enjoyed many scientific advances in understanding its development, structure, and function since these early postulations. Despite the long history of its study, the brain continues to generate human interest and inspire its investigation in all fields of modern science. In recent years, the knowledge and technology to isolate and manipulate stem cells *in vitro* (Reynolds and Weiss 1992; Uchida, Buck et al. 2000) and the demand for medical therapies to treat intractable brain diseases such as Parkinson's Disease (Lindvall 2003; Marshall, Novitch et al. 2005; Bauer, Tempfer et al. 2006) have initiated active research into understanding the fundamental characteristics of neural stem cells (NSCs) and neural progenitor cells (NPCs) in both the developing brain and the mature brain. The focus of this thesis project was to investigate the regulatory mechanisms, which underlie the switch from proliferation to differentiation in the developing brain using a visually powerful *in vivo* approach to bridge the gap between basic research and real life medical applications, such as neural stem cell transplantations. The open questions in the field addressed here are: What are the genetic and mechanistic profiles of neural stem/progenitor cells and which genes play an activity-dependent role in maintaining and/or initiating change within these profiles.

1.1 Neurogenesis in development

The brain is a complex organ composed of millions to trillions of cells. Even the brain of the common fruit fly boasts circuits possessing computing power that is yet to be rivaled by any man-made technologies to date. It is the neural stem cells that produce all the components, both neurons and macroglia, of this complex network during development (Gotz and Huttner 2005; Kriegstein and Alvarez-Buylla 2009). Embryological *Xenopus* studies confirmed the Spemann-Mangold organizer to be essential in the production of embryological neural stem cells during gastrulation and helped elucidate the mechanisms of neural induction (Hemmati-Brivanlou and Melton 1997; Sasai and De Robertis 1997). Once the neural epithelium is established after neural induction, it is the precise orchestration of the NSC/NPC proliferation and differentiation which determines the proper development of the brain (Farkas and Huttner 2008). Although there is much excitement surrounding the phenomena of adult mammalian neurogenesis, this thesis will focus on developmental neurogenesis.

1.1.1 Semantics of NSCs verses NPCs

The term "stem cell" has various meanings depending on the field of study as well as the opinion of the researcher using it. However, most stem cell researchers apply two fundamental criteria to define a cell as a stem cell: self-renewability, ideally an unlimited number of cell divisions, and multipotency, the ability to give rise to many types of

differentiated cells (Rao 2006). Strictly adhering to this definition, a *neural stem cell* (NSC) is a cell that has the unlimited capability of giving rise to itself and to numerous different types, if not all types, of neuronal and glial cells of the nervous system. It is not to be confused with *embryonic stem cell*, which has been shown not only to give rise to an entire nervous system, but in fact, it can give rise to an entire organism (Okabe, Forsberg-Nilsson et al. 1996). However, operationally, a neural stem cell is defined by its ability to generate a neurospheres with both neurons and glia in culture (Zappone, Galli et al. 2000). The term *neural progenitor cell* (NPC) is often used more broadly; it is a blanket term that describes a neural cell that can generate different progeny regardless of any limits on its self-renewal capacity. A *precursor cell* is used to describe a cell with a lineage that is restricted to a specific fate; thus, a *neuronal precursor* is a cell destined to become a neuron. Some researchers may disagree with these narrow interpretations outlined above because the current research is showing that the differences between the terms are more like a gradient rather than a defining line; for example, evidence show that a neural precursor which gives rise to neurons may eventually itself become a glia (Kriegstein and Götz 2003; Anthony, Klein et al. 2004). In this thesis presentation, given the unknown characteristics of the NSCs/NPCs in my experimental system, I will use term I have defined more loosely, NPC.

1.1.2 Neural stem cells, neural progenitor cells, and glia

Current understanding about developmental neurogenesis is based primarily on the rodent cerebral cortex, however, the principles have been shown to apply to other regions of the brain as well as other vertebrates. In fact, studies show many processes that occur during development are often recapitulated to a certain extent in the adult brain (Kriegstein and Alvarez-Buylla 2009). Pioneers of the field report three basic categories of NSCs and NPCs, each with differing cell-biological features (Figure 1.1-A). I will briefly review them below focusing on identifying markers, morphology, and cell division behavior; the details of which will be expanded upon later in this chapter. A developmental timeline of these cell-types is provided as a visual in (Figure 1.1-B).

1.1.2.1 Neuroepithelial cells

The neural plate and the neural tube are established following neural induction and the completion of gastrulation. They are composed of a single layer of cells called neuroepithelial (NE) cells in a layer of cells called ventricular zone (VZ), a defined region adjacent to the ventricle (Boulder 1970). The VZ is pseudostratified because of the dividing cells undergo interkinetic nuclear migration (Sauer 1935; Sauer and Walker 1959; Sidman, Miale et al. 1959; Fujita 1962; Hayes and Nowakowski 2000). At the time of neurogenesis, these cells have the morphology of radial glial cells (RG). They are highly polarized along the apical-basal axis with their cells bodies attached to the apical surface lining the ventricular lumen and their process extending to the basal lamina. Prominin-1 (CD133) is found selectively at the apical plasma membrane (Weigmann, Corbeil et al. 1997; Corti, Nizzardo et al. 2007) while tight-adherens junction associated proteins like afadin (AF6) are found at the basal plasma membrane (Ikeda, Nakanishi et al. 1999). It has been shown some of these markers are important for maintenance of polarity (Zhadanov, Provance Jr et al. 1999), which in turn maintains the proliferative

status of these cells (Aaku-Saraste, Oback et al. 1997). The neuroepithelial cells (NEC, Figure 1.1-A1) are true NSCs.

1.1.2.2 Radial glial cells

The closure of the neural tube signifies the completion of neurulation. After which, neurogenesis proceeds and the cortex thickens as more cells are added in layers. The NE cell while maintaining its polarity elongates its basal process to remain in contact with the pial surface of the cortex. These cells, known as radial glia (RG, Figure1.1-A2), with longer processes have 24nm microtubules and 9nm intermediate filaments which span the entire cortical wall; they are related to but are distinct from NE cells. The RG cell can be thought of as lineage restricted NPCs and as the differentiated progeny of neuroepithelial cells (Kriegstein and Götz 2003). Over a relatively short span of development, the radial glia replace the neuroepithelial cells as the major cell type lining the VZ, and as a result, radial glia give rise to most of the neurons and glia of the brain (Gotz, Hartfuss et al. 2002; Anthony, Klein et al. 2004).

The RG cells retain some properties of NE cells but gradually acquire some astroglial- associated characteristics. Like the NE cells, radial glia also form a pseudostratified layer along the ventricular wall and share the following properties: express intermediate filament protein nestin (Lendahl, Zimmerman et al. 1990; Wei, Shi et al. 2002), are highly polarized, and express CD133, PAR3 (Naoyuki, Syu-Ichi et al. 2002), and ZO1 (Aaku-Saraste, Hellwig et al. 1996) at the apical surface. In contrast to NE cells, RG cells begin to express genes also found in astroglia such as: astrocyte specific glutamate transporter (GLAST) (Lehre, Levy et al. 1995; Shibata, Yamada et al. 1997), the Ca+ binding protein S100ß (Tabuchi and Kirsch 1975; Haglid, Hamberger et al. 1976), glial fibrillary acidic protein (GFAP) (Antanitus, Choi et al. 1976; Levitt and Rakic 1980; Garcia, Doan et al. 2004; Casper and McCarthy 2006), vimentin, and brain-lipid-binding protein (BLBP) (Feng, Hatten et al. 1994), conversion of tight junctions to adheren junctions (Aaku-Saraste, Hellwig et al. 1996; Stoykova, Gotz et al. 1997), and association with blood vessels by the basal process (Misson, Edwards et al. 1988; Takahashi, Misson et al. 1990). The changes in the RG membrane and its basal associations permit cross-communication with extracellular events in the brain through contacts with the extracellular matrix and neighboring cells, as well as the rest of the body through contacts with blood vessels. With the progression of neurogenesis, there is a gradual transition from symmetrical divisions to asymmetrical divisions and a gradual restriction of linage potential, which consequently accounts for the high degree of heterogeneity in neurogenic pools (Kriegstein and Götz 2003; Itsykson, Ilouz et al. 2005). The gradient of changes is such that it would be difficult to track and characterize a single cell or cell-type using only one marker. Even with complex immunohistochemical analysis of a neurogenic region, it would only amount to a snap-shot of an ever changing landscape. However, with *in vivo* time-lapse imaging, it would it be possible to observe a single cell as it switches its identity from one type to another, like watching a maple tree changing from green to red with the seasons. It would also allow intervention of that switching process to investigate how a gene of interest may be involved in the transition.

1.1.2.3 Basal progenitors

Controversy surrounds the origins of this type of NPC. Whether or not the basal progenitor cell (BP, Figure 1.1-A3), also known as intermediate or transient progenitor cells (IPCs or TPCs), are differentiated NE cells or RG cells, all agree that these progenitors are a distinct class of NPCs (Miyata, Kawaguchi et al. 2004; Noctor, Martinez-Cerdeno et al. 2007; Attardo, Calegari et al. 2008). It was previously thought BP cells, identified by the marker TBR2, were unique to the cortex. However, TBR2 expressing cells have been reported in *Xenopus* midbrain (Brox, Puelles et al. 2004), suggesting that this progenitor type may be more widespread and present in other brain regions. Morphologically, they can be distinguished from NE cells and RG cells by the absence of their apical-basal contacts. Their nuclei translocate to the basal region of the VZ and form the subventricular zone (SVZ). The SVZ is not pseudostratified because nuclei of BP remain in one place during cell division. They also express different proteins—for example, non-coding RNA SVET1 (Tarabykin, Stoykova et al. 2001) and the TBR2 related genes (Englund, Fink et al. 2005), CUX1, and CUX2 (Nieto, Monuki et al. 2004; Zimmer, Tiveron et al. 2004). It has been reported that basal progenitors may function to increase the number of neurons by performing several, perhaps a pre-set number of, rounds of symmetrical divisions that may end with a final round of symmetric divisions that results in two daughter neurons (Noctor, Martinez-Cerdeno et al. 2004; Martinez-Cerdeno, Noctor et al. 2006; Noctor, Martinez-Cerdeno et al. 2007; Pontious, Kowalczyk et al. 2008).

1.1.3 Patterns of division

The neural stem cell research field recognizes two basic patterns of cell division: symmetric and asymmetric. Further sub-divisions are distinguished in terms of the cleavage plane and whether the resulting daughter cells are both proliferative cells, both differentiated cells, or one of each cell type. Much of what is known about neurogenesis and patterns of division was observed in *Drosophila* as reviewed by (Boone and Doe 2008). Until symmetric and asymmetric division events were observed in *in vitro* time-lapse images of rodent cortical slice cultures (Kosodo, Toida et al. 2008), it was thought those events were unique to invertebrates. It was then realized that fundamental developmental events such as neurogenesis were evolutionarily conserved across species including both vertebrates and invertebrates. Furthermore, this high degree of conservation illustrates that what is observed in this study of *Xenopus* NPCs may also be applicable to other species. In any case, there is a huge body of work which focuses on the exact bio-molecular mechanisms that coordinate the patterns of division but I will only highlight but a very, very small portion of this literature; a simplified cartoon is provided as a visual aid (Figure 1.1-C).

1.1.3.1 Symmetric, proliferative division

A division event that results in two of the same type of cells is called symmetric. Most symmetric divisions are proliferative except for the terminal symmetric division that results in two differentiated cells, also known as symmetric, differentiative divisions. Classically, symmetric divisions of the NE cells and the RG cells are thought to have a vertical cleavage plane meaning the plane of division is perpendicular to the apical surface; in fact patterns of division were once classified as vertical and horizontal.

Recently, it has been observed that a vertical cleavage plane can result in an asymmetric division forcing researchers to look more closely at the event (Kosodo, Roper et al. 2004). As in other cell systems with apical-to-basal polarized cells such as NE cells and RG cells, the positioning of the mitotic spindle apparatus is crucial in determining whether or not a vertical division will be symmetric or asymmetric. If the spinal-pole position is exactly perpendicular so that the bisection occurs through the apical plasma membrane, the result will be a symmetrical division. However, if the spindle-pole is positioned slightly askew so that the cleavage furrow does not pass through the apical plasma membrane, the result will be an asymmetrical division (Attardo, Calegari et al. 2008); see (Figure 1.1-C1). Since the positioning of the spindle in NE cells and RG cells is highly dependant on the polarity of the cells, it can be extrapolated that the loss of polarity in these cells can favor asymmetric divisions. The details of the relationship between polarity and plane of division have not been completely elucidated for BP cells but only symmetric, proliferative and symmetric, differentiative divisions have been observed in BP cells of the rodent cortex. One other point must be mentioned in the context of symmetrical divisions. It is generally believed that for symmetric divisions, the cytoplasm, membrane, and the cell fate determinates within those compartments are equally divided among the daughter cells resulting in two cells with the same characteristics (Zhong and Chia 2008). During the symmetrical division events of NE cells and RG cells, it has been shown some division events result in both the daughter cells inheriting a portion of the radial process which contact the pial surface of the brain (Huttner and Kosodo 2005; Kosodo, Toida et al. 2008) while others show that the process inherited by only one of the two proliferative daughter cell (Miyata, Kawaguchi et al. 2001). The fate of the radial process is thought to be important in maintaining stemness. Because the origin of the radial process is thought to be associated with the cytokinesis machinery, it could play a part in directing the apical-basal axis of the cleavage plane. Therefore, its maintenance in the daughter cells may be predictive of future symmetrical divisions. Time-lapse i*n vivo* imaging may be helpful in addressing the validity of this theory.

1.1.3.2 Asymmetric, neurogenic division

A division event that results in two different types of cells is called asymmetric (Figure 1.1-C2/3). During cortical development, an asymmetric division event most often results in a proliferative cell and a neuronal cell (Knoblich 2001). It is thought that asymmetric divisions result in an unequal distribution of maternal cytoplasm accounting for the resulting difference in characteristics of the daughter cells (Chenn and McConnell 1995). The orientation of the cleavage plane of a neuroepithelial cell or a radial glia may be horizontal or, as explained above, vertical with respect to the apical surface of the cell (Smart 1973; Knoblich 2008). It is interesting to note that before the onset of neurogenesis, the genes regulating polarity are down-regulated correlating with the increase of asymmetric divisions (Aaku-Saraste, Hellwig et al. 1996).

1.1.4 Key regulators of neurogenesis

A complex set of cellular events determine the proper development of the brain. Among those are the regulators of neurogenesis. Many molecules and signaling pathways both cell autonomous and non-autonomous control the switch of NSCs/NPCs from

proliferation to differentiation, death or senescence. There were many insights about neurogenesis from studies of Drosophila again showing the fundamental nature of these mechanisms as reviewed by (Sgambato, Vanhoutte et al. 1998; Egger, Chell et al. 2008). The regulation of neurogenesis has been investigated from several vantage points and the players involved have been categorized and reviewed in different ways depending on the writer's particular research interests such as transcription factors, epigenetic control, miRNA regulators, and external signaling factors (Shi, Sun et al. 2008), cell-cycle state and cell fate (Cremisi, Philpott et al. 2003), or cell polarity and the symmetry of division (Zhong and Chia 2008), to name just three of the many reviews on this subject. The difficulty in standardizing a classification system lies in the fact that many players involved in neurogenesis do not fit neatly into one category; in fact, their functions are often related to and/or overlapping with other categories creating a very complex network. Table 1.1 highlights some regulatory pathways pertinent to this thesis. Some pathways have been extensively studied in the spotlight of neural stem/progenitor cells and neurogenesis. Others have only recently debuted onto the scene from other fields both related to and not related to neuroscience such as from the embryology and cancer biology. Cell-adhesion molecules that dictate cell-polarity and identity (Section 1.1.2 and 1.1.3) and neurotransmitter initiated pathways (Section 1.1.6) are discussed in brief elsewhere. Needless to say, there are many opportunities for intellectual contribution in the field of neurogenic mechanisms.

1.1.5 Neural progenitor cell markers

Cell-specific markers are a valuable tool in identifying and following a specific population of cells in developmental biology. In stem cell biology, markers are used to study the transition from one cell-type to another; thus, temporally expressed cell-specific markers that are indicators of "stemness", differentiation, and cell-cycle state are even more valuable (Abramova, Charniga et al. 2005). Cell-specific markers that are temporally and spatially unique allow researchers to work with a relatively homogenous pool of experimental material; this will reduce variably in the results in addition to making the work more easily interpretable by others in the field using the same markers.

1.1.5.1 Known NSC/NPC markers

The difficulty in identifying NSC/NPC specific markers is that a stem cell is a stem cell is a stem cell. Since the mechanisms that govern cell cycle and division events are shared among stem cells of different tissues, so are the markers. Therefore, only a limited number of neural stem cell specific markers have been identified; some have already been mentioned earlier in this chapter. Among the more popularly used markers are cell-surface markers like CD133, structural markers like nestin and vimentin, RNA binding proteins such as Musashi1 (Kaneko, Sakakibara et al. 2000), and transcriptional regulators such as the Sox-family of transcription factors (Bylund, Andersson et al. 2003; Graham, Khudyakov et al. 2003; Komitova and Eriksson 2004; Ekonomou, Kazanis et al. 2005; Wegner and Stolt 2005; Tonchev, Yamashima et al. 2006; Wang, Stromberg et al. 2006) and Pax6 (Warren, Caric et al. 1999; Estivill-Torrus, Pearson et al. 2002; Englund, Fink et al. 2005), and cell-cycle regulators such as REST (Ballas, Grunseich et al. 2005; Ballas and Mandel 2005) and Geminin (Aigner and Gage 2005). Other molecules that are known to co-localize with these markers and known to be also

expressed in non-neuronal stem cells are extensively utilized in the field of neurogenesis, stem cell and cancer biology such as the Octamer-binding Protein (Oct) family of transcription factors (Okuda, Tagawa et al. 2004; Chin, Shiwaku et al. 2009), MCMs (Ryu and Driever 2006), Ki-67 (Scholzen and Gerdes 2000), and Fibroblast Growth Factor (FGF) (Katoh and Katoh 2005; Kosaka, Kodama et al. 2006). The use of known markers is not without drawbacks; for example, nestin is also present in reactive astrocytes (Clarke, Shetty et al. 1994), Schwann cells, and developing muscle cells (Sejersen and Lendahl 1993); so there may be a danger in characterizing a non-NSC/NPC if the markers are used blindly. The other disadvantage in using known markers is that it limits what can be learned about NSCs/NPCs in general. It would be akin to using blinders to focus on a tree in forest of trees; interesting observations might be missed. Therefore, there is a need to add to this short list of markers by using such research tools as non-hypothesis driven microarrays; so that the field is not restricted to studying only just one type of NSC/NPC.

1.1.5.2 Sox2 as aNPC marker

Sox2 is a member of the Sox-family of transcription factors known to be expressed in NSCs/NPCs (Graham, Khudyakov et al. 2003; Komitova and Eriksson 2004). It is categorized in the sub-family group B which is specific to the central nervous system (CNS). Thus, Sox2 is closely related to Sox1 and Sox3 which are also known to be expressed in NSCs/NPCs (Wegner and Stolt 2005; Tonchev, Yamashima et al. 2006). The rat Sox2 amino-acid sequence has over 90% identity with human, mouse, and chicken and has over 85% sequence identity with *Xenopus* and zebrafish (Katoh and Katoh 2005). In *Xenopus*, Sox2 is required for early neuroectoderm differentiation (Kishi, Mizuseki et al. 2000). However, at later stages of development, it has been shown to maintain NSC identity (Bylund, Andersson et al. 2003; Graham, Khudyakov et al. 2003). Sox2 has also been shown to be involved in the regulation of many neurogenesis related pathways such as Shh (Favaro, Valotta et al. 2009) and the Wnt/β-catenin (Agathocleous, Iordanova et al. 2009) pathways.

Sox2 is characterized by a High Mobility Group (HMG-box) that binds DNA elements and the Sox123C domain. It also has a POU domain that allows it to bind to other transcription factors which suggest that Sox2 transcription factor works as a hetrodimer. The genomic sequence of these regions is well conserved across all vertebrates. Similarly, the Sox2 promoter is characterized by specific domains (Wiebe, Wilder et al. 2000; Zappone, Galli et al. 2000) whose sequences are conserved in human, rat, and mouse; these domains are also thought to be very well conserved across species (Katoh and Katoh 2005). It has been identified that the Sox2 transcription factor binds to a specific binding domain on the FGF4 promoter and enhances FGF4 expression (Ambrosetti, Basilico et al. 1997; Ambrosetti, Scholer et al. 2000). The Sox2 binding domain present on the FGF4 promoter requires Sox2 to form a complex with another known NSC/NPC marker, Pou5F1/Oct3/Oct4 which I will identify as Oct3 (Okuda, Tagawa et al. 2004; Favaro, Valotta et al. 2009). Given the conservation of both Sox2 and Oct3 sequences and their consistent co-expression with FGF4 across vertebrates (Katoh and Katoh 2005), it likely that the enhancer elements of the promoter for FGF4 will be shared in our system.

1.1.6 Role of activity on neurogenesis

Brain activity in the normal development of the brain has always been a subject of study. A classic example is in the visual system where *in utero* spontaneous visual activity has been correlated with the proper development of the visual system in mammals as reviewed by (Huberman, Feller et al. 2008). In recent years, there has been a growth of interest in the role of activity specifically regulating NSC/NPC proliferation and differentiation. Evidence has already been demonstrated in the normal adult brain where it has been shown that enriched environments (Bruel-Jungerman, Laroche et al. 2005), exercise (van Praag, Kempermann et al. 1999; Olson, Eadie et al. 2006; Pereira, Huddleston et al. 2007), and learning and memory (Parker, Anderson et al. 2005) increases neurogenesis and that these increases were dependent on neurotransmitter activity (Zeng, Cai et al. 2004; Bursztajn, Falls et al. 2007; Ge, Pradhan et al. 2007; Platel, Lacar et al. 2007; Nakamichi, Takarada et al. 2009) and activity-dependent signaling cascades (Dworkin, Malaterre et al. 2009; Kriegstein and Alvarez-Buylla 2009). And in the pathological adult brain, conditions such as seizures showed that random global brain activity induces neurogenesis (Parent and Murphy 2008; Porter 2008; Kuruba, Hattiangady et al. 2009).

A potential role of activity-dependent mechanisms in the regulation of neurogenesis in the normal developing brain is suggested by the presence of neurotransmitters such as GABA and glutamate at embryonic stages; these molecules are thought to act as trophic factors (Zeng, Cai et al. 2004; Platel, Lacar et al. 2007). There is also evidence that neurotransmitter- and calcium-dependent signaling affect mechanisms of differentiation (LoTurco, Owens et al. 1995; Sadikot, Burhan et al. 1998; Gandhi, Luk et al. 2008). All these observations in the adult and the developing brain taken together indicate that NSCs/NPCs respond to neural activity but its exact role is still an open question.

1.2 Microarray

It has been 15 years since the first DNA microarrays. The technology has been embraced by many fields requiring high-throughput DNA/RNA analysis of small samples. With the completion of whole genome sequencing projects, the DNA microarray provides a systematic approach to measuring the complete transcriptional signature of any cellular pool at any given developmental, physiological, and pathological process of several model systems; the *X. laevis* genome has yet to be entirely completed but already partial representations have been used to design arrays to look at several developmental processes. Expression profiling has provided researchers with an access pass to observe not only entire regulatory systems but also networks of systems by revealing concerted changes in the transcriptome of a single or a population of cells. It has been valuable in identifying previously uncharacterized changes in gene transcription for a given process of a cell such as during the proliferation and differentiation of NSCs/NPCs.

1.2.1 History of microarrays

The advancement of microarray technology involved numerous seemingly disparate fields such as mechanics, robotics, micro-fabrication, chemistry, molecular biology,

micro-fluid dynamics, enzymology, optics, bioinformatics, and statistics, to name just a few. Moreover, microarray technology has not been limited to DNA/RNA; present iterations include the bio-chip, lab-on-chips, and antibody chips. Therefore, in addition to large scale genotyping and gene expressions profiling, now microarrays are used for single nucleotide polymorphism detection, alternative splicing detection, siRNA/microRNA profiling, chromatin immunoprecipitations, gel electrophoresis, and even protein profiling. It is also noteworthy to recognize that the other technologies involving pre-microarray processing (which will be discussed below) and post-microarray processing (which is the work of statisticians and data base managers) were developed in order to fully capitalize on the potential benefits of the microarray technology.

1.2.1.1 Microarray chips

The high-throughput high-density DNA microarray chip evolved from the Southern blot. It differs from the Southern blot in that a known DNA sequence (probe) is attached to a substrate and the sample (target) is probed for the presence of a DNA/RNA fragment complementary to the probe. The use of a collection of a distinct set of DNA probes in an array for the purposes of expression analysis was first described in 1987 by (Kulesh, Clive et al. 1987). This array was made by dot-blotting the probe onto filter paper. The modern glass based microarray was first described in 1995 by (Schena, Shalon et al. 1995), who spotted 45 complementary DNA (cDNA) probes on to a glass slide. Then impressively within the year, 1000 probes were arrayed in the same fashion (Schena, Shalon et al. 1995) while 135,000 probes were arrayed (Prickaerts, Koopmans et al. 2004) using a method called photolithography (Fodor, Read et al. 1991) currently adapted by Affymetrix. In 1997, a complete genome array of yeast was published (Lashkari, DeRisi et al. 1997), and soon after, complete and specialized microarrays of other genomes were made available commercially. The *Xenopus laevis* whole genome Affymetrix array consists of more than 32,400 probe sets where a set consists of 10-12 different probes representing more than 29,900 transcripts; which translates to nearly 400,000 probes on one chip.

1.2.1.2 Target handling technology

Aside from the miniaturization of the microarrays chips themselves, advancements in molecular biology have been essential in pushing the limits of microarray technology. In the introductory microarray study, 5µg of target material (Schena, Shalon et al. 1995) was required which calculates to 165-500µg of total RNA (totRNA) if it is assumed that 1-3% of totRNA is message RNA (mRNA). Since one cell contains 10-30pg of totRNA, that amounts to 1.6×10^6 to 2×10^7 cells needed for one array experiment (Nygaard and Hovig 2006). One solution was to expand samples *in vitro*; it is a recognized method for microarray experiments and was used successfully in many studies. The problem is that the microenvironment in the culture dish may vastly differ from the *in vivo* environment. The other solution was to develop methods to reduce the amount of RNA needed as starting material. There are two focuses: signal amplification and high-fidelity sample amplification.

The former strategy involves improving target labeling technology both for pre-hybridization and post-hybridization of the chip. Several proprietary enzymatic and non-enzymatic target labeling techniques have been developed in lieu of using modified nucleotides which interfere with the amplification processes. Additionally, signal amplification methods such as dendrimer technology (Stears, Getts et al. 2000) and tyramide signal amplification (Karsten, Van Deerlin et al. 2002) were developed to amplify detectable signal after hybridization but before reading of the chips.

The latter strategy involves improving linear amplification methods. One basis of this procedure is based on the Eberwine method (Eberwine, Yeh et al. 1992). The general steps involved reverse-transcribing message RNA (mRNA) using an oligo-dT primer encoding a T7 RNA polymerase priming site. Then the T7 polymerase was used to convert mRNA to complementary DNA (cDNA) followed by the use of the cDNA to produce amplified antisense RNA (aRNA). A variation of this method involving performing multiple rounds of amplification has been used successfully for even single cell experiments. Currently, many kits using the Eberwine method are available commercially which aids in reducing variation between experiments. An alternative method developed by Kurimoto *et al* uses polymerase chain reaction to linearly amplify the cDNA into cDNA instead of aRNA before performing a round of *in vitro* transcription to produce labeled aRNA (Kawaguchi, Ikawa et al. 2008); currently there is no known kit available which directly uses this method. However, it is believed that this method is basis for the NuGEN kit used in this thesis. The proprietary method called SPIA amplification appears to be a modification of the method described by Kurimoto *et al* where the cDNA is amplified to cDNA.

The final comment within the scope of sample handling is this: With more sensitive amplification methods, there was a need to obtain cleaner starting material more consistently. This resulted in the improvement of extraction techniques ranging from *in situ* extraction of totRNA in amplification buffer (Kawaguchi, Ikawa et al. 2008) to advanced DNA/RNA binding supports such as beads and specialized silica membrane containing columns. NuGEN released a new kit in the spring of 2009 incorporating the *in situ* extraction technique which claims to faithfully amplify mRNA from a single cell for use in standard sized microarray chips.

1.2.1.3 Target harvesting technology

Another pre-microarray process that has been improved is sample-harvesting technologies. With microarrays becoming more sensitive and more specific to cell type and cell processes, there was a need to harvest more a homogeneous sample of cells. One technology that has been improved is in the field of fluorescence assisted cell-sorting technology (FACS). Cell sorting has long been used in hospitals to sort blood cells by the gallons. Now with the advancement of fluorescent labeling, optics, and liquid handling, FACS boast sorting of even milliliters of starting samples to sort as few as 300,000 cells. Another related technology is the genetically transactivated fluorescent labeling of a specific cell population at specific developmental time points using cell-specific temporal markers such as those described in the previous section. Many researchers combined these two fluorescence based technologies by making transgenic reporter mice. A very

recent fluorescent based method is called translating ribosome affinity purification (TRAP). This method involves immunoaffinity purification of a fluorescent protein tagged ribosomal transgene and their mRNA cargo; the ribosomal transgene expression is driven by cell type specific regulatory elements in bacterial artificial chromosome (BAC) transgenic mice (Doyle, Dougherty et al. 2008; Heiman, Schaefer et al. 2008). Transgenesis in *X. laevis* is still in its nascent stages thus in this thesis, I take advantage of the fluorescent marker technology using plasmid electroporation to label cells of interest which are then hand harvested. An entirely different harvesting method available today is laser capture microdissection where a laser is used to cut and capture a section of tissue facilitated by a computer aided laser guidance system and a microscope; this method allows for spatial resolution and has been used to look at regional differences of cells within a complex tissue. In general, the harvesting technologies assist researchers in reducing the complexity of the target by enriching for specific cell-types.

1.2.2 Microarrays in neuroscience

The complexity of the brain has delayed the application of microarray technology in neuroscience. However, recent developments as described above have made it possible for many researchers to make valuable contributions to the field. Microarray contributions in neuroscience can be divided into three groups: molecular characterizing of the developmental stages both of the individual neurons and the brain as a whole, building a molecular map of the different regions of the brain, and molecular phenotyping of neurological conditions and diseases (Serafini 1999; Cao and Dulac 2001; Luo and Geschwind 2001; Díaz 2009). Many advances have been made since then but still some challenges remain some of which were encountered in this thesis. One issue is the non-neuronal basis of commercially available arrays; for example, there are arrays available specifically geared toward profiling cancer related genes. Although there are available neuro-arrays, many neuron specific transcripts are still under-represented in the current arrays, allowing low expressing but significant genes to remain undetected and thus, undiscovered. Furthermore, despite the intense effort the NIH Neuroscience Microarray Consortium, http://np2.ctrl.ucla.edu/np2/home.do, has made to provide a globally available microarray database specifically for neuroscientists, it is lacking in a comprehensive database linking genome sequencing projects, gene annotation projects, in addition to all the other microarray projects put together. Therefore, it forces individual researchers to constantly "reinvent the wheel" when analyzing the complex results of a microarray experiment. Adding to frustration is that even the tools available to cluster microarray data are non-neuronal based, making the exercise even more difficult.

1.2.3 Profiling NSCs/NPCs

Developing and adult NSCs and NPCs can be isolated and purified using various methods including those described above. Inroads have been made regarding their *in vivo* anatomical location in the CNS, their functional significance, and their molecular signature. However, the process of gaining a deeper understanding of these stem cells is hindered by the fact that any given pool of neural stem cells is heterogeneous and cells in various states of differentiation are closely intermingled. Needless to say, the more rigorous the field is in defining each population of NPCs in various different organisms highlighting both common themes as well differences, the more useful the defined

populations will be in formulating and testing specific hypothesis that will be relevant to the field.

Microarray technology has been used to profile and characterize gene expression of various stem cells populations, including neural stem cells (Easterday, Dougherty et al. 2003; Kawaguchi, Ikawa et al. 2008). And in turn, the gene expression signatures have been used to more precisely define and identify the various *in vivo* and *in vitro* stem cell populations. Ongoing investigations are being conducted to carefully characterize NSCs and NPCs as well as their progression from one state to another (Ahn, Lee et al. 2004); but the consensus is that there is a lot more work to be done in this field.

Since preliminary data from our lab identifies a pool of activity-dependant proliferative NPCs, further studies with these NPCs would be enhanced by the identification of their genetic expression profiles. In this way, the observation of NPCs from this lab can be translatable to NSCs/NPCs of other species sharing similar profiles. In particular, it will be interesting to compare our results with other studies showing activity related increases NPC proliferation and integration, such as in exercise or learning and memory.

1.3 *In vivo* imaging of the developing brain

Until recently, imaging of NSCs/NPCs has been overshadowed by that of the neuron. With the advent of the Golgi stain, the neuron has captured the imagination. As the technology to look more closely at the neuron advanced, its structure began to give away its function. Fluorescent protein tagging and laser assisted microscopy coupled with time-lapse imaging revealed that they are perpetually in motion. Newly born neurons in the developing and adult brain actively migrate away from their birthplace, they take on various shapes in the course of their journey, and once they reach their destination, they extend and retract processes which then undergo constant reconstruction. However, beginning in the 1960's the imaging eye turned toward NSCs/NPCs.

Studies such as those performed by Altman and Das (Altman and Das 1965) emerged contradicting the long standing dogma that stated the adult brain is static. Spurred by the song bird studies by Goldman and Nottebohm (Goldman and Nottebohm 1983) and encouraged by the primate studies by Kornack and Rakic (Kornack and Rakic 1999), Eriksson published the seminal 1998 paper which showed evidence of neurogenesis in the adult human brain (Eriksson, Perfilieva et al. 1998). Until then, the adult human brain was considered incapable of supporting an introduction of new cells. However, since neurogenesis occurs naturally in the adult brain, the manipulation of endogenous neurogenic pools within or introduction of NSCs/NPCs into the adult brain to treat brain diseases became a possibility. This resulted in an explosion of research into understanding NSCs/NPCs, both in the developing and adult brain (Sohail 2009). Naturally with this wave, came the adaptation of known imaging tools and development of more genetic tools to look at NSCs/NPCs followed by an increased desire to see more.

1.3.1 Looking at neurogenesis

The majority of information regarding the neurogenesis is from static experiments. Goldman and Nottebaum used the radioactive hydrogen molecule attached to thymidine to label dividing cells in song birds. 5-bromo-2-deoxyuridine (BrdU) became popular in the late 1980's and was the marker used by Kornack, Rakic, and Eriksson; it is still popular now (Taupin 2007). Tritiated thymidine, BrdU and other halogenated reagents (CldU and IdU) are markers of DNA synthesis only and not markers of S-phase of the cell cycle or cell division. This single fact is the source of several drawbacks to its use; for example it can label cells undergoing DNA damage repair or DNA duplication without division. An alternative method was developed by Buck *et al* using 5-ethynyl-2-seoxyuridin (EdU) which labels s-phase cell cycle progression (Buck, Bradford et al. 2008). However, the relevant problem of using the aforementioned reagents is the requirement to sacrifice the animal and the inability to observe the same cell over time.

These disadvantages lead to the advancement of techniques such as animal and tissue preparation and technology such as 2-photon and spinning disk confocal microscopy to be able to observe the same cell over time. An example is the organotypic slice culture which has been indispensable for electrophysiologist for decades. These slices have been shown to be capable of neurogenesis, *in vitro* survival for more than 6 months, and sustaining repeated imaging sessions (Raineteau, Rietschin et al. 2004; Gogolla, Galimberti et al. 2006). Several labs have already used organotypic slice cultures successfully to reveal break-through results, especially in the study of neurogenic division patterns (Chenn and McConnell 1995; Miyata, Kawaguchi et al. 2001; Noctor, Flint et al. 2001; Miyata, Kawaguchi et al. 2004; Noctor, Martinez-Cerdeno et al. 2004; Attardo, Calegari et al. 2008). For example, until Noctor *et al* showed with time-lapse imaging of cortical slice culture that horizontal cleavage planes can result in symmetrical divisions (Noctor, Martínez-Cerdeño et al. 2008), it was generally thought that horizontal cleavage planes only resulted in asymmetrical divisions (Figure 1.2). Without time-lapse imaging of the same cell, it would have been difficult to correlate a static BrdU experiment capturing a dividing cell with a horizontal cleavage plane with another BrdU experiment capturing two proliferative daughter cells and conclude that horizontal cleavage planes can result in symmetrical divisions.

Another technique for observing the same NPC over time is using superficial readily accessible brain tissues such as the mouse olfactory bulb for *in vivo* imaging of migrating and integrating NPCs (Mizrahi, Lu et al. 2006); however, this technique cannot be used to observe NPCs at the site of neurogenesis. Finally, the zebrafish which has been a model organism in embryology has also become a model organism to look at brain development *in vivo* (Köster and Fraser 2004); however, techniques to deliver reporter constructs are currently not as routine as those in *Xenopus*. The development and use of these techniques to observe neurogenesis illustrates that there is a call for and a value in watching neurogenic events live as it happening.

1.3.2 The albino *Xenopus laevis* model system

The albino *X. laevis* tadpole has unique advantage as a model system for the purposes of imaging the process of neurogenesis. First, the skin of the tadpole is

transparent and the central nervous system (CNS) is superficial thus making it amenable to *in vivo* time-lapse imaging in an intact and virtually unprocessed animal. It has long been used to study neuronal dynamics, such as dendritic arbor growth and development using fluorescent dye labeling or electroporated fluorescent proteins encoded in DNA plasmids to visualize cells with laser microscopy (Haas, Sin et al. 2001; Haas, Jensen et al. 2002; Wu and Cline 2003; Bestman, Ewald et al. 2006); I proposed a cell-specific promoter to drive expression of fluorescent protein to label a specific cell population using this delivery method. Second, in addition to fluorescent proteins, other genes of interest (GOI) can be expressed by plasmid introduction. GOI can be expressed as fusion proteins tagged with fluorescence for purposes of visualizing specific protein actions and locations. Or they can be used in overexpression and knockdown paradigms using functionally disruptive forms of the GOI (Bestman and Cline 2008; Chiu, Chen et al. 2008). Using the same delivery method, morpholinos can be introduced into tectal cells to functionally knockdown GOI expression. In this way, genes can be functionally characterized *in vivo*. Third, the visual system in *Xenopus* is a relatively simple network where the retinal ganglion cell axons directly innervate tectal cells. Thus, questions regarding how physiological activity affects tectal cell development can be addressed (Sin, Haas et al. 2002; Aizenman and Cline 2007). Finally, the most important property of this system is that the retina and the tectum continue to develop throughout the larval stages of development and the neurogenic pool is still active (Straznicky and Gaze 1972). Thus, by using the same imaging and labeling techniques used routinely in the lab, it is possible to observe *in vivo* neurogenesis events (Figure 1.3).

1.3.2.1 Development of the tectum

The developmental timeline for the *X. laevis* nervous system has been extensively characterized including that of the visual system; extensive development of the visual system occurs between stages 39 and 49. Retinal ganglion cells (RGCs) from the eye first innervate and transmit visual information to the optic tectum beginning stage 39 (Holt 1983). The RGC pool in the eye expands continuously even beyond metamorphosis. Thus, although the topographic retinotectal map is initially established by stage 45 (O'Rourke and Fraser 1990), it is still undergoing experience-dependent refinement at the stages studied in this thesis. The constant refinement occurs because the tectum is continuously accommodating and integrating the incoming axons from the new retinal ganglion cells by expanding its own pool of tectal cells and reorganizing its synaptic connections. During the period between stages 45 and 49, visual stimulation drives many aspects of tectal circuit development including the fine restructuring of the retinotectal topographic map, the maturation of RGC axons arbors, the RGC synchronized elaborations of tectal cell dendrites (Bestman and Cline 2008), the refinement of receptive fields (Tao and Poo 2005) and the development of the circuits pertaining to the detection and processing of visual inputs (Engert, Tao et al. 2002; Aizenman and Cline 2007; Pratt, Dong et al. 2008; Dong, Lee et al. 2009). The development of a functional retinotectal circuit is especially relevant during these stages because the tadpoles deplete their yolk supply by stage 47 and the need to forage for food is required beyond stage 47. By stage 49 the optic tectum is laminated and there is a decrease in the rates of structural rearrangements of retinal axons and tectal cell dendrites as synaptic connections become stronger and more stable (Sakaguchi and Murphey 1985); experiments by Pranav Sharma

show at the later stages of *X. laevis* development the NPCs are less proliferative indicated by the decrease in BrdU uptake at later stages (Figure 1.4). Finally, the development of tectal neurons from NPCs to integrated neuron covers a span of days (Figure 1.5) where as in the mouse it has been known to take as long as a month. The short developmental timeline of the *X. laevis* brain and its cells, NPCs and neurons, is another advantage of this model system.

1.3.2.2 Activity-dependent development

Activity-dependent development is the unifying focus of the Cline lab. In keeping with tradition, one aspect of this thesis investigated the role of visual activity in regulating NPC behavior with a particular interest in discovering genes that may play a role in regulating activity-dependent NPC proliferation and differentiation. One such candidate is CPG15 which has been the focus of other works in the lab relating to activity-dependent plasticity.

Visual deprivation affects NPC proliferation. Data from currently unpublished work of Pranav Sharma in the Cline laboratory has directed much of this thesis investigation into activity-dependent mechanisms in *X. laevis* NPCs. He took advantage of a sequential exposure technique which uses two different halogenated thymidine analogs (IdU and CldU) to track the history of dividing cells (Vega and Peterson 2005). He reports that altering the visual experience of the tadpole results in changes in NPC behavior. He demonstrates that 48h of visual deprivation increases cell proliferation by increasing the re-division rate of already proliferating cells (Figure 1.6). His experiments ultimately suggest that the role visual experience plays in neurogenesis is to push NPCs toward differentiation and away from proliferation.

CPG15. Candidate Plasticity Gene 15 or Neuritin is a glycosylphosphatidyl inositol (GPI)-linked activity-induced protein that is highly conserved between *Xenopus* and humans (Nedivi, Javaherian et al. 2001). It was shown to be up-regulated in response to light and be involved in activity-dependent promotion of dendritic growth (Tadahiro, Zhen et al. 2008). CPG15 is also thought to play a role in extending the critical period in dark-reared animals which naturally suggest that it is involved in signaling pathways that mediate synaptic plasticity (Lee and Nedivi 2002). The findings most relevant to NPCs are that the soluble form of CPG15, CPG15-2 has been shown to rescue early cortical progenitors from apoptosis and promote neuronal survival in rodent cortical cultures (Putz, Harwell et al. 2005) and has been shown to enhance the differentiation effect of NGF in the immortalized neuronal cell-line, PC12 (Cappelletti, Galbiati et al. 2007). It is undeniably interesting that this highly conserved activity-dependent gene plays all these roles. One cannot help but speculate if CPG15 is also involved in activity-dependent regulation of proliferation of NPCs in *X. laevis.*

Table 1.1 | Pathways that are involved in neurogenesis. These pathways have been shown to be involved in different processes of neurogenesis such as proliferation events and differentiation events. References to some of the implications of these pathways are displayed as well. Note: This is an incomplete list.

Pathway	Implications in NPCs	References
Pathways mediated by cell-extrinsic factors		
Wnt-Frizzled (Canonical Pathway)	Differentiation pathway Stabilized ß-catenin knock-in results in large brains ß-catenin knock-down results in small brains LRP6 co-receptor for Wnt reduced granule NPCs	(Toledo, Colombres et al. 2008) (Chenn and Walsh 2003) (Zechner, Fujita et al. 2003) (Zhao, Li et al. 2007)
Wnt-Frizzled (Non-Canonical Pathway)	Wnt/PCP pathway activation causes differentiation through Wnt7B/Dishevelled	(Li, Chong et al. 2005)
Notch	Hes-genes activated by Notch/Delta maintains stemness Notch1 knock-down increases differentiation Conditional knock-down of Notch1 depletion of NPCs Deleting Delta-like decreases radial glial pools	(Lasky and Wu 2005) (Yoon and Gaiano 2005) (Yoon, Nery et al. 2004) (Yoon and Gaiano 2005)
Ephrins	EphA4 promotes cell proliferation in glioma cell-line EphB regulates neurogenesis in adult hippocampus	(Fukai, Yokote et al. 2008) (Chumley, Catchpole et al. 2007)
Sonic Hedge Hog	Shh null mice have reduced brain size Over-expression in adult hippocampus increases neurogenesis	(Machold, Hayashi et al. 2003) (Dahmane, Sanchez et al. 2001)

Pathway	Implications in NPCs	References
Growth Factors	EGFR disruptions causes cortical dysgenesis TGFα, ligand knock-down causes decreased proliferation FGFR1 deletion causes decreased proliferation in hippocampus FGF2 knockdown reduced proliferation *In vivo* administration of FGF increases NPCs *In vivo* administration of EGF increases NPCs	(Sibilia, Steinbach et al. 1998) (Tropepe, Craig et al. 1997) (Ohkubo, Uchida et al. 2004) (Raballo, Rhee et al. 2000) (Craig, Tropepe et al. 1996) (Kuhn, Winkler et al. 1997)
Hormones	ERß deletion shown to increase neuronal loss in adult mice TRα deletion inhibits proliferation by affecting cell-cycle	(Wang, Andersson et al. 2003) (Lemkine, Raji et al. 2005)
Metalloproteinases	MMPs are temporally and spatially differentially expressed MMPs have differential roles in development of CNS as reviewed by two papers	(Vaillant, Didier-Bazes et al. 1999) (Mannello, Tonti et al. 2006) & (Agrawal, Lau et al. 2008)
Stress Related	Depression causes decreased neurogenesis Anti-depressive therapies increase neurogenesis Glucocorticoids affect neurogenesis in adults HSF1 and HSP70 expression associated with neurogenesis	(Eisch, Cameron et al. 2008) (Encinas, Vaahtokari et al. 2006) (Mirescu and Gould 2006) (Yang, Oza et al. 2008)
Pathways mediated by cell-intrinsic factors		
Apoptosis and Survival	Apoptosis determine size of neurogenic pool Bcl-2 show spatial and temporal brain expression Bcl-2 over-expression mice have large brains Bcl-2 play a role in differentiation	(Lindsten, Golden et al. 2003) (Novack and Korsmeyer 1994) (Martinou, Dubois-Dauphin et al. 1994) (Akchiche, Bossenmeyer et al. 2009)
Differentiation and Proliferation	Proneural genes assist in cell-cycle exit and differentiation while stemness genes inhibit differentiation	(Bertrand, Castro et al. 2002)

Pathway	Implications in NPCs	References
Signal Transduction pathways		
MAPK	MAPK transduces RTK activation by growth factors MAPK activated by integrins and work through Rac	
PKA	CREB activation results in NPC proliferation CREB involved in survival and differentiation of new neurons	(Dworkin, Malaterre et al. 2009) (Jagasia, Steib et al. 2009)
Ca-Calmodulin	CREB and HDACs activation by CaKM	(Hsieh, Nakashima et al. 2004)

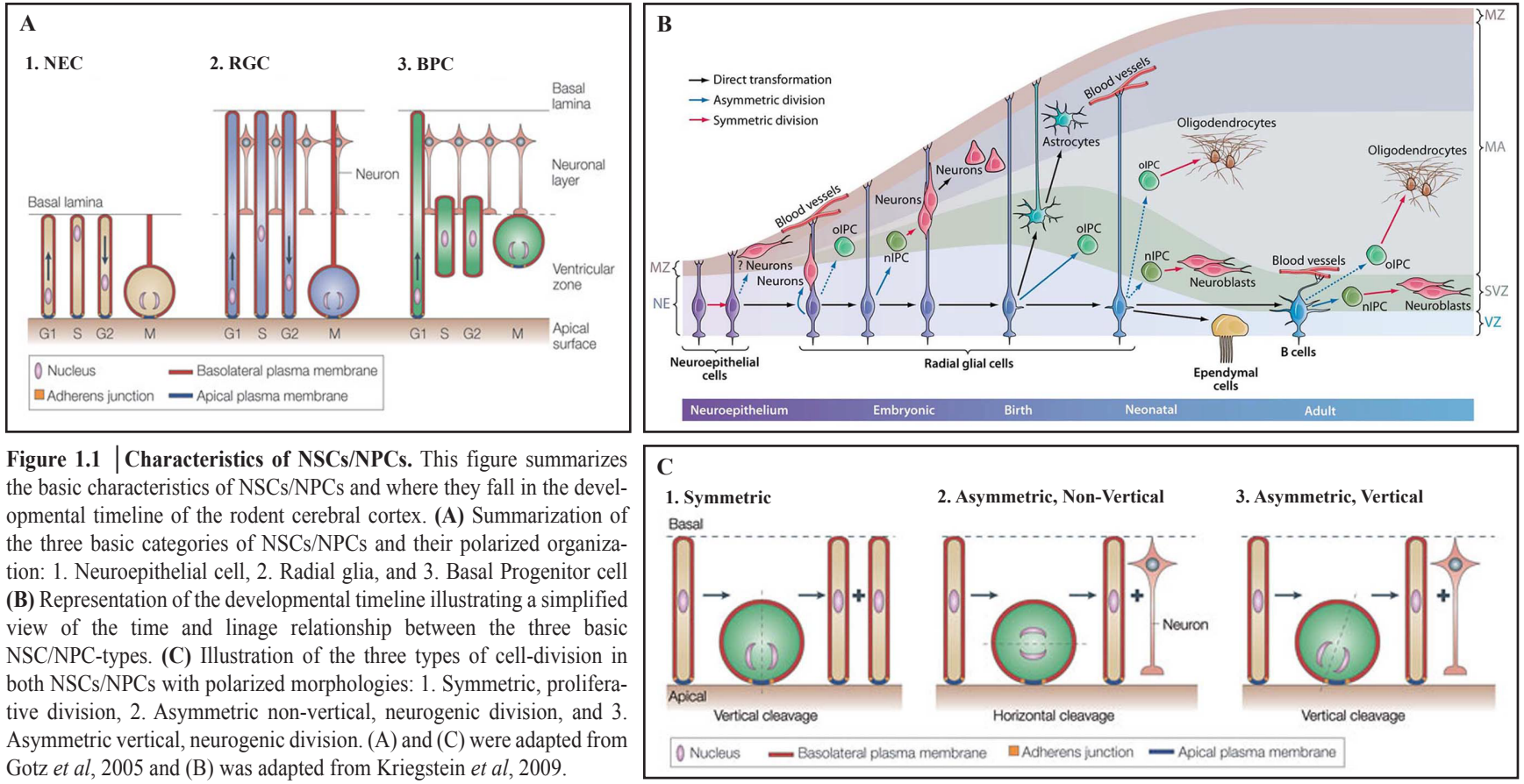

Figure 1.1 | Characteristics of NSCs/NPCs. This figure summarizes the basic characteristics of NSCs/NPCs and where they fall in the developmental timeline of the rodent cerebral cortex. **(A)** Summarization of the three basic categories of NSCs/NPCs and their polarized organization: 1. Neuroepithelial cell, 2. Radial glia, and 3. Basal Progenitor cell **(B)** Representation of the developmental timeline illustrating a simplified view of the time and linage relationship between the three basic NSC/NPC-types. **(C)** Illustration of the three types of cell-division in both NSCs/NPCs with polarized morphologies: 1. Symmetric, proliferative division, 2. Asymmetric non-vertical, neurogenic division, and 3. Asymmetric vertical, neurogenic division. (A) and (C) were adapted from Gotz *et al*, 2005 and (B) was adapted from Kriegstein *et al*, 2009.

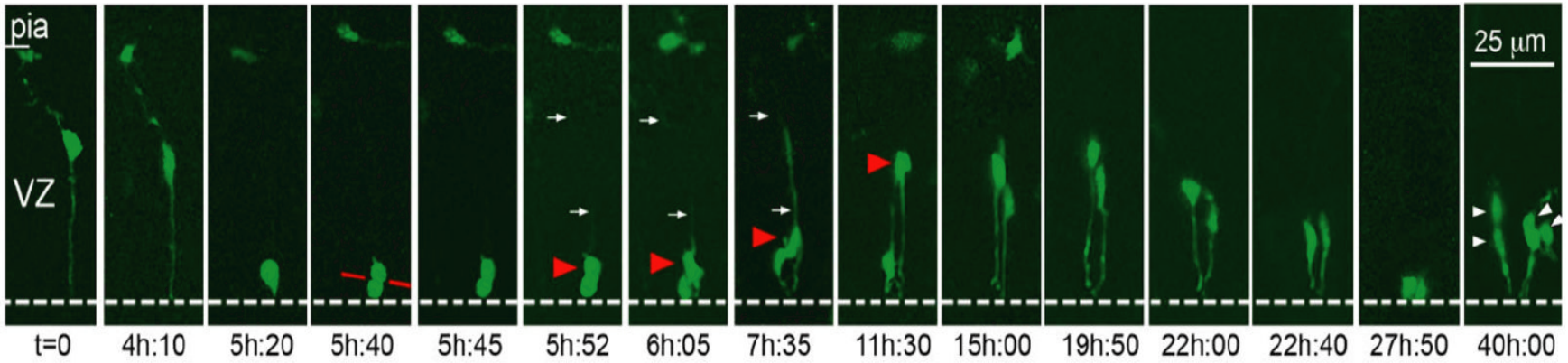

Figure 1.2 | Time-lapse imaging of cortical slice culture. Image series shows a horizontally oriented cleavage plane resulting in a symmetric proliferative division. A single bipolar RG cell at E13 is shown in G1-phase at t = 0. The RG cell body rose slightly in the VZ before descending to the ventricular surface (t = 5h:20m). The pial fiber became very thin and faint during mitosis but was detected post hoc. The RG cell divided with a horizontal cleavage plane (red line) at t = 5h:40m. After division the soma of the basal daughter cell (red arrowhead) moved away from the ventricle at a faster rate than its apical sibling. This behavior might be interpreted to signify an asymmetric fate for the daughter cells. Nonetheless, extended time-lapse imaging demonstrated that both daughter cells retained contact with the ventricle, resumed IKM, and divided at the ventricular surface (t = 40 h). Authors classified this RG division as symmetric proliferative. An unrelated cell with the morphology of a tangentially migrating cell was present in the marginal zone of the viewing field from 5–11 hours. Time elapsed is shown in either minutes (m), or hours and minutes (hh:mm) as indicated below each sequence. Figure and legend adapted from Noctor *et al.* 2008.

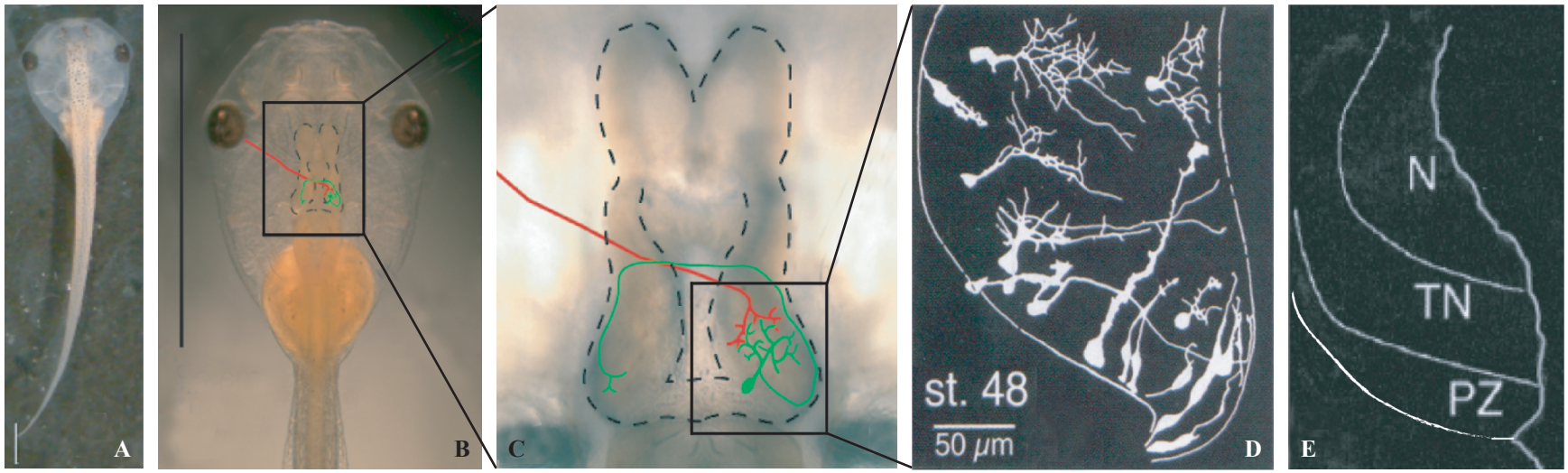

Figure 1.3 | The brain of albino Xenopus laevis tadpole: An in vivo model system. (A&B) Early stages of the albino X. laevis tadpole is transparent and the brain superficial making in vivo imaging possible. **(C)** Magnification of forebrain and optic tectum with illustration of contralateral projecting retinal ganglion cell axon (red) and optic tectal neuron (green). **(D)** Drawings of tectal neurons reconstructed from in vivo time-lapse images. Cells lining the ventricle tend to have radial glia-like morphologies. Cells near the ventricular zone of radial glia-like cells appear to be younger neurons with simple dendritic arbors. Cells more rostal-lateral appears to be more mature with elaborated dendritic trees. **(E)** The optic tectum is divided into three basic zones: proliferative zone (PZ) where the neural progenitors are located, tectal neuron zone (TN) where most of the cells bodies are located, and the neuropil (N) where all the processes are located. All images are adapted from Bestman *et al*, 2007 and Wu *et al*, 1999.

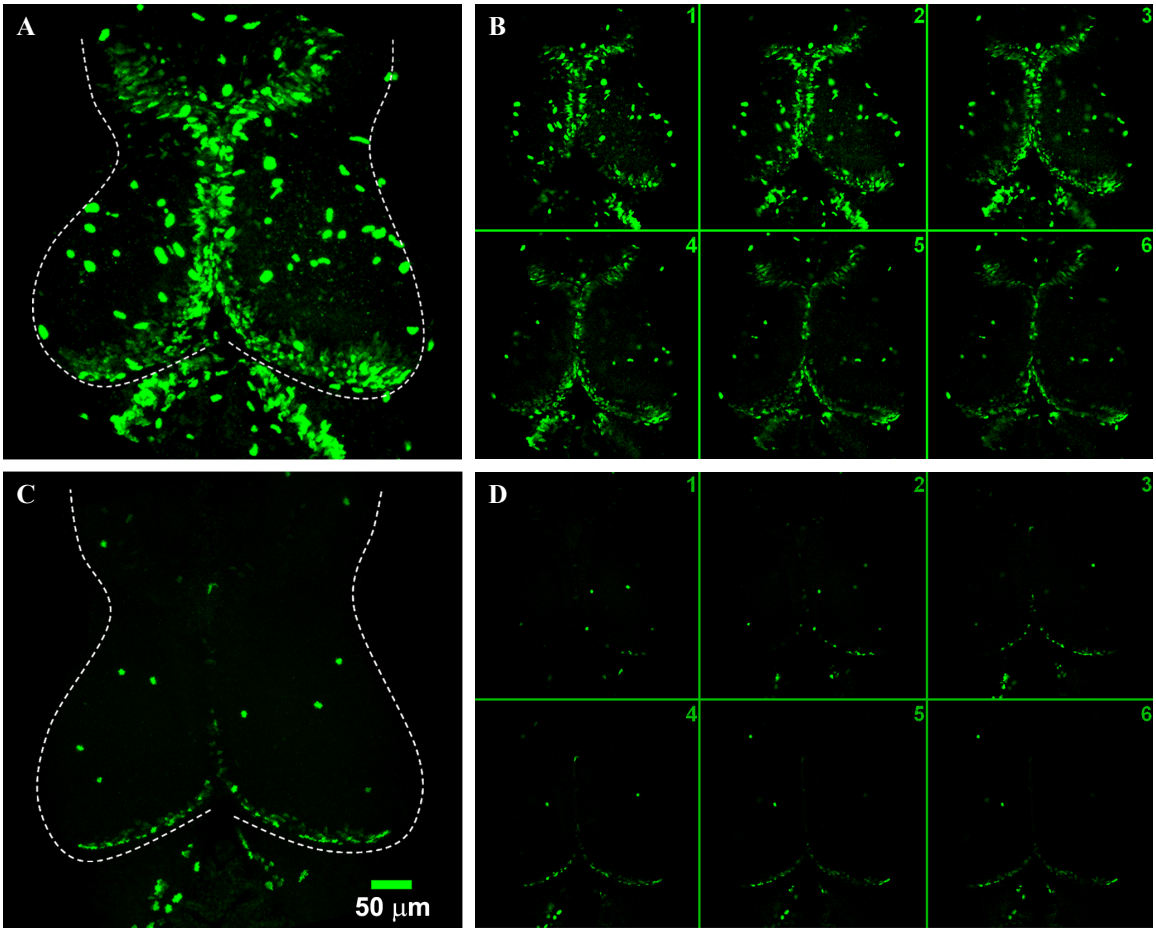

Figure 1.4 | Brain of X. laevis differ in proliferative property at different stages. Decrease in XdU incorporation at stage 49 indicates the brain at older stages contains less proliferative cells than at younger stages. Stage 46 **(A, B)** and 49 **(C,D)** tadpoles were labeled with 2 hr exposure to XdU. A and C are projections of a z-series of horizontal confocal sections through the midbrain. Samples of single optical sections are shown from dorsal to ventral in B and D. XdU incorporation decreases significantly from stage 46 to stage 49. Figure and legend adapted from unpublished data of Pranav Sharma in the Cline laboratory.

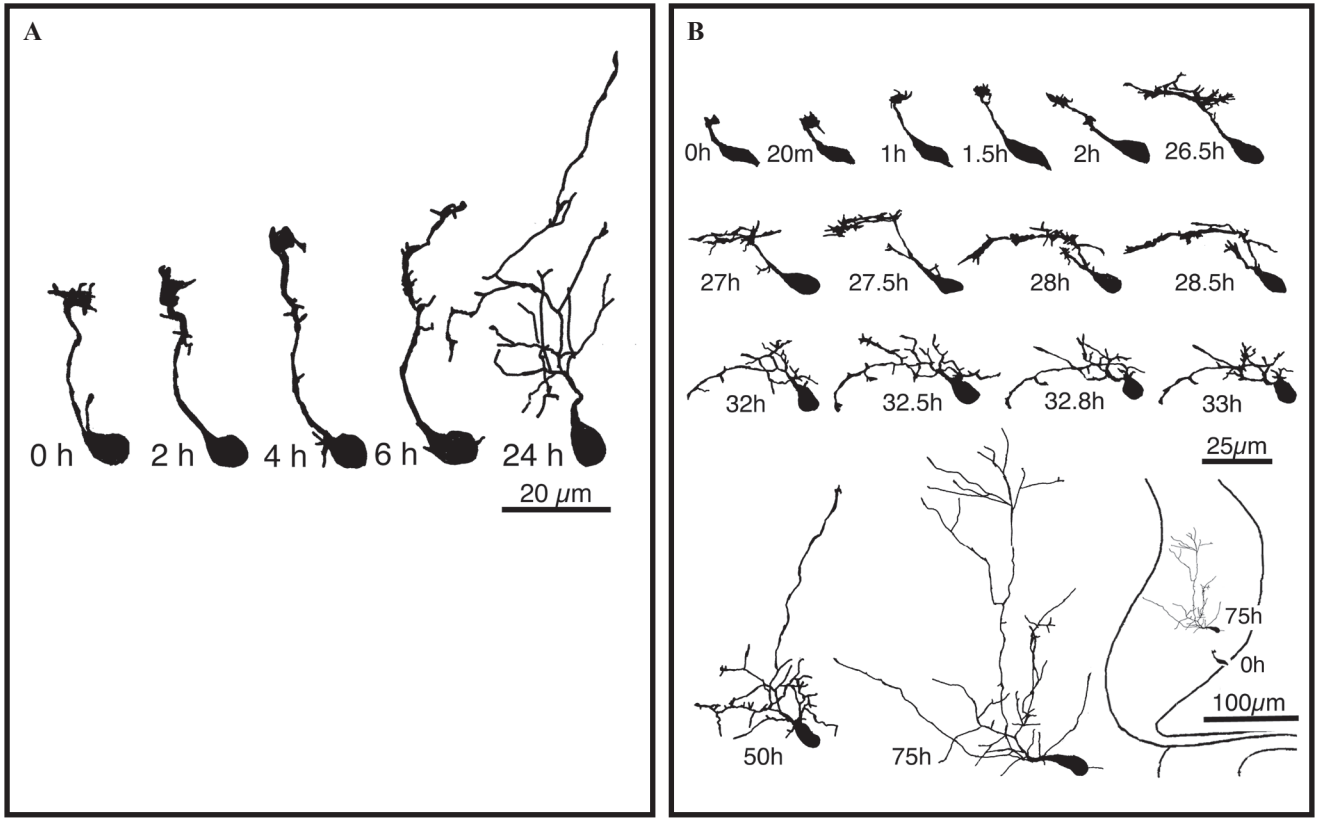

Figure 1.5 | Time-lapse images: Neural progenitor-like cell to neuron in 75hrs. DiI iontophoresis was used to label cells. 2hrs after dye labeling, images were taken with confocal microscopy. **(A)** Neuronal cell can elaborate a complex dendritic tree with-in 24hrs. **(B)** Neural progenitor-like cell residing in the progenitor zone adjacent to the ventricle can migrate, elaborate a dendritic tree, and extend an axon all within 75hrs illustrating that the process of neurogenesis spans days instead of months. Images adapted from Wu *et al*, 2003.

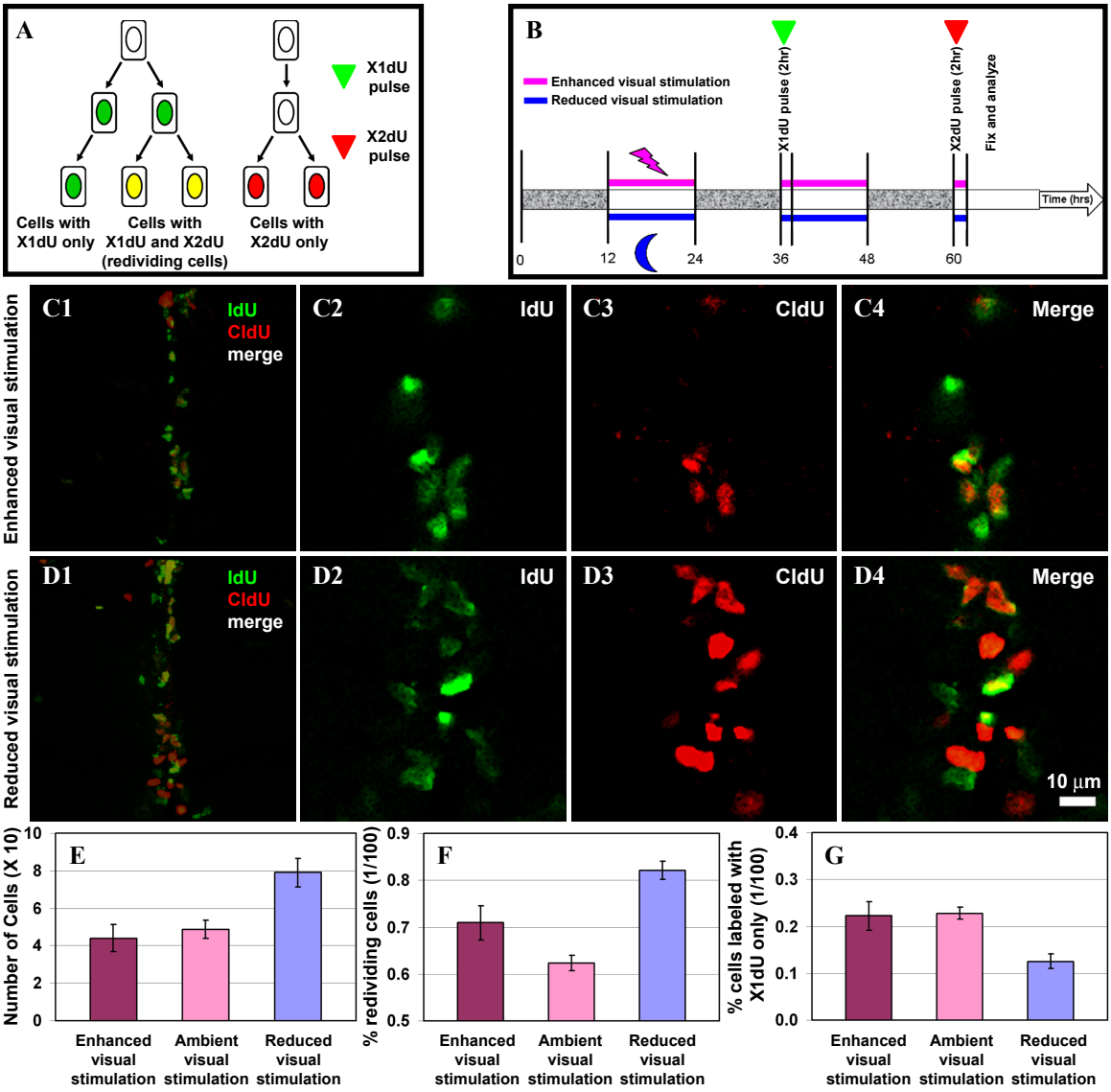

Figure 1-6 | Visual deprivation increases cell proliferation in optic tectum. Altering the visual experience of the tadpole results in changes in NPC behavior. **(A)** Cartoon of the results of the assay to detect the division history of proliferating cells. Green cells: X1dU only. Red cells: X2dU only. Yelllow cells were dividing during exposure to X1dU and divided again during exposure to X2dU. **(B)** Timeline of the experimental protocol. The 12h dark/12h light rearing conditions are shown as shaded and white bars. During the 12h 'light' period animals were either exposed to normal ambient light, enhanced visual stimulation or dark. Animals were exposed to IdU (X1dU) for 2h and allowed to develop in the absence of X1dU for 24 hours, after which they were exposed to CldU (X2dU) at the times marked by the green and red arrows, respectively. Protocol reveals the fraction of proliferating cells (labeled with X1dU and/or X2dU) that were re-dividing (double labeled with X1dU and X2dU), stopped dividing (X1dU only) or started dividing (X2dU only) at the time when the animals were exposed to X2dU. **(C-D)** Images of the dorsal midline ventricular layer of the optic tectum of tadpoles with visual experience, C1-4, or deprived of visual experience, D1-4, labeled with anti- X1dU (green; D,H) and anti-X2dU (red; E,I) C ,G. Merged images of the complete z-series showing the X1dU and X2dU-labeled cells through the depth of the 30 µm cryostat section. C2-4 and D2-4: Magnified single optical images from the z-series in C1 and D1 showing a fraction of cells labeled with X1dU only, X2dU only and both X1dU and X2dU. **(E)** Graph of total number of XdU-labeled cells. **(F)** Percentage of X1dU and X2dU-labeled cells. **(G)** Percentage of X1dU-only labeled cells Scale bar = 10 µm for C2-4 and D2-4. This figure and legend was adapted from the unpublished work of Pranav Sharma in the Cline lab.

Chapter 2 A Reporter for NPCs

Specifically driving expression of a fluorescent reporter construct in NPCs first required the identification of a NPC-specific marker. Neural stem cell/neural progenitor cell reporters in conjunction with mouse transgenic have been used with great success in NSC/NPC characterization and isolation. For example, the Nestin (Mignone, Kukekov et al. 2004), Sox1 (Barraud, Thompson et al. 2005), and Sox2 reporter (D'Amour and Gage 2003; Miyagi, Nishimoto et al. 2006) have been generated and used in previous NPC/NSC studies. Transgenesis of *Xenopus tropicalis and laevis* have also been shown to be useful in generating reporter lines. An available NSC/NPC reporter in *Xenopus* is Pax6, however, it showed ubiquitous expression in the CNS, as illustrated by transgenesis (Hirsch, Zimmerman et al. 2002; Ogino, McConnell et al. 2006) and immunohistochemistry (Figure 2.1-A/B). With the availability of various reporters, initial efforts were made to utilize a reporter that has been previously characterized; however, bulk electroporation (Whole Brain Electroporation, WBE) of gift plasmids did not suit the needs of this project. The mouse Nestin reporter from the Grisha Enikolopov laboratory at Cold Spring Harbor Laboratory (CSHL) did not express by WBE at all, and the mouse Musashi1 reporter from the Steven Goldman laboratory at the University of Rochester showed late and dim expression at PTD2; Musashi1 immunohistochemistry performed showed ubiquitous expression at stage 47 at the time (Figure 2.1-B/C). The mouse Sox2 promoter from the Angie Rizzino laboratory never made it to the Cline laboratory. Thus, given the results of preliminary results, the decision was made to search and characterized a reporter that fit the criteria of specificity and rapid 24hr expression. Sox2 was decided upon due to its proliferative zone immunohistochemistry staining pattern, the availability of its complete bacterial artificial chromosome (BAC) sequence, and its versatility as a transcription factor with a known and characterized binding sequence. Then, a Sox2 based reporter plasmid was designed and cloned, and its specificity was confirmed with immunohistochemistry.

2.1 Sox2 in the *X. laevis* tectum

Xenopus Sox2 (xSox2) has been identified in embryological *Xenopus* studies concerning the neural inductive actions of the Spemann organizer (Mizuseki, Kishi et al. 1998; Sasai 2001). xSox2 (*X. laevis and X. tropicalis*) gene has been fully sequenced along with its BAC clone (*X. tropicalis*) which is available commercially from the Children's Hospital of Oakland Research Institute (CHORI) BAC-PAC library (Cat.#ISB-345F12).

2.1.1 xSox2 in tadpole stage 46 to stage 49

Although, xSox2 has been shown to be present during the development of the nervous system at embryological stages, it had yet to be determined if the tadpole stages of interest (Methods 2.2.3) also expressed xSox2 especially by the NPCs in the tectum. Immunohistochemistry confirmed its presence in NPC's in the tectum at stage 46 to stage 49 (Methods 2.2.5 and Results 2.3.1); this allowed me to use it as the basis of the reporter construct.

2.1.2 Sox2 as a transcription factor

Sox2 is a transcription factor whose binding domain has been identified and characterized as an enhancer of FGF4; it has been used successfully in cell culture (Ambrosetti, Basilico et al. 1997; Ambrosetti, Scholer et al. 2000). It forms a hetrodimer with Oct3 and binds to a short sequence within an expression enhancer element of the FGF4 promoter region. Oct3 and FGF4 was shown to be expressed in *Xenopus* and also shown to play a role in neural development (Riou, Delarue et al. 1998; Snir, Ofir et al. 2006). As to whether or not Oct3 and FGF4 are expressed in the tadpole stages of interest could not be determined using immunohistochemistry due to the lack of cross-reacting antibodies. However, to emphasize a point made earlier, these elements, Sox2, Oct3, and FGF4, have all been shown to be expressed together to maintain stemness in other model systems (Srivastava, Shenouda et al. 2006).

2.2 Methods

Initially two strategies for designing a reporter construct using Sox2 as a marker were considered in parallel. The first strategy was to use the BAC xSox2 clone to isolate a possible promoter region using recombineering (Methods 2.2.1). The second was to take advantage of Sox2 as a transcription factor; the Sox2/Oct3 binding domain construct (Sox2/Oct3.mFGF4 and mFGF4-only) was a gift from the Basilico lab and was used to clone several fluorescent protein expression plasmids (Methods 2.2.2). In the end, the Sox2/Oct3.mFGF promoter sequence strategy prevailed because of its compact nature.

2.2.1 Generation of 9kb reporter by recombineering

Given that the mouse Sox2 promoter region is a 6kb fragment of DNA upstream of the ATG site of the Sox2 exon (Wiebe, Wilder et al. 2000; Zappone, Galli et al. 2000), a 9kb fragment upstream of the xSox2 ATG was cloned out of the xSox2 BAC using recombineering (Copeland, Jenkins et al. 2001). A double selection method was used to aid in determining positive clones. First the xSox2 BAC purified using Clontech BAC Purification Kit (Clontech, Mountain View, CA, Cat.#740579) was introduced into the SL102 bacterial cells using a previously described method from (Copeland, Jenkins et al. 2001); all recombineering bacteria, shuttle plasmids, and protocol were gifts of NCI-Frederick at http://recombineering.ncifcrf.gov/. For the first round of recombineering (Figure 2.3-A), a neomycin/kanamycin cassette (neo/kan) from PL451 plasmid was designed to target to xSox2 BAC 9kb upstream of the ATG. The neo/kan targeting vector was subcloned using primers 5' HA1-Forward-XhoI (F; JLO-P#47) and 3' HA1-Reverse-HindIII (R; JLO-P#48) for the 5' homologous arm and primers HA2-F-BamHI (JLO-P#49) and HA2-R-SacII (JLO-P#50) for the 3' homologous arm; restriction enzymes used to open the PL451 vector are indicated by the primer name. The neo/kan targeting vector was introduced into the xSox2 BAC containing SL102 bacteria and clones were screened using kanamycin and chloramphenicol (both positive screen) and ampicillin (negative screen). The neo/kan-xSox2 BAC was introduced again into SL102 to prepare for the next step. For the second round of recombineering (Figure 2.3-B), a plasmid containing eYFP flanked by ISce1 site was designed to retrieve a 9kb fragment of XSox2 BAC containing both the neo/kan cassette and the ATG of xSox2; the plasmid was a gift of Joerg R. Leheste at New York College of Osteopathic Medicine of NYIT. The retrieval vector was subcloned using HA1-F-XbaI (JLO-P#53) and HA1-R-BglII (JLO-

P#54) as described above and HA3-F-BglII (JLO-P#30) and HA3-R-XhoI (JLO-P#55); ISce1-eYFP vector was opened using the restriction enzymes XbaI and SpeI. The retrieval vector was introduced into the neo/kan-XSox2 containing BAC for recombineering; the positive clones were positive for ampicillin and kanamycin resistance and were negative for chloramphenicol resistance. Finally, the Neo/Kan was removed by restriction enzyme reaction near the FRT site. Recombineering procedures were performed with the assistance of Yeon Lee, a previous member of the Cline laboratory. The final product (9kb.P/Sox2-eYFP, JLO#57) was used to make transient transgenics using intra-cytosolic sperm transplantation (Amaya and Kroll 1999) or I-SceI meganuclease transgenesis (Ogino, McConnell et al. 2006) or to transiently express fluorescent protein in the tectal cells using WBE (I-SceI Transgenesis Figure 2.3-C, 9kb.P/Sox2-eYFP WBE Figure 2.2-A,B,C, and Methods 4.1).

2.2.2 Generation of Sox2/Oct3.mFGF4 construct by subcloning

The Sox2/Oct3.mFGF4 fragment was subcloned out of the plasmid described in (Ambrosetti, Scholer et al. 2000). It contains 6 tandem repeats of the Sox2/Oct3 hetrodimer transcription binding site followed by a minimal FGF4 promoter element; Sox2/Oct3 plasmids were gifts of Claudio Basilico at New York University. The Sox2/Oct3.mFGF4 promoter was then subcloned into a promoterless eGFP plasmid (eGFP-1HM) using SacI and BglII from the original plasmid. The eGFP-1HM (JLO#72) was made by removing the CMV from the Clontech eGFP-N1 vector (Clontech, Mountain View, CA, Cat.#6085-1); eGFP-N1 was cut with AseI and NheI, blunted with large fragment Klenow, and closed using Roche Rapid Ligation Kit (Roche Diagnostics, Mannheim, Germany, Cat.#11636379001). The eGFP-1HM (JLO#72) was cut with SacI and BglII to subclone the Sox2/Oct3.mFGF4 fragment. Additionally, a control plasmid with only the mFGF4 promoter (Gift of Basilico Lab) was also constructed. The mFGF promoter was subcloned using the same restriction enzymes into eGFP-1HM. These products (Sox2/Oct3.mFGF4-eGFP, JLO#75 and mFGF4-eGFP, JLO#74) were expressed in tectal cells using WBE (Methods 4.1 and Figure 2.2-D to F) and their specificity in Sox2+ cells was confirmed using immunohistochemistry (Methods 2.6).

2.2.2.1 Construction of Sox2/Oct3.mFGF4-Gal4VP16-14xUAS.mFGF4 plasmids

Initial WBE experiments with Sox2/Oct3.minFGF4-eGFP (JLO#75) showed that the fluorescent protein expression in the cells after 24hrs was not sufficient to visualize them reliably; likely because Sox2/Oct3.mFGF4 promoter action is weak thus fluorescent protein levels may not reach the detection threshold within 24hrs. In order to increase the expression of eGFP using this promoter, the Gal4VP16-UAS strategy was used as described in (Köster and Fraser 2001) with one modification.

14xUAS.mFGF. The original 14xUAS plasmid used in the Fraser laboratory contains 14 tandem UAS repeats followed by ElB (Köster and Fraser 2001), a minimal promoter; the UAS repeats do not work effectively without the minimal promoter. However, experiments showed that the 14xUAS.E1B in the absence of Gal4VP16 will promote low level transcription (personal communication, Kasandra Burgos). Thus, in order to reduce non-specific background expression of genes following the 14xUAS.E1B, the E1B minimal promoter was replaced with the mFGF4, the FGF4 minimal promoter. The

14xUAS fragment was cut out of Fraser Lab Plasmid ID#147 with a 5' HindIII cut and 3' SalI cut. And, the mFGF4 fragment was cut out of my plasmid Sox2/Oct3.mFGF4-eGFP (JLO#75) with a 5' BamHI cut and 3' AgeI cut. The SalI and BamHI cuts were blunted with large Klenow fragment and the two fragments were cloned into a vector opened with 5' AgeI and 3' HindIII.

Sox2/Oct3.mFGF4-Gal4VP16-eGFP. The first step in constructing a Gal4-UAS plasmid was ligation of the Sox2/Oct3.mFGF4 fragment with the Gal4VP16 fragment. The Sox2/Oct3.mFGF4 was cut from its original Basilico plasmids with 5' SacI and 3' BglII restriction enzymes. The Gal4VP16-polyA was cut from the Fraser Lab Plasmid ID#102 with 5' BamHI and 3' HindIII. The two fragments were ligated into a vector cut with 5' HindIII and 3' SacI. In the case of Sox2/Oct3.mFGF4-Gal4VP16-eGFP (JLO#87), eGFP-1HM was cut appropriately and the fragments were ligated as a triple fragment ligation. This construct can be used in conjunction with any plasmid containing UAS repeats; when electroporated with WBE by itself, it has low level eGFP expression although the Gal4VP16 has its own stop codon and poly-A tail.

Sox2/Oct3.mFGF4-Gal4VP16-14xUAS.mFGF4-eGFP. Once the plasmid Sox2/Oct3.mFGF4-Gal4VP16-eGFP was completed, it was opened with 5' AgeI and 3' HindIII. The 14xUAS and mFGF4 fragments described above were ligated as a triple fragment ligation to produce Sox2/Oct3.mFGF4-Gal4VP16-14xUAS.mFGF4-eGFP (JLO#95).

Sox2/Oct3.mFGF4-Gal4VP16-14xUAS.mFGF4-TurboGFP.NLS. TurboGFP is a variant of GFP that is visible quicker (Evrogen, Moscow, Russia, Cat.#FP512). The first step in constructing Sox2/Oct3.mFGF4-Gal4VP16-14xUAS.mFGF4-TurboGFP.NLS was to subclone the NLS sequence 3' to TurboGFP. This was done by amplifying the NLS from Clontech DSRed2-Nuc plasmid (Clontech, Cat.#632408) using 5' primer XbaI-NLS-F (JLO-P# 87) and 3' primer NotI-NLS-B (JLO-P# 88) and TA-cloning into a shuttle vector (TA-Cloning Kit for sequencing, Invitrogen, Cat.#K4575-01). TurboGFP-NLS was made by a triple fragment ligation: amplifying the TurboGFP with 5' primer AgeI-TurboGFP-F (JLO-P#85) and 3' primer BamHI-TurboGFP-B (JLO-P#86), subcloning out the NLS fragment from TA-NLS (JLO-#96), and opening eGFP-1HM with 5' NotI and 3' AgeI which removes the eGFP. Once TurboGFP-NLS (JLO#98) was constructed, Sox2/Oct3.mFGF4-Gal4VP16-14xUAS.mFGF4 was inserted by subcloning out the promoter fragment from Sox2/Oct3.mFGF4-Gal4VP16-14xUAS.mFGF4-eGFP (JLO#95) with 5' SacII and 3' AgeI, opening TurboGFP.NLS (JLO#98) with 5' AgeI and 3' SacII, and ligating the two fragments together. Sox2/Oct3.mFGF4-Gal4VP16-14xUAS.mFGF4-TurboGFP.NLS (JLO#100) was used for the cell-picking protocol. This construct was visible within 16hrs of WBE and it was found predominately in the nucleus; the most likely reason for its cytosolic presence is the leakage of the fluorescent protein out of the nucleus despite the NLS sequence.

Other variations and colors. Several other variations and colors were made of this construct but were not used extensively in this thesis. Some may be useful for further

investigative and subcloning efforts. The complete library of my plasmids and primers are listed in the Appendix for reference purposes.

2.2.2.2 Construction of the 14xUAS.mFGF-Kaede plasmid

Kaede is a photoconvertible fluorescent protein which converts from green to red upon UV exposure (Mizuno, Mal et al. 2003; Dittrich, Schäfer et al. 2005; Mannello, Tonti et al. 2006). It was used to track daughter cells for the imaging section of this thesis. It was made by subcloning Kaede out of a plasmid obtained from the Svoboda lab using 5' AgeI and 3' NotI. The fragment was then ligated into eGFP-1HM (JLO#72) and opened with 5' NotI and 3' AgeI, effectively replacing the eGFP sequence with Kaede to make a promoterless Kaede plasmid (PML-Kaede; JLO#122). For the final step, 14xUAS.mFGF4 fragment was subcloned out of 14xUAS.mFGF-TurboGFP (JLO#114) with 5' HindIII and 3' AgeI and ligated it into the PML-Kaede (JLO#122) using the same restriction enzymes. This construct was made with assistance from Mohana Gudurvalmiki, currently in the Cline laboratory. The 14xUAS.mFGF4-Kaede plasmid (JLO#123) was used in conjunction with the driver plasmid described above, Sox2/Oct3.mFGF4-Gal4VP16-eGFP (JLO#87).

2.2.3 Animal husbandry and staging of *Xenopus* tadpoles

Albino *Xenopus laevis* tadpoles were obtained from the lab colony or from a commercial source (Nasco, Fort Atkinson, WI). They were raised in 0.1x Steinberg's solution. They were subjected to a 12hr/12hr light-dark cycle in incubators set at 16°C or 24°C unless otherwise stated. Staging of animals were conducted according to the Nieuwkoop and Faber descriptions and drawings (Nieuwkoop and Faber 1994) and these resources: http://www.bio.davidson.edu/people/balom/StagingTable/xenopushome.html and http://www.engr.pitt.edu/ldavidson/NieuwkoopFaber/Frame1.html. Animals at stage 46 were determined by visualizing the intestines at 2 to 2-1/2 torsions; this stage is reached by ~4 days of incubation at 24°C. One day later (~24hrs), stage 47 is reached; animals at st47 were determined by 3 to 3-1/2 revolutions of the intestines. The final stage of interest is reached 1 to 2 days after stage 47 and lasts ~5 days; animals at st48 were determined by the appearance of a shiny gold abdomen at 1to 2 days after stage 47. Animals at st49 were determined by incubation time only. Generally, animals at the stages of interest were kept at 24°C, while prior to these stages animals may have been kept at 16°C to slow growth and stagger animals for scheduling daily experiments.

2.2.4 Immunohistochemistry methods

Animals first were subjected to a microwave assisted antigen retrieval protocol according to (Paupard, Miller et al. 2001). After which, immunohistochemistry was preformed according to (Chambaut-Guérin, Hérigault et al. 2000).

2.2.4.1 Microwave antigen retrieval protocol

Animals were anesthetized in 0.02% MS-222 (3-Aminobenzoic acid ethyl ester, Sigma-Aldrich, St. Louis, MO, Cat.#A9830). Then using a dissection microscope, the skin above the brain and the dura was peeled back to expose the tectum. The animals were prefixed in 4% paraformaldehyde (PFA, Sigma Aldrich, Cat.#158127) for 5mins and no longer than 10mins on ice in a 6-well plate. After pre-fixation, the 6-well plate

was place afloat in a cold water bath in the microwave and microwaved on high power for 15secs. After microwave antigen retrieval, they were fixed further in 4% PFA for 2hrs at room temperature (RT) and then cryoprotected overnight or up to a month at 4°C in 30% sucrose; both fixatives were made fresh in 0.1M phosphate buffer (PB; 0.08M Sodium phosphate monobasic anhydrous, 0.02M Sodium phosphate dibasic anhydrous, and pH7.4 with sodium hydroxide). The brains were dissected out after overnight fixation and prepared for cryosections by embedding with Cryo-OCT compound (Adwin Scientific, Addison, IL, Cat.#4583); brains embedded in Cryo-OCT could be stored at -80°C indefinitely. Sections were cut as 40µm thick horizontal sections onto positively charged glass slides with the assistance of Kim Bronson, a former member of the Cline laboratory and stored at -20°C until ready for immunohistochemistry.

2.2.4.2 Immunohistochemical staining protocol

Sections were briefly thawed before washing 2 times with 0.1M PB for 20mins at RT. Then they were incubated for 30mins in blocking solution (5% normal goat serum; Vector Laboratories, Burlingame, CA, Cat.#S-1000 and 0.3% Triton X-100, Sigma-Aldrich, Cat.#T9284 in 0.1M PB) before incubation with primary antibody diluted in antibody dilution buffer (0.1M PB and 0.03% Triton X) at 4°C overnight (16+hrs). After primary antibody incubation, sections were rinsed 4 times for 10mins with rinsing buffer (0.1M PB and 0.3% Triton). Appropriate secondary antibodies in antibody dilution buffer were incubated at RT for 1hr. Then sections were rinsed 1 time for 10mins with rinsing buffer and 2 times for 10mins with plain 0.1M PB before being mounted with mounting medium and covered with a glass cover slip. Stained sections were stored at -20°C.

2.2.5 Immunohistochemistry for xSox2

Animals at stage 47/48 were used for this experiment. Primary antibodies, anti-human Sox2 Rabbit polyclonal antibody (Chemicon/Millipore, Billerica, MA, Cat.#AB5603) was used at 1:200 dilution and PSA-NCAM mouse monoclonal antibody (Chemicon/Millipore, Cat.#MAB5324) was used at 1:500 dilution. Secondary antibodies, Goat anti-rabbit IgG Alexa 488 (Invitrogen, Carlsbad, CA, Cat.#A11008) and goat anti-Mouse IgM Alexa 488 (Invitrogen, Cat.#A21042) was used at 1:500 dilution. Fluorescence was imaged using Zeiss LSM 510 Meta Confocal microscope. I noticed that the some lots of the Sox2 antibody worked well, but others did not work as consistently.

2.2.6 BrdU assay

Stage 47/48 animals were used for the BrdU assay. Animals were anesthetized using 0.02% MS-222 before BrdU (1mg/ml in water; Sigmal-Aldrich, Cat.#B9285) was pressure injected into the pericardial sac using a pulled glass pipette (Methods 4.1.1). Visualization of injection was made possible by the addition of 0.01% Fast Green (Sigma-Aldrich, Cat.#F7252). Animals were allowed to recover at RT. They were sacrificed 2hrs after BrdU injection and 24hrs after Brdu injection.

BrdU immunohistochemistry was performed according to (Peunova, Scheinker et al. 2001) with some modifications. Animals were first subjected to antigen retrieval (Methods 2.2.4.1) but instead of cryoprotection with sucrose, they were dehydrated in 70% ethanol overnight at 4°C. Next day, the brains was dissected out and placed in DNA

denaturing solution (2N HCl and 0.5% Triton X-100 in PB) for 2hrs at RT. Before overnight (~24hrs) incubation at 4°C with primary antibody, the brain was washed with PB 3 times for 10mins; anti-BrdU antibody was diluted 1:200 in PB (Accurate Chemical, Westbury, NY, Cat.#OBT0030). Then the brains were washed clear of primary antibody with 3 washes of PB for 20mins at RT. The secondary antibody, anti-rat-FITC conjugated IgG (Chemicon/Millipore, Cat.#AP136F), was diluted 1:500 in PB; the brains were incubated with secondary antibody overnight (~24hrs) at 4°C. Then the brains were washed 3 times for 20min with PB before being mounted individually in wells created by 2 binder-hole reinforcement stickers on a glass slide. The wells were filled with Vectashield Hard-Set mounting medium (Vector Laboratories, Cat.#H1400) or Vectashield mounting medium with PI and a cover glass was place atop carefully as to not create any bubbles. Slides were stored at -20°C until imaging. Imaging was performed either with a 2-photon microscope or the Zeiss Meta confocal microscope.

2.2.7 Sox2/Oct3.mFGF4 promoter specificity assay

Animals at stage 47 were electroporated by WBE (Methods 4.1) with Sox2/Oct3.mFGF4-eGFP. 1day, 2days, and 3days later, they were sacrificed, fixed, and stained (Methods 2.2.4). Sox2 Rabbit polyclonal antibody was used at 1:200 dilution and Alexa-633 tagged secondary antibody (Invitrogen, Anti-Rabbit IgG Cat.#A21072) was used at 1:500 dilution. Before cover glass mounting, sections were PI stained with Vectashield with PI (Vector Laboratories, Cat.#H1300). Slides were stored at -20°C until ready for imaging.

Three-color fluorescence data was gathered using the Zeiss LSM 510 Meta confocal microscope: 488nm Argon for green eGFP, 514nm Argon for PI, and 633nm Hene for far-red Alexa-635. Serial sections were taken at 1μm with each channel optimized for each color. Data for endogenous Sox2 and exogenous eGFP (Sox2/Oct3.mFGF4-eGFP, JLO#75) colocalization experiment was visualized using Imaris Software. First PI was used to locate cell bodies. Then cell bodies with eGFP expression were located and endogenous Sox2 immunostaining colocalization was determined by eye for each eGFP+ cell (Figure 2.5). The number of eGFP expressing Sox2+ cells were counted and divided by the total number of eGFP expressing cells multiplied by one hundred to give a percentage of colocalization.

2.3 Results

2.3.1 xSox2 localization in the tectal NPCs of *X. laevis*

The polyclonal rabbit Sox2 antibody against the human Sox2 protein was used to test for xSox2 expression along the VZ of the stage 47/48 tectum (Figure 2.4; Methods 2.2.5). xSox2 expression analysis performed at stage 46 thru stage 49 showed similar results (Experiments performed by Pranav Sharma). Then, to confirm the NPC nature of the xSox2 labeling cells, the tectum was also analyzed using the PSA-NCAM antibody and BrdU (Methods 2.2.6). PSA-NCAM is a neuron associated cadheren protein and an early neuronal marker which appears once a neuronal fate is determined (Bonfanti 2006). The results of the PSA-NCAM immunohistochemistry (Figure 2.4-B) show complementary membrane staining relative to the Sox2 results (Figure 2.4-A). A 2hr BrdU chase showed BrdU incorporation in the VZ in the Sox2+ cells (Figure 2.4-C). A more interesting

observation was even though BrdU has been known to clear the animal within hours of introduction (personal communication, Hollis Cline) a 24hr chase of BrdU showed an expanded zone of labeled cells indicative of proliferation over the 24hr period (Figure 2.4-D).

2.3.2 Sox2/Oct3.mFGF4-eGFP plasmid specificity verification

Immunohistochemistry showed that the Sox2/Oct3.mFGF4-eGFP plasmid expression was 90% colocalized with endogenous Sox2 expression on post transfection day 1 (PTD1). The expression level decreased on PTD2 at 74% colocalization and further decreased on PTD3 at 22% colocalization (Figure 2-5). Also, noted in the immunohistochemical images were by PTD3, eGFP expressing cells began to extend processes and began to appear more like neurons. In comparison, the control Clontech eGFP-N1 plasmid showed 62% colocalization on PTD2 and 58% colocalization on PTD3; the brain for PTD1 was not available for analysis due to inadequate staining. These values coincide with the percentage for random transfection: 50% chance of plasmid transfection into a NPC vs. 50% chance of plasmid transfection into a non-NPC considering these two cell types. The control plasmid mFGF4-eGFP was not visibly expressing fluorescent protein at PTD1 and PTD2 but by PTD3, there was 95% colocalization indicative of the weak promoter activity of the minimal FGF4 promoter sequence. PTD1 verse PTD3 of the Sox2/Oct3.mFGF4-Gal4VP16-14xUAS.mFGF4-TurboGFP-NLS plasmid was not performed due to the unavailability of the Chemicon Sox2 antibody at the time. Several other antibody sources were investigated but none cross-reacted with xSox2; however, given that precautions were taken to limit run-away 14xUAS promoter activity as well as its verification by preliminary microarray experiments, the Sox2/Oct3.mFGF4-Gal4VP16-14xUAS.mFGF4-TurboGFP-NLS (JLO#100) plasmid appears to function similarly to the Sox2/Oct3.mFGF4-eGFP plasmid.

2.4 Conclusion

The Sox2/Oct3.mFGF4 reporter fluorescently marks cells that endogenously express Sox2 protein. The specificity verification experiment showed high correlation of cells with exogenously expressing fluorescent protein with Sox2+ immunostaining the first day post-transfection. This suggested that the Sox2/Oct3.mFGF4 reporter construct marked Sox2+ cells, at least initially. Fluorescent proteins have a half-life of longer than one week in the *Xenopus* model system. Therefore, the decrease in colocalization of fluorescent protein and Sox2 immunostaining was suggestive of Sox2+ cells exiting the proliferative state and possibly entering a differentiative state with the down-regulation of endogenous Sox2 protein since Sox2 expression has been shown to not only be a maintainer of stemness (Graham, Khudyakov et al. 2003), but also an inhibitor of differentiation (Agathocleous, Iordanova et al. 2009). The dual roles for Sox2 may be possible by its POU domain which allows it to work as a hetrodimer transcription factor. Given that Sox2 binds with Oct3 to express stem cell associated genes such as FGF4 and Nanog (Rodda, Chew et al. 2005), it can be speculated that Sox2 may bind with a different transcription factor for its role as a differentiation inhibitor. With the reporter construct verified, it was ready to be used for NPC cell identification in the microarray experiments and the imaging experiments.

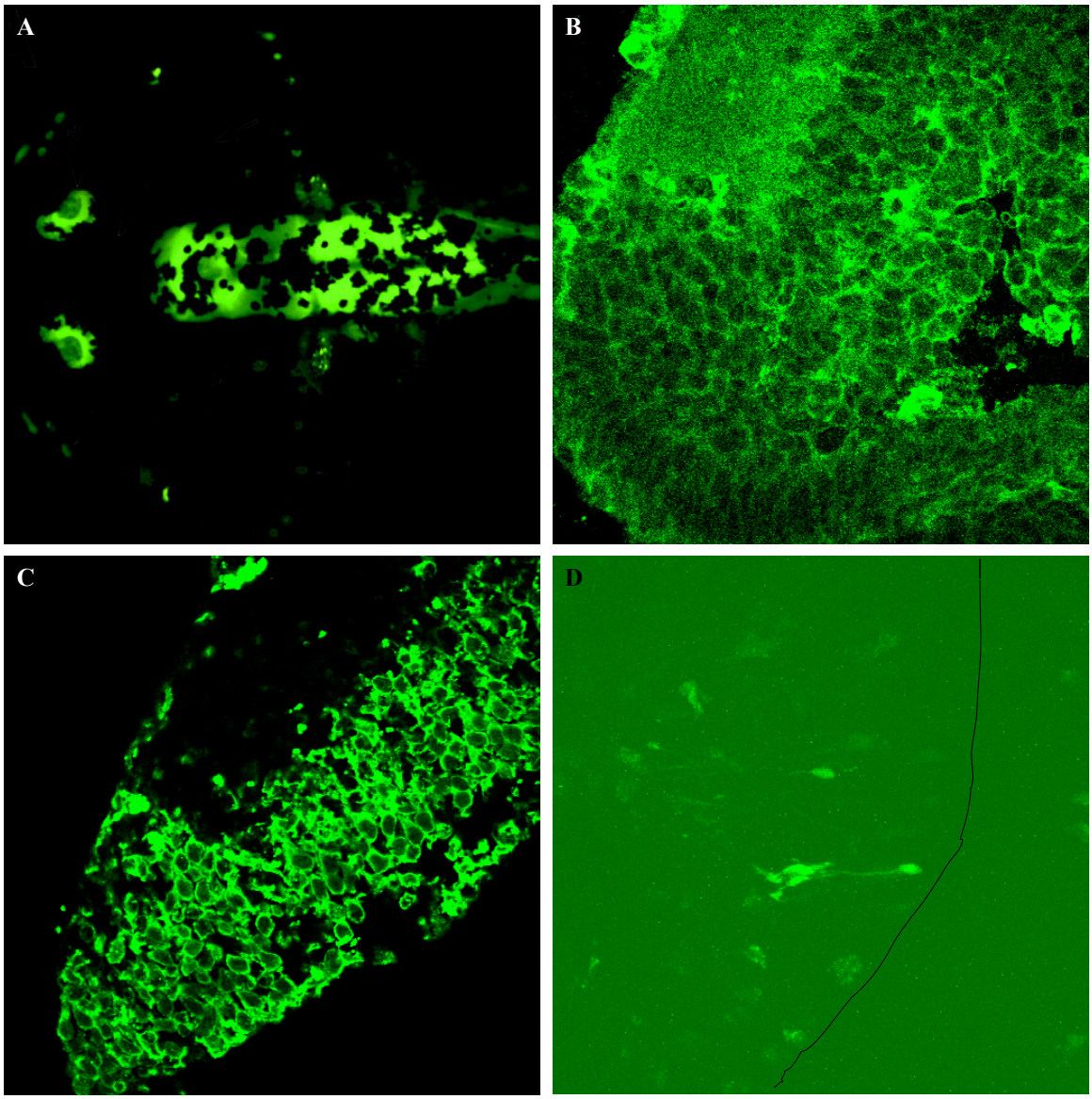

Figure 2.1 | Preliminary results of previously characterized NPC/NSC reporters. These images show previously characterized NPC markers did not fit the criteria for use in this project; they were not specific and not rapidly expressing. **(A)** Pax6-GFP Xenopus tropicalis transgenic tadpole at stage 45 show pan-CNS cell labeling. **(B)** Immunohistochemical staining with Rb-polyclonal anti-msPax6 illustrates Pax6 may be expressed throughout the tectum at stage 47/48. **(C)** Immunohistochemical staining with Rb-polyclonal anti-huMsi1 shows ubiquitous staining at stage 47/48. **(D)** MsMsi1 promoter driven huGFP at PTD2 showing very dim labeling of potential Xenopus NPC. Reminder: Immunohistochemical staining may be indicative of true protein expression or lack of specific cross-reactivity with Xenopus laevis homologous proteins. (A) was adapted from Hirsch, Zimmerman et al. 2002. (D) Plasmid huMsi1 was gift of Steven Goldman laboratory.

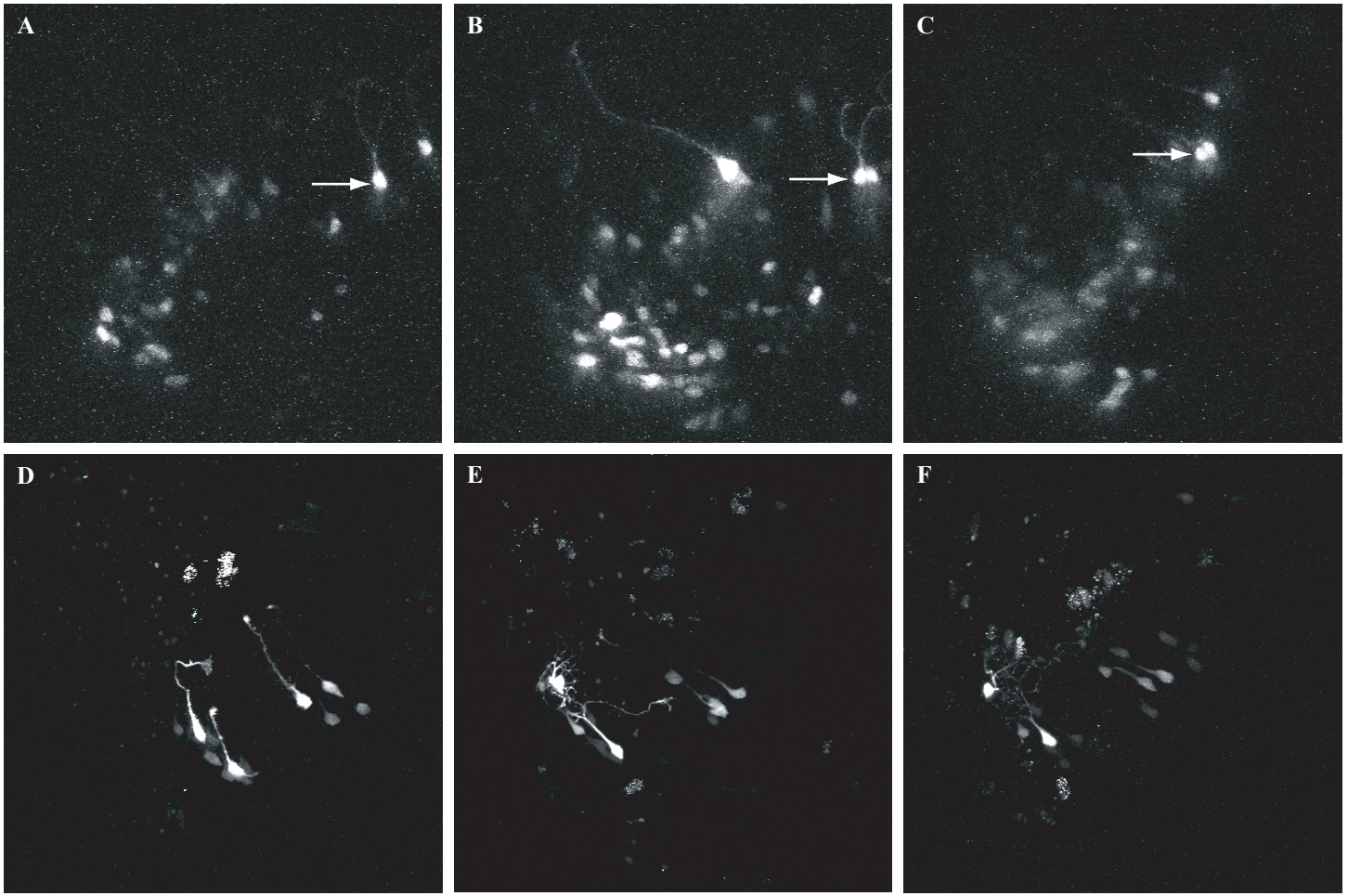

Figure 2.2 | Bulk electroporation of 9kb.P/Sox2-eYFP and Sox2/Oct3.mFGF4-eGFP. These images were taken 24hrs after WBE. **(A-C)** Expression of 9kb.P/Sox2-eYFP shows very weak eYFP expression PTD1. Expression increases on PTD2 but again decreased PTD3. This may be due to Sox2 being down-regulated in the cells. Arrow indicated a division event captured. **(D-F)** Expression of Sox2/Oct3.mFGF4-eGFP show similar expression pattern as 9kb.P/Sox2-eYFP over three days. There was an increase in cell number but no readily identifiable division event was noted here.

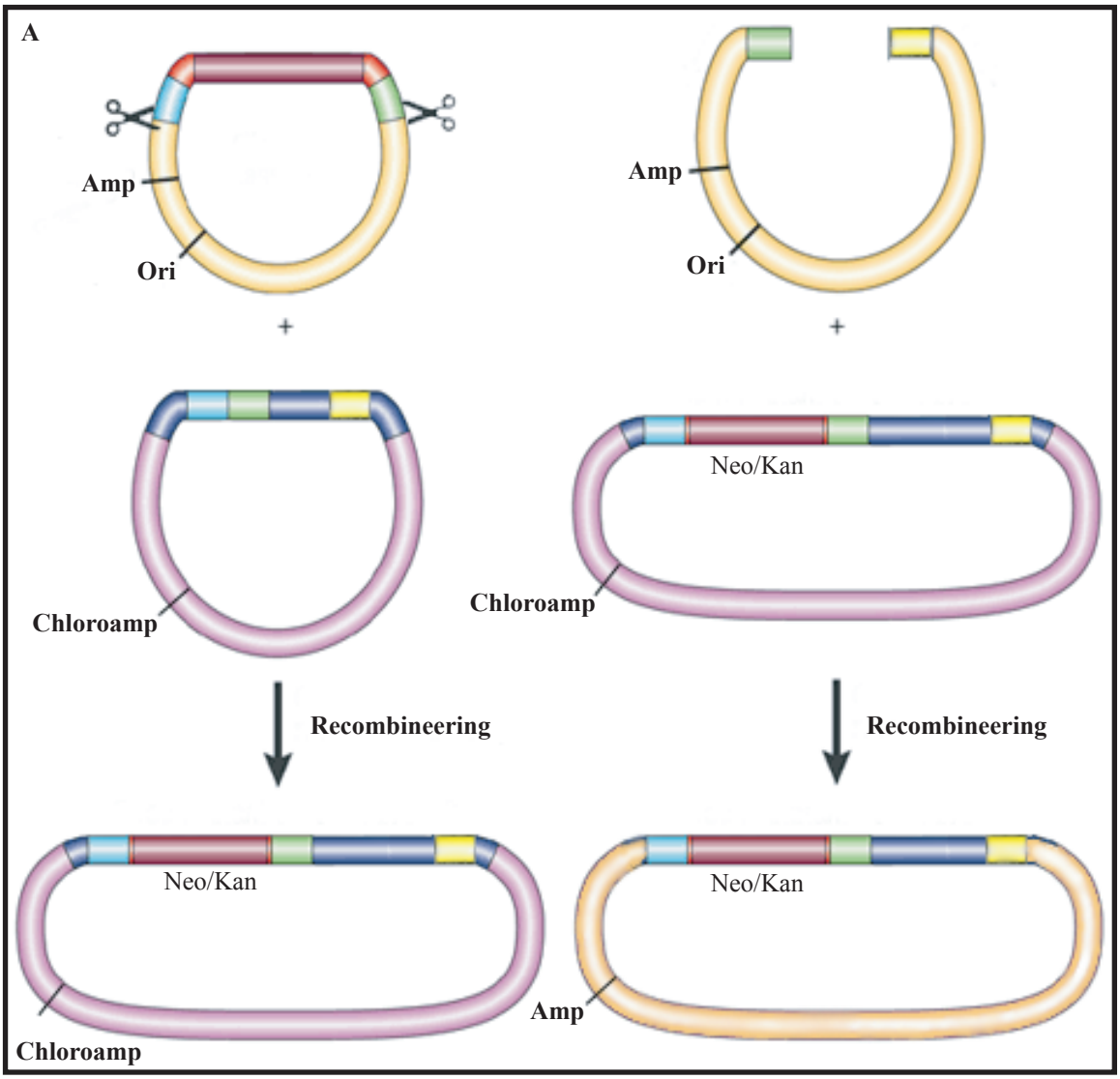

Figure 2.3 | Two-step recombineering of 9kb.P/Sox2-eYFP reporter construct. (A) Strategy. **(B)** I-SceI transgenic tadpole at 2-cell.

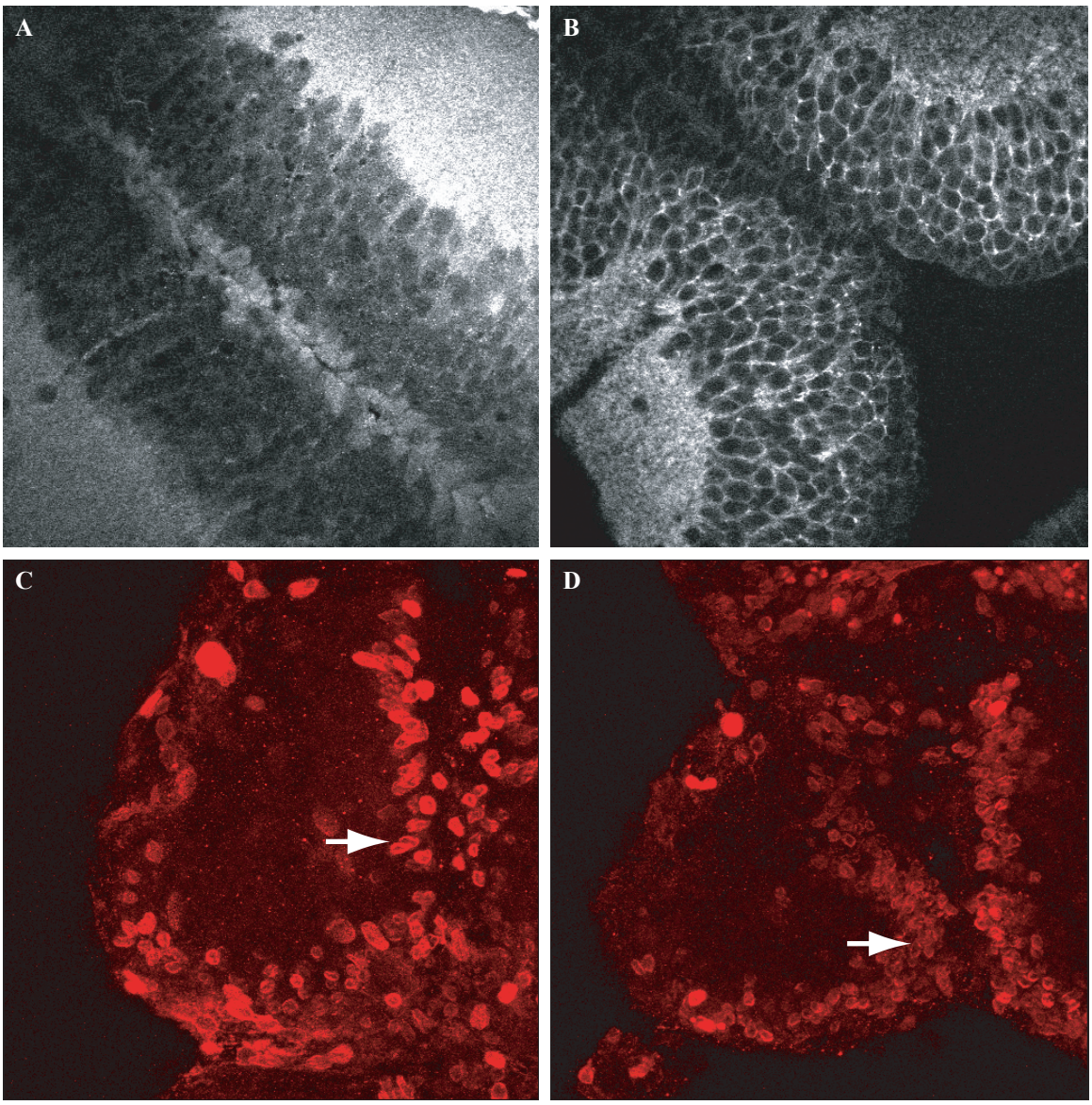

Figure 2.4 | Neural progenitor cell immunohistochemical staining. Stage 47/48 tadpoles were sacrificed, cryo-sectioned, and stained for endogenous proteins. **(A)** Rb-polyclonal anti-Human Sox2 antibody labels the cells in the proliferative zone. **(B)** Ms-monoclonal anti-PSA-NCAM antibody label complementary to the Sox2 labeling cells. **(C)** 2hr BrdU chase shows labeling of one pseudo-layer of cells in the proliferative zone. **(D)** 24hr BrdU chase shows expansion to 2-3 layers of cells indicative of proliferation over the 24hr period. Both BrdU images were 15microns in depth. Arrows indicate the location of cells which proliferated over the 24hr period.

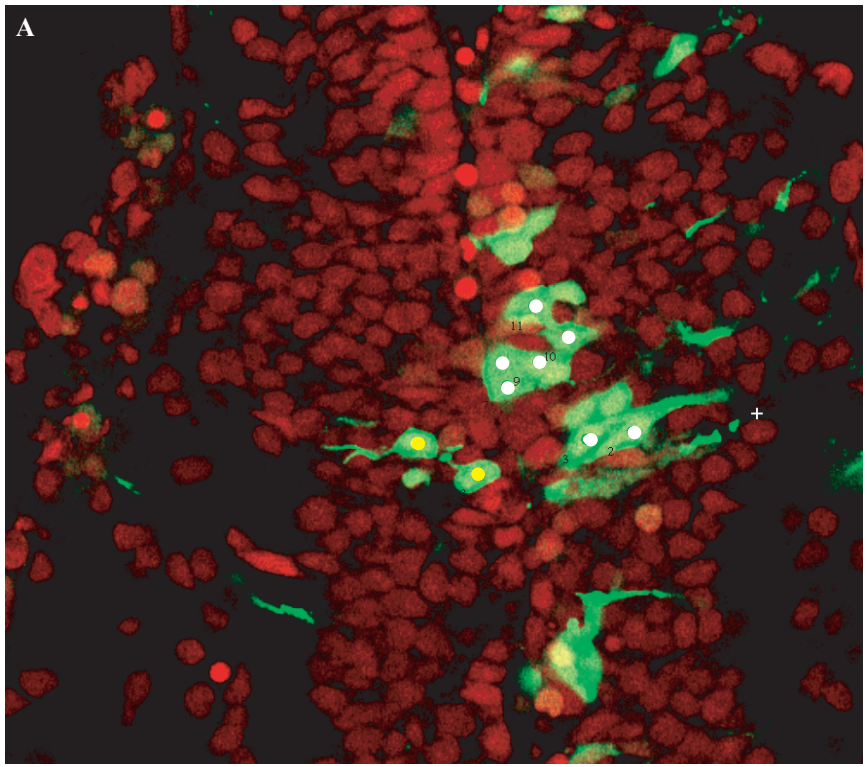

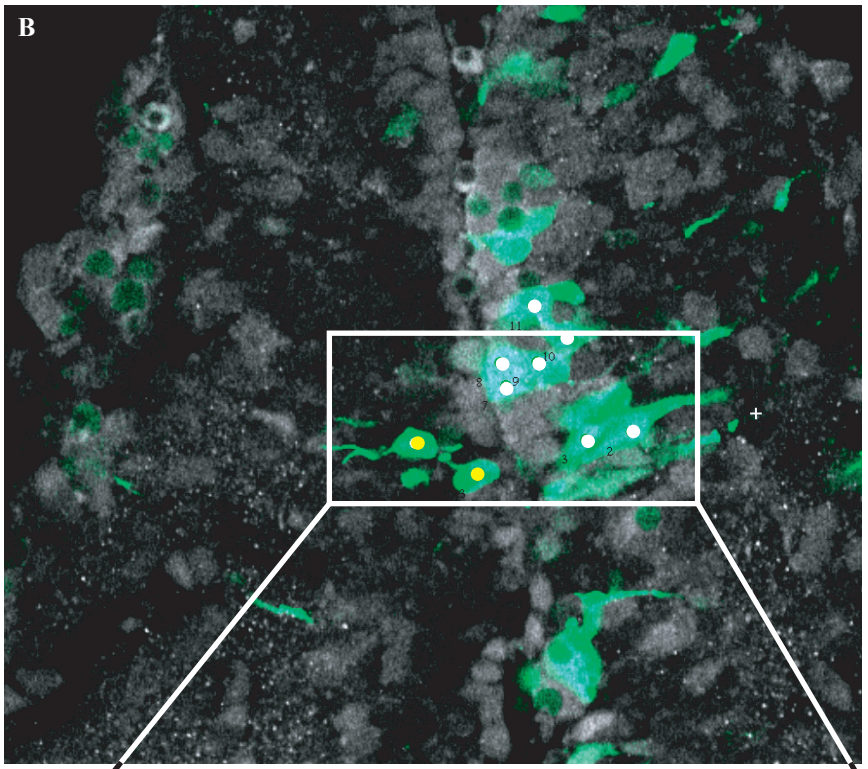

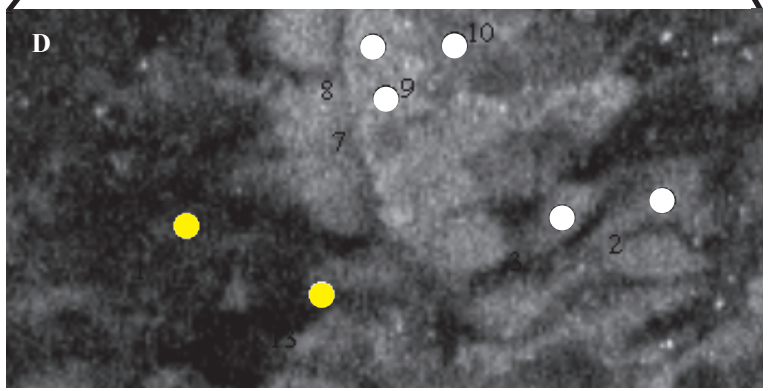

Experimental Condition	Post Transfection Day	% Colocalized	% Non-colocalized
eGFP	1	n/a	n/a
eGFP	2	62	38
eGFP	3	58	42
mFGF-eGFP	1	n/a	n/a
mFGF-eGFP	2	n/a	n/a
mFGF-eGFP	3	95	5
Sox2/Oct3-eGFP	1	90	10
Sox2/Oct3-eGFP	2	74	26
Sox2/Oct3-eGFP	3	22	78

Figure 2.5 | Sox2/Oct3.mFGF4-eGFP plasmid verification. Plasmid was transfected with electroporation and animals sacrificed at PTD1, 2, and 3. **(A)** Exogenous plasmid expression was imaged in the GFP channel (488nm) and over laid with PI (514nm) to locate the cell bodies. **(B)** GFP channel was overlaid with the Sox2 immunohistochemistry in Far-Red (633nm). Yellow dots indicated non-colocalization and white dots indicated colocalization. **(C)** Results of colocalization experiment. **(D)** In-set enlarged

Chapter 3 Microarray

3.1 Methods

The use of microarray experiments as a tool to gain a better understanding of the *X. laevis* model system is new to this lab. Much time was spent on experimental design and sample preparation, largely because the intent was to isolate an indentified cell type for the microarray experiments, minimize the number of cells per sample, and accurately and consistently amplify the small amount of available RNA. Even in the beginning, it was fairly apparent how a microarray experiment can encompass an entire thesis project on its own. What was accomplished in this thesis is by no means complete and it is hoped that what was learned during this thesis effort will provide a stepping stone to many more such experiments.

3.1.1 Isolation of a homogeneous pool of cells

The tectum of the *X. leavis* as described earlier is very heterogeneous; this is true for all animals and especially true during development. Preliminary microarray experiments which compared entire mid-brains containing the tectum and tegmentum of stage 43 and stage 48 tadpoles showed very few significant differences (Results 3.2.3) due to this heterogeneity. This prompted the need to use a homogenous pool of tissue. Several methods were considered, and they are described below in detail.

3.1.1.1 Panning for cells

The first technique considered for the harvest of a homogeneous pool of cells was panning as described in (Barres, Silverstein et al. 1988). This method required the identification of a suitable cell-surface marker. Such markers used in FACS of NSCs/NPCs from mammalian brain are LEX/SSEA-1 (Capela and Temple 2002; Capela and Temple 2006) and CD133 (Corti, Nizzardo et al. 2007). However, antibodies against these proteins did not cross-react with *X. laevis* tissue. Another strategy used in FACS is negative sorting (Pruszak, Sonntag et al. 2007). PSA-NCAM was a candidate for a negative sorting strategy since it is expressed by cells that appear to have migrated away from the proliferative zone as illustrated in the immunohistochemistry (Results 2.3.1); however this would not have assured a homogenous pool of cells with a common innate characteristic. Thus a strategy where an exogenously expressed cell surface protein driven by a cell-type specific promoter was planned to be employed after an initial negative panning step with PSA-NCAM.

GPI anchored Flag-GFP used as a proof of principle. This plasmid was a gift of Pranav Sharma. For the proof of principle experiments, this GPI anchored Flag-tagged GFP was driven by a CMV promoter. One day before the panning experiment, cells in the animals at stage 47/48 were transfected by WBE and a 100mm panning plate (Corning, Cat.#30167) was prepared by overnight incubation at 4°C with Rb-polyclonal anti-Flag antibody (Sigma, Cat.#F7425) diluted 1:1000 in Tris Buffered Saline (TBS: 50mM Trizma base, Sigma-Aldrich, Cat.#T6791; 150mN NaCl, Sigma-Alrich, Cat.#S7653; pH7.6 with HCl, Sigmal-Aldrich, Cat.#320331). On the day of the panning experiment, the panning dish was briefly washed with zero-divalent Steinberg's solution

(ZdSS: 58.18mM NaCl; 0.67mM KCl, Sigmal-Aldrich, Cat.#P9333; 4.62mN HEPES, Sigma-Alrich, Cat.#H7523; 0.40 EDTA, Sigma-Aldrich, Cat.#E1644; pH7.4 with NaOH, Sigma-Aldrich, Cat.#72068) 3 times and blocked with 0.5% NGS in ZdSS for 1hr at RT. In the meantime, 40 brains were dissected into ZdSS, incubated at RT for 15mins, and triturated with a fire-polished glass pipette. When the panning plate was ready, the blocking solution was removed; the dissociated cells were plated and incubated at RT for 1hr on a shaker set on low. The supernatant was removed and the panning plate was briefly washed with ZdSS 3 times for 5mins on the shaker. The plate filled with ZdSS and visually scanned for green expressing cells. None was to be found.

Trouble shooting the panning plate. The panning plate was thought to be the easiest to trouble shoot. First, serial dilutions of the anti-Flag antibody were plated (1:250 to 1:10,000 in TBS) using the same protocol above, but instead of using electroporated cells, secondary antibody goat anti-rabbit IgG-FITC (Chemicon; Cat.#AP307F) at a dilution of 1:1000 in TBS was used to visualize the plate. This simple experiment showed that the problem was in the panning plate preparation. Then, the protocol was modified; no shaking during the wash and blocking solution resulted in sufficient anti-Flag plating indicating that if agitation was to be used to aid in mixing steps, it must be done very gently if at all; however, the idea of Laser Capture Microdissection was pursued before other aspects of the panning protocol were optimized further.

3.1.1.2 Laser Capture Microdissection

After struggling to initiate the panning protocol, Laser Capture Microdissection (LCM) was considered. This method had one very desirable advantage: LCM allowed for the use of morphology to collect cells that are spatially related. Since, it is known that NPCs that take up BrdU were located lining the ventricular wall, it was possible to microdissect out those particular layers of cells. LCM was also appealing due to the fact that preliminary experiments by Pranav Sharma suggested differences in the pools of NPCs depending on their location in the tectum as described earlier.

The first step in preparing the brain for LCM is to section it into 3-15μm sections. Two methods could be used for this step: cryosections or paraffin sections. Since paraffin sections required some form of harsh aldehyde fixing prior to paraffin embedding, it was the least desirable (Scicchitano, Dalmas et al. 2006). Cryosections can be made either with flash-frozen tissue or with minimally fixed tissue. Fresh flash-frozen tissue was the most desirable because unlike fixing tissue where cellular components are chemically cross-linked and potentially damaged leading to poor totRNA yield, flash-freezing tissue preserved the integrity and quality of the totRNA best (Scicchitano, Dalmas et al. 2006; Peh, Lang et al. 2009). Both methods of cryo-sectioning were attempted as described in detail below.

Cryosections of PFA fixed brain tissue. Brains of tadpoles at stage 47/48 were dissected out after anesthetization with MS-222 and placed in 2% PFA in PB for 15mins at RT. Then they were washed clean of PFA 3 times for 10mins with PB and cryoprotected in 30% sucrose either for 1hr at RT and embedded in Cryo-OCT or in increasing concentrations of sucrose in PB: 5% for 30mins, 10% for 30mins, 15% for

30mins, 20% overnight and embedded in 1part Cryo-OCT and 1 part 20% sucrose (Barthel and Raymond 1990). The brains embedding in only Cryo-OCT were then cut at neg20° into 16µm and 20µm sections and the brains embedded in a Cryo-OCT/sucrose mixture were cut at -15° into 12µm and 16µm sections. After sectioning, all groups were subjected to Hematoxylin & Eosin (H&E), only Hematoxylin, or only Eosin staining (detailed below). The morphology of 16µm and 20µm sections appeared to be intact. The morphology of the 12µm sections was slightly disturbed with the presence of sectioning artifacts: cracking of the tissue perpendicular to the path of the sectioning knife. The 20µm sections with gave the best morphology (Figure 3.1) but considering thinner is better for LCM purposes; the thinner 16µm tissue was used for subsequent experiments. And, as far as which staining protocol was superior, Eosin-only staining showed the best outline of cell boundaries compared to the other staining methods. Microdissection of 16µm, Eosin-only stained tissue was carried out according to the Zeiss P.A.L.M. LCM manual and the captured tissue was RNA extracted as described below in (Methods 3.1.2.1).

Hematoxylin and eosin staining (H&E). RNase-free H&E kit (HistoGene LCM Frozen Section Staining Kit; Molecular Devices, Sunnyvale, CA, Cat.#KIT0401) was used to H&E stain the sections. Manufacturer's suggested protocol was followed with no changes. A modified protocol recommended by the NIH Laser Capture Microdissection Core Laboratory was used for Hematoxylin-only and Eosin-only. For Hematoxylin-only: 70% Ethanol for 1min, wash in RNase-Free water (Invitrogen, Cat.#10977-023) for 15secs, Meyers Hematoxylin stain (Sigma-Aldrich, Cat.#MHS16), wash 15secs, 1xAutomation Buffer (GeneTex, Irvine, CA, Cat.#GTX73344) for 15secs, 70% ethanol for 1min, 95% ethanol for 1min times 2, and Xylene for 1min times 2. For Eosin-only, 70% Ethanol for 1min, wash for 15secs, 1xAutomation Buffer for 15secs, 70% ethanol for 1min, 95% ethanol for 1min, Eosin stain (Sigma-Aldrich, Cat.#E4382), 95% ethanol for 1min times 2, and Xylene for 1min 2 times.

Cryosections of flash-frozen tissue. RNA extraction experiments (Methods 3.1.2.1) show that even with light PFA fixing RNA quality checked by NanoDrop was less than desirable. Therefore, flash frozen tissue sections were attempted. Tadpole brains were dissected out after anesthetization with MS-222. They were either quickly embedded Cryo-OCT in a Tissue Tek Cryomold (Sakura, Torrance, CA, Cat.#4565) or cryoprotected by incubation in an increasing concentrations of sucrose in PB (5%, 10%, 20%, 30% and 50% on ice) for 15min each and then placed in OCT as described above. The mold was placed on dry ice in a Styrofoam container with a lid; the molds are completely frozen within 30secs. Then the flash frozen brains were sectioned using Cryo-OCT into 16µm sections and H&E stained using HistoGene kit. Both methods produced sections which sustained extreme damage from ice crystal artifacts (Figure 3.1); the difficulty of the flash- freezing protocol may be due the aqueous nature of the young tadpole brain. The use of glycerol in DMSO was suggested by (Rosene, Roy et al. 1986) as well as used of high osmotic pressure during sucrose based cryoprotection (Palluault, Slomianny et al. 1992) but neither methods were attempted due the their late discovery; they may be worth investigating in the future if LCM is attempted again.

Cryosections of alcohol fixed tissue. A lighter alcohol fixing protocol was attempted instead. A modified methacarn solution (8 parts Methanol and 1 part Glacial Acetic Acid) as suggested by (Cox, Schray et al. 2006) was used for a 15min fix followed by cryoprotection with 30% sucrose in PB and sectioning as described above. Then the sections were H&E stained and visualized under the LCM microscope. Again, this was a truncated exercise because the sections appeared no better than the flash frozen sections.

Miscellaneous methods using RNA-Later. Other methods were attempted including the use of RNA-Later (Ambion, Cat.#AM7020). RNA-Later was used prior to PFA fixing in an attempt to preserve the RNA in the tissue, but it did not compare to fresh frozen tissue. RNA-Later did not help preserve morphology in fresh tissue confirming the manufacturer's warning that RNA-Later is not a preservative.

3.1.1.3 Hand-picking cells

After months of struggling with tissue preparation for LCM, hand-picking of cells was attempted as a last resort, and it is the method that triumphed in the end; however, it was not without its own trials and tribulations. The final protocol is described below.

Tissue dissociation. Animals were anesthetized in MS-222 and their mid-brains were dissected out and placed in a 1.5ml microtube containing 270µl of amphibian phosphate buffered saline (APBS) with 0.1% EDTA (Sigma, Cat.#E6635) as described in http://www.urmc.rochester.edu/SMD/mbi/xenopus/Protocols/TissueCultureReagents.pdf. APBS is composed of 113mM sodium chloride (Sigma, Cat.#S7653), 8mM sodium phosphate dibasic (Sigma, Cat.#S5136), 1.5mM potassium phosphate monobasic (Sigma, Cat.#P8416), and pH7.7 with sodium hydroxide (Sigma, Cat.#72068) until all 5-10 brains are dissected. Then 30µl of 2.5% Trypsin-EDTA (Invitrogen, Cat.#15090-046) added to the APBS resulting in the final working concentration of 0.25% Trypsin-EDTA. The brains were incubated undisturbed at RT for 15mins and the reaction was inactivated with 1x the reaction volume (300µl) of Defined Trypsin Inhibitor (Invitrogen, Cat.#R007100). The brains were gently triturated with a large bore fire-polished glass Pasteur pipette and transferred into a 15ml Falcon tube containing the cell-picking medium which contains 4 parts L15-Leibovitz medium (Invitrogen, Cat.#11415-064), 5 parts APBS, and 1 part 10% Bovine Calf Serum (Invitrogen, Cat.#16010167) in a total volume of 10mls. The brains were let to rest for 15mins on ice and then using a smaller bore fire-polished glass Pasteur pipette, they were triturated again. The dissociated cell mixture was plated onto 3 wells of a 4-well rectangular plate (Nunc, Cat.#267060); the last well was filled with just cell-picking medium to act as a cell washing station. Once the cells were plated, they were allowed to settle in the plate on top of the microscope stage for 15mins. A timer was set for 90mins just prior to the addition of Trypsin to indicate the end of the cell-picking session.

Glass pipette pulling. Cell-picking pipette were made according to the Sutter P-1000 and P-97 Pipette Cookbook, http://www.sutter.com/contact/faqs/pipette_cookbook.pdf, for large diameter tipped needles. 1mm thick walled glass pipettes (World Precision Instruments, Sarasota, FL, Cat.#1B100-4) were pulled with the following parameters: Heat at Ramp +25, Pull at 0, Velocity at 140, Time at 100, and Pressure at 200. Slight

changes were made to the ramp and velocity until a desirable taper was achieved. The pipettes were broken with the glass-on-glass technique at the natural breaking point to make a tip with ~50μm orifice. If the glass-on-glass technique is done properly, it results in an orifice with a relatively smooth cut edge; however, if a smooth edge is not obtained, it is recommended to use a pipette beveller to smooth the edges which reduces cell membrane shearing during aspiration. All these techniques are described in detail with corresponding images in the cookbook.

Microscope set-up. The Zeiss Axiovert 200 inverted microscope was used to visualize the cells. The condenser was taken off to accommodate the micromanipulator and pipette holder. The micromanipulator was a 3-axis hydraulic micromanipulator (Narishige, East Meadow, NY, Cat.#MO-202U) attached to course manipulator (Narishige, Cat.#MMN-1) mounted on a bracket designed for the Zeiss Axiovert 200 (Narishige, Cat.#NZ-19 with NR2). A microinjector set (Narishige, Cat.#IM-9B) was used to hold to cell-picking pipette and aspirate/inject cells.

Experiments. Cells at stage 47 were transfected by WBE with Sox2/Oct3.mFGF4-Gal4VP16-14xUAS.mFGF4-TurboGFP-NLS (JLO#100) plasmid at a concentration of 2μg/μl; when morpholinos were used, the morpholino concentration was at 0.5μM. 24hrs (PTD1) or 5days (PTD5) later ~8 brains were dissected, dissociated, and plated. Glass pipettes used for aspirating cells were filled almost to the top of the pipette with cell-picking medium then loaded onto an oil-filled microinjector syringe. The pipette was not filled to the top to allow for a very tiny air bubble which helped in the visualization of the media-oil interface; cell contact with the oil was avoided because it made it difficult to separate the cells from the oil. The pipette tip was positioned in the middle of the field of vision and lowered so that the tip is about 0.5mM above the bottom of the dish with the course manipulator and the well was scanned by moving the stage. Once a green fluorescent protein expressing cell was located, it was positioned below the pipette tip. The micromanipulator was used to lower the pipette tip directly above the cell of interest and the microinjector was used to aspirate the cell into the pipette. When ~25 cells were aspirated into the pipette, the pipette was elevated, and the stage was moved so that the cleaning well is in the field of vision. Then the pipette was lowered again so that the tip was 0.5mM above the bottom of the well and the cells were gently ejected out of the pipette. And the cell-picking process was repeated until the timer set at 90mins ended. The pipette was reloaded with fresh cell-picking medium and all the cells in the cleaning well, 100-200 in total, were aspirated into the clean pipette. If morpholinos were used, the red filter was used to confirm morpholino content before aspiration at this time. Then the pipette holder was removed from its holder on the micromanipulator, the pipette tip was placed in the bottom of an RNase/DNase-Free 1.5ml microtube by hand, and the cells were ejected into the tube. Pipette tip breakage was not an issue because the RNA purification protocol used a column which eventually filtered out the glass from the sample. Then the cells were spun down at 1000g in a microcentrifuge, and as much of the medium were removed as carefully as possible as not to disturbed the cells at the bottom. The green cells at the bottom of the tube were visualized using the epiflourecence on the microscope before 15μl of Extraction Buffer (EB of PicoPure Kit) was added to it. Finally, the buffer and cells were mixed well by flicking the tube by hand before spinning

down briefly and incubated at 42°C for 30mins. At this point, the cells can be stored at -80°C until the rest of the RNA isolation protocol could be performed in tandem with rest of the cell samples; the PicoPure kit was used for the RNA isolation step.

3.1.2 RNA target handling

Target handling introduces the most variation to microarray experiments. Currently commercially available amplification kits are consistent enough that there is very little variation between amplification reactions; however, because of the variability in column performance, many commercially available kits for extraction of RNA result in very different amplification results. Additionally, when handling picograms of material which is then amplified 100million-fold or more, it is only logical that any variation in starting material will translate into great changes in the end product.

3.1.2.1 Extraction of RNA

Two commercially available kits were tried and the one that was column-based was preferred because if its ease of use. The first kit was the Epicentre Biotechnologies ArrayPure Nano-scale RNA Extraction Kit (Epicentre, Madison, WI, Cat.#MPS04050) and the other was the Molecular Devices PicoPure RNA Isolation Kit (Molecular Devices, Cat.#KIT0204); both kits avoid using the organic solvents used in traditional Trizol and phenol-chloroform RNA extractions.

Epicentre ArrayPure. The protocol in this kit was similar the traditional method of Trizol RNA extraction except it used a proprietary lysis solution and a proprietary protein precipitation solution which avoided the use of the phenol-chloroform. Once the cells were lysed, the proteins were precipitated, spun down, and discarded. The RNA was then precipitated with isopropanol, spun down, dried, and resuspended; there was no column. The drawback to this kit was that the pellet was not visible making it very difficult to not aspirate the pellet while removing the excess supernatant.

Molecular Devices PicoPure. This was a column-based kit and like all column matrixes, the performance was most variable for the very small molecules and the very large molecules. However, the advantage of this kit was in its simplicity of use: lyse, load, wash, dry, and elute. The step that was most critical was the drying step; if the column was not dried properly, solvents were introduced into the sample. They would then disrupt the initial steps of the amplification reaction and result in a low amplified product yield. This was the kit that was used for these array experiments. As a final note, purified totRNA quality slowly deteriorates over time even at the recommended -80°C and does not sustain freeze-thaw very well; thus, multiple freeze-thaw cycles should be avoided if possible. It is best practice to move on to the amplification protocol on the same day as the isolation step.

3.1.2.2 Amplification of RNA

There were several commercially available RNA amplification kits which claimed a final yield of micrograms of aRNA from picograms of totRNA; however, the claims were based on optimally clean totRNA for such published yields which was not the case at hand.

Molecular Devices RiboAmp HS Plus. The decision to use this kit (Molecular Devices, Cat.#KIT0515B) was based on the familiarity of the brand name and its claim of generating micrograms of amplified RNA (aRNA) sufficient for a standard format GeneChip from 100-500pg of totRNA. This kit uses 2 rounds of in vitro transcription and is based on the Eberwine method. The first experiment was a set of 4 mid-brains; they were dissected out and place in 100µl of EB and the protocol for cell pellets in the PicoPure manual was followed. Two dilutions of each sample were used for the amplification protocol: 5ng (RiboAmp.1dilA-4dilA) was the maximum input (recommended: 500pg-5ng) and 200pg (RiboAmp.1dilB-4dilB) was near the validated low input (absolute low: 100pg). Then the product protocol for RiboAmp HS was followed exactly and 4 of the 8 amplifications were hybridized onto GeneChip *X. laevis* Genome 1.0 arrays (Results 3.2.1, Affymetrix, Cat.#900492) using RiboAmp HS suggested protocol for GeneChips; amplified RNA was analyzed with the Agilent Bioanalyzer to assure quality. These GeneChips were run by Wen Wen Lin a former member of the Tim Tully laboratory. Another trial using 500pg of input also yielded sufficient aRNA for microarray experiments, but as the results of the preliminary experiments showed the fault of this kit is in its inconsistency (Results 3.2.1).

Epicentre TargetAmp 2-round Biotin Kit 3.0. The decision to use this kit was based on personal searches on Google for small input amplification kits. Epicentre's claim of 8µg of amplified RNA from 50pg was superior to the RiboAmp Kit. It uses the same type of protocol as the Molecular Devices TargetAmp kit. This kit (Epicentre, Cat.#TAB2R71024) was tried three times without success. The first trial used the recommended minimum and recommended maximum input amounts of 50pg and 500pg of totRNA from previously isolated RNA used for the RiboAmp HS reaction. The second trial used newly isolated RNA. The last trial used two positive controls sent to me from Fred and Hank of TargetAmp technical resources: Human totRNA and Hela totRNA. Neither positive controls used at the maximum input amount resulted in adequate amplification. The fault of this kit was likely in the very small reaction volumes of 5-10µl. I postulated that because of the small volumes used in this kit, any changes in volume due to evaporation during incubation would result in deleterious reaction conditions.

NuGEN WT-Ovation Pico Kit. The amplification kit that was finally settled upon was the NuGEN kit (NuGEN, Cat.#3300); at that time there was a choice of using the Ambion/Applied Biosystems MessageAmp II or the NuGEN kit. Ambion is a known name in RNA handling and both its RNAqueous Micro Kits, another column-based purification kit, and its MessageAmp II kits were highly recommended for processing picograms of RNA target (Chris John, Microarray Core Facility at Cold Spring Harbor Laboratory); however, the NuGEN kit was more appealing for two reasons: it was based on a newer RNA amplification technique that did not require two rounds of *in vitro* transcription as in the previous two kits and it was the kit preferred by Chris Johns, the Cold Spring Harbor Core Microarray Facility manager for picograms of RNA. The manufacturer recommended protocol was followed exactly with two modifications. The first modification was the use of 100% ethanol when 80% ethanol was called for during the cleaning steps. The second modification was in the last purification step. It called for

the recombining of reactions that had been previously divided into two; this was not done. The two reactions were kept separate because the recommended Zymo-columns often overloaded and clogged giving reduced yield. As a result, the final product needed SpeedVac-ing to reduce its volume in preparation for the labeling step.

The NuGEN labeling kit was also used: FL-Ovation cDNA Biotin Module V2 (NuGEN, Cat.#4200). This labeling kit uses a proprietary labeling technique which claims to produce a higher percentage of labeled fragments than the traditional *in vitro* transcription labeling with biotinylated nucleotides. The protocol first calls for fragmentation of the amplified cDNA (a-cDNA) and then labeling of the fragments. Because, a larger percentage of fragments were labeled using this kit, less target input was needed: standard format GeneChips required 15-18µg of aRNA but using WT-Ovation and FL-Ovation, only 4-5µg of amplified cDNA was required for comparable signal.

Two preliminary experiments using the NuGEN kit were performed using GeneChip *X. laevis* Genome 1.0 arrays. The first preliminary experiment was just a proof of principle experiment using stage 48 brains: 1 sample was totRNA isolated from 1 brain each and the other sample was totRNA isolated from pool of 4 brains. The isolated totRNA was quantified using the Nanodrop and the quality of checked by Agilent Bioanalyzer. The input for all four samples was 500pg (NuGEN1.1-4) and the results of the microarray are discussed in (Results 3.2.2). The second preliminary microarray experiment was performed using the recommended maximum of 5ng (NuGEN2.1dilA-4dilA) and the recommended minimum of 500pg (NuGEN2.1dilB-4dilB). Two brains of stage 43 (NuGEN2.1dilA/B and 2.2dilA/B) and two brains of stage 48 (NuGEN2.3dilA/B and 2.4dilA/B) were used resulting in a total of eight samples. The results of these experiments are discussed in (Results 3.2.3). Both experiments using NuGEN kits used the NuGEN suggested protocol for hybridization of GeneChips; the Affymetrics suggested protocol was used to wash and scan the chips. Chris John and members of the CSHL Microarray Core Facility assisted in the wash and scan of the chips for both the above discussed experiments.

It is worth noting that a new kit from NuGEN called WT-Ovation One Direct RNA Kit was released just as the amplification step for my experiments was beginning. This kit is superior in that the RNA extraction step is an *in situ* one-step process which does not require alcohol precipitation or the use of a column; this translates to less variation in the RNA isolation step. It also claims sufficient amplification of 10pg of input or 1 cell for a standard format array which require 5µg of amplified product. There was no time to trouble shoot a new kit, thus the old tried and true kit was used; however, it would benefit subsequent microarray experiments to try this new kit because the fewer cells that need to be picked means less time it will take to pick them and less opportunity for contamination from unwanted cells. Additionally, biological replicates would be possible because sufficient number of cells could be picked from one tadpole brain which would make the microarray comparisons more statistically powerful.

3.1.2.3 RNA quality control

Two methods were used to access the quality of the totRNA inputs and the amplified RNA product. The website http://biomedicalgenomics.org/RNA_quality_control.html shows a very comprehensive tutorial on how the access the quality of RNA on both the Nanodrop UV-spectrometer and the Agilent Bioanalyzer.

Nanodrop UV-spectrometer. NanoDrop® ND-1000 UV-Vis Spectrophotometer enables remarkably accurate analyses of extremely small samples with high reproducibility. This technology is an improvement from the older UV-spectrometers because it only requires 1-1.5µl of sample. The output of the spectrometer trace denotes the concentration as well as hints at the quality of RNA. The accuracy range is suggested between 0.3ng/µl to 4300ng/µl. Although, experiments with repeated measurements of the same sample below 1ng/µl showed a great variation in the readings suggesting that concentrations below 1ng/µl are not accurate.

Agilent Bioanalyzer. The Agilent Bioanalyzer is a Lab-on-Chip technology that can analyze DNA and RNA. It is an advanced version of gel electrophoresis. It is still cheaper to run gels the old fashion way if you have many micrograms of sample; however, the Agilent Bioanalyzer becomes the preferred method of RNA analysis if you have picograms to nanograms of very precious sample. In the case of microarrays, it was used to analyze input totRNA as well as analyze amplified product. Some of the microarray experiments performed in this thesis used this technology to check RNA quality before or after amplification. The manufacturer protocol was followed exactly for both the RNA Pico kit (Agilent Technologies, Santa Clara, CA, Cat.#5067-1513) and RNA Nano kit (Agilent, Cat.#5067-1511).

3.1.3 Microarray experiments using Sox2/Oct3 plasmid

The plasmid used for the final set of microarray experiments was Sox2/Oct3.mFGF4-Gal4VP15-14xUAS.mFGF4-TurboGFP-NLS (JLO#100). The first microarray experiment was used to validate the construct. The second and final experiment was used to find candidate genes for morpholino design; the morpholinos were used in the imaging experiments of this thesis.

3.1.3.1 Microarray validation of plasmid specificity

Tadpoles at stage 47/48 were transfected by WBE with JLO#100 and processed as above (Methods 3.1.1.3). Twelve rounds of picking over two days were performed for each condition, PTD1 and PTD5. For each condition, all twelve rounds were pooled together, extracted in one column, and eluded in 20µl. The concentration of the two samples was determined using the NanoDrop analyzer. Approximately 5ng was used for each reaction; 6 reactions for each condition were amplified. All amplified cDNA for each condition were pooled together and 3 GeneChip *X. laevis* Genome 1.0 arrays were run. This resulted in 3 technical replicates at the level of chip hybridization and reading for each of the two conditions; cartoon of work flow is depicted in (Figure 3.2) as Preliminary Method. This experiment was performed with the assistance of Chris Johns at the CSHL Core Microarray Facility. The results of this experiment are discussed in (Results 3.2.4) and referred to as PreND1vPreND5.

3.1.3.2 Final experimental treatments rational

The rational for the experimental conditions of the final microarray experiment was based on several factors. Consideration of controls, results of preliminary experiments of Pranav Sharma, and personal interests in a single gene all played into the design of this experiment. A total of six comparisons were made in the final microarray experiment.

Table 3.1 | List of microarray comparisons executed in the final microarray experiment.

Comparison	Rational for comparison	Conditions
ND1vND5	NPCs verse Differentiated Neurons	Normal 12/12 light-dark cycle
ND1vSMC	NPCs at Early Stage 48 verse NPCs at Late Stage 48	Normal 12/12 light-dark cycle
DD1vLD1	Proliferative NPCs verses Differentiating NPCs	**Dark:** Light deprived after WBE **Light:** Light enhanced with flashing LEDs during 12hrs light and normal 12hrs dark
DD5vLD5	Proliferative NPCs verses Differentiated Neurons	
CPG12vCMo12	Early genes affected by functional CPG15 knockdown	12hrs of CPG15 functional knockdown
CPG24vCMo24	Later genes affected by functional CPG15 knockdown	24hrs of CPG15 functional knockdown

NPCs verses Neurons. This comparison was the initial impetus for the microarray experiments. A molecular characterization of NPCs of *X. laevis* tectum had not been conducted until now. Microarray analysis was used as a non-hypothesis driven experiment to broadly scan the entire genome for transcripts expressed in NPCs. Since the cells expressing Sox2/Oct3.mFGF4 driven eGFP has been shown to decrease in colocalization with endogenous Sox2 protein and show more neuronal morphology by PTD3 (Results 2.3.2), I postulated that PTD5 FP positive cells would be neurons. Thus, the comparison between PTD1 and PTD5 was designed to compare transcripts in NPCs and differentiated neurons. Additionally, a stage matched control (SMC) comparison was performed to test whether PTD1 and PTD5 cells were different because of differentiation and not simply different because of the 5 days of development that occurred between the harvest periods.

Visually-deprived verses visually-experienced animals. Preliminary data from the Cline laboratory suggest that visually-deprived animals were shown to have significantly more NPC proliferation compared to animals with visual experience as detected by double XdU incorporation studies mentioned earlier (Section 1.3.2.2). This suggested that visual activity may promote NPC differentiation, thus it would appear that visual experience decreased XdU incorporation. One interpretation is that NPCs remain proliferative in visually-deprived animals because they lack the signals to trigger the

switch to the differentiated state. This suggests that the proliferative state is a 'default' state. The intent of microarray comparison of visually-deprived verses visually-experienced animals was to find genes that promote or restrict the switch between proliferation and differentiation.

CPG15 verses Control CPG15. Morpholinos against CPG15 were used for a set of experiments because CPG15 has many interesting roles in brain development: its expression is increased by activity and light deprivation, acts as a tropic factor for cortical NPCs, and aids in differentiation of PC12 cells. The comparison between NPCs exposed to CPG15 morpholinos and control-CPG15 morpholinos was intended to identify genes that may be involved in CPG15 signaling pathway concerning NPC survival.

3.1.3.3 Final microarray experiments

Many details for the experimental protocol of the final microarray experiment were the culmination of all that was learned from the preliminary experiments; however, there are still avenues for optimization for subsequent microarray experiments.

Final cell harvesting protocol. Weekly batches of animals (~200 tadpoles) were divided into two groups: one set was grown at 24°C while the other set was grown at 16°C until their development was 1day delayed at which time they were placed at 24°C so that 2 sets of animals could be processed in a week. It took one full week of harvesting of cells for one condition. First ~100 tadpoles grown at 24°C were transfected by WBE; then ~50 were used for the PTD1 harvest and ~50 were used for the PTD5 harvests. The next day after the beginning of the first set, ~100 tadpoles grown in the combination of 16°C and 24°C were transfected by WBE so that the harvesting sessions were staggered by a day.

For Normal PTD1 (ND1) and Normal PTD5 (ND5), animals were grown in 12/12 light-dark cycle. For visually-deprived animals (called Dark PTD1 or DD1 and Dark PTD5 or DD5), tadpoles were grown in normal 12/12 light-dark cycles until stage 47 when they were transfected by WBE and wrapped in aluminum foil until harvest at PTD1 and PTD5. For visually-stimulated animals (called Light PTD1 or LD1 and Light PTD5 or LD5), the tadpoles were grown in normal 12/12 light-dark cycles until stage 47 when they were transfected by WBE and placed in the chamber with rows of flashing green LED lights on top called the light-box. The LEDs were set to turn on and off at 1 Hz during the 12hr light-cycle and turn off during the 12hr dark-cycle. For the CPG15 morpholino (called CPG) and CPG15 control morpholino (called CMo), stage 47 tadpoles were transfected by WBE with both the lissamine-tagged (red) morpholino and the Sox2/Oct.mFGF4 plasmid (JLO#100) at the same time. Tadpoles for the CPG15 set were grown in normal 12/12 light-dark cycle and harvested at PT12hrs (CPG12 and CMo12) and PTD1 (CPG24 and CMo24). Harvest of PTD5 of CPG15 morpholino was not possible because no FP positive cells with red-lissamine tagged CPG15 morpholino could be recovered at PTD5, suggesting that knockdown of CPG15 killed the cells. Finally, for the SMCs, tadpoles were grown at 12/12 light-dark cycle and were transfected by WBE 24hrs prior to what would have been PTD5 harvest day for the other sets.

Final target handling protocol. Animals at stage 47 were prepared and harvested as described in (Methods 3.1.1.3). Twelve rounds of picking over two days were performed for each condition. All twelve rounds were pooled together before column purification and divided into 5 equal volumes. Then 5 columns were processed separately and carried through till the end of the microarray experiment for each condition. This was done because the columns offered the most variation and thus the most statistical power. Each column was eluded twice using 11µl of eluent, EB; many modified protocols for column elution suggested that eluding the column twice increased yield and consistency of product; this resulted in ~20µl of totRNA. Then without analyzing its concentration, 5µl of extracted totRNA was used in the amplification reaction. Input was calculated to be totRNA from ~100cells. The input was not measured for RNA concentration because the NanoDrop and the Agilent Bioanalyzer PicoChip were not accurate for such low concentrations. And, SpeedVac-ing of the eluate was not done because a previous trial of concentrating eluate from the column also resulted in a high concentration of contaminants that hindered the amplification reaction. Amplification was performed as described in (Methods 3.1.2.2). The amplified products were hybridized to the new *X. laevis* GeneChip 2.0 (Affymetrix, Cat.#901216) according the NuGEN FL-Ovation protocol manual. The work flow is depicted in (Figure 3.2) as Final Method. The washing and reading of the chips were according to Affymetrix suggested protocol; this was done with the assistance of Mohana Gudurvalmiki of the Cline laboratory and Jerry Lee of Dark Neuroscience, Inc.

3.1.4 Microarray analysis

There were six datasets resulting from the six comparisons detailed above. There were two parts to the microarray analysis. One part was analyzing the results of the chips themselves; this included the algorithms to normalize the probe signal to the statistical analysis performed to create the six datasets of differentially regulated genes. The other part involved data mining the six resultant very large datasets to assemble a tractable list of candidate genes to be tested further using an imaging protocol.

3.1.4.1 Chip analysis

The .CEL extension files of the each chip which contain all the signal information on each of the probes will be referred to as the chip dataset. The first-pass quality control experiments on the first three preliminary experiments were done by Affymetrix GCOS software. The software outputs an image of all the signals on the chips, background-noise to signal values, percent present/absent/marginal calls, and the presence/absence of housekeeping genes and spike controls. The image of the signals shows whether or not the probes equally hybridized over the entire chip. The background/noise and signal values indicated the strength of the probe signals over noise. The percent present/absent/marginal call values is qualitative; generally speaking a value of 50% or higher is preferred, but this is not a hard and fast rule. Finally, the housekeeping genes and spike controls indicated the quality of the hybridization.

Some of the CEL-files were analyzed by AffyQC to evaluate the quality of hybridization for individual chips. Briefly, the linear model, fitPLM (R package), was

applied and beta weights for each probe were plotted back onto the two dimensional chip surface. This method would reveal edge effects, bubbles, splotches, etc. Chips with severe features were excluded from analysis.

The analysis of the chip dataset obtained from the Sox2 PreND1vPreND5 experiment and the final experiment was done using an analysis program developed by DART Neuroscience. Briefly, RMA (Irizarry, Ooi et al. 2003) was applied with standard defaults to derive gene expression values. Gene expression values then were subjected to a BoxCox transformation to make residuals (error variance) across biological replicates more normal and homogeneous. Finally, a bootstrapping method was used to derive p values for treatment effects on a gene by gene basis. The datasets created contained those genes whose significance had a p-value of <0.01 and will be referred to as raw datasets.

3.1.4.2 Microarray data analysis

The datasets from each of the comparisons ranged in numbers and could include 1000's of differentially regulated genes. A program called JMP was used to filter down the data into a more manageable set. JMP was used to combine datasets according to user-set criteria. For example, you can ask the program to identify significant genes in one dataset that are also significant in another dataset. By combining datasets in this fashion, it mathematically reduced the false positive rate; a true reduction of the false positive rate would require independent replication of the experiment. Because the criteria used to compare and combine the datasets are determined by the user, it is heavily biased by any assumptions made by the user, as will be discussed below. Presented here are the comparisons that yielded some of the candidate genes and the rationale behind the comparisons. The term filtered dataset will be used for JMP datasets as well as other automated methods used to "filter" the raw datasets.

ND1vND5 and DD1vLD1. The JMP program was used to identify significantly differentially regulated genes in the ND1vND5 raw dataset with a p-value <0.01, which were also significantly differentially regulated in the DD1vLD1 raw dataset with a p-value <0.01 and only display the genes that were regulated in the same direction; meaning, that the genes were up-regulated or down-regulated in both the raw datasets. The rationale for this exercise was based on the assumption that ND1 FP-expressing cells were cells that were more likely to be bonafide NPC than the PTD5 FP-expressing cells and DD1 FP–expressing cells were cells that were more likely to be actively proliferative than the LD1 FP-expressing cells. Therefore, the genes that were differentially regulated in the same direction in ND1vND5 and DD1vLD1 should be the differentially expressed genes that were more likely to regulate proliferation of NPCs. This method of comparison results in a virtual p-value of $<0.01^2$ or <0.0001.

ND1vND5 and DD5vLD5 same. The JMP program was used to identify differentially regulated genes with a p-value <0.01 in these 2 datasets. The rationale of this comparison was also to select for transcripts that may maintain NPCs in a proliferative state. In addition to the assumption about the comparison of ND1vND5 mentioned above, we assumed that FP-expressing cells in DD5 animals would be more likely to be immature or proliferative than the FP-expressing cells in the LD5 samples.

The genes identified by this comparison may be biased toward more long-term activity-dependent transcripts while the first comparison may be biased toward more immediate activity-dependent transcripts.

ND1vND5 and ND1vSMC same. Again, a similar user criterion as above two was set between ND1vND5 and ND1vSMC and the raw datasets used for this comparison were differentially regulated genes with p-value <0.01. Here, we assumed that late stage 48 NPCs have less proliferative capacity than early stage 48 NPC, based on previous XdU incorporation data by Pranav Sharma at stage 48. Accordingly, the ND1vSMC dataset was used to conjunction with ND1vND5 dataset to identify genes that may be involved in maintaining the proliferative activity of stem cells, or maintaining 'stemness'.

DD5vLD5 and CPG24vCMo24 opposite. The user set criterion for this set was unique in that we used JMP to identify differentially expressed genes in the DD5vLD5 and CPG24vCMo24 raw datasets with p-values <0.01 which were regulated in opposite directions; meaning that the a gene was up-regulated in one raw dataset but down-regulated in the other. The assumption made in this comparison was any activity dependent gene showing regulation in one direction should be regulated in the opposite direction if CPG15 is knocked down with the morpholino. In this way, genes that were up or down regulated by CPG15 may be revealed by this comparison. A similar comparison of oppositely regulated transcripts in CPG12vCMo12 and DD1vLD1 might be expected to identify immediate early gene candidates required for survival of active NPCs.

DD1vLD1 not ND1vSMC. This was another unique method to compare the raw datasets. We set the JMP criteria to filter out significantly regulated genes in the DD1vLD1 in the raw dataset with p-values <0.01 that were not significantly regulated in the ND1vSMC raw dataset with p-values <0.01. This type of "not" comparison does not mathematically decrease the p-value as the previous "and" comparisons. Nevertheless, the rationale for this comparison was to identify genes in the NPC which may induce differentiation as a result of physiologically relevant activity. We assumed that FP-expressing cells in the DD1 are NPCs in the proliferative state and those FP-expressing cells in the LD1 are NPC that are less proliferative because they have been exposed to a differentiation signal downstream of physiological activity. The genes that are differentially expressed in the DD1vLD1 raw dataset are genes involved in maintaining proliferation (DD1) or in promoting differentiation (LD1). Moreover, we assumed genes that were not differentially regulated in ND1vSMC were involved in maintaining stemness because both ND1 and SMC are FP-expressing NPCs which were proliferating. Therefore, this "not" comparison was assumed to output a filtered dataset of genes involved in activity-dependent differentiation.

ND1vND5 and ND1vSMC and DD1vLD1. This comparison brought the infinite possibilities of the JMP program to another level of possibilities. This was a three-way filter looking for genes that were significantly regulated in three raw datasets. This comparison does increase the statistical power virtually from the original p-value of 0.01 to 0.01^3 or 0.000001. The rationale is that all three comparisons select for genes that

distinguish between an active proliferative state and either a less proliferative state or differentiated neurons (Table).

Unfortunately, despite JMP being an *almost* automatic method used to pare down the raw datasets, the filtered datasets provided by JMP were still too large to test all the candidates using our *in vivo* imaging protocol. Fortunately, there were several genes that appeared more than once in the various filtered datasets which focused our attention on a smaller list of candidates. We also used an unquestionably biased method of considering a pathway of interest and scanning through all the raw datasets to see if any genes in the pathway are differentially expressed in the JMP comparisons. We used this method because we felt that the assumptions made for the JMP comparisons may have filtered out some potentially interesting genes. The only truly unbiased method used to pick a candidate gene was to choose the one gene that seemed to be the most differentially regulated in several of the raw data sets.

Another program used look at the data was called Ingenuity Pathway Analysis or IPA. This was a pathway analysis program that organized the input dataset into known pathways. The input datasets were all the raw datasets consisting of transcripts which were differentially expressed with p-value <0.01 and the filtered datasets from the JMP analysis. The outputs of Ingenuity were schematics of known signaling pathways in which hits from the input dataset were marked in a gradient color according to their relative increased (red) or decreased (green) expression pattern in the input dataset. The power of this tool is not in determining the details of a single gene; for example, the output of the pathway analysis does not indicate that if a gene was up-regulated in the pathway then another gene in the pathway would be expected to be down-regulated The true advantage of this tool is in the organizing of large sets of regulated genes in a complex biological process into a more comprehendible visible model. It integrates known scientific literature which reflects both the ambiguity in the literature known about the networks and genes and bonafide variations in the biology. It aids in placing a single gene in the context of the larger more complex system that is the entire biological process occurring within a cell.

There are two limitations to using Ingenuity for this particular set of experiments. The first is this program is rodent-centric meaning that all the genes must be entered as mouse gene names. If the original data are not from mouse microarrays, the gene name must be converted into mouse-terms. For *X. laevis* where not all the genes have been annotated, this limits the dataset that can be entered into the program. Only 11,972 of the 33,442 genes were representable in mouse-terms. The second drawback is that this program lacks neuroscience knowledge. Many signaling pathways relate specifically to cancer and aging. Despite these shortcomings, it was still valuable in highlighting the possible signaling pathways that may be involved in the given the dataset. Several raw datasets and JMP filtered datasets were analyzed using Ingenuity. Yet, because of the infinite possibilities of JMP, there is still more interesting analysis to be done using this tool.

The last method used to analyze the raw datasets was to compare it gene-by-gene with previously reported NPC microarray datasets. This can be done painstakingly by hand; using the Excel or Jmp "Find" function, I can locate genes in these datasets with genes in the reference dataset; both complete raw datasets for PreND1vPreND5 and ND1vND5 were used (ComND1vComND5 for combined). For small datasets like the one presented in (Easterday, Dougherty et al. 2003), time was not an issue. The alternative method uses the "Join Datasets" functions in JMP. There are currently thousands of cataloged microarray datasets available, both curated and not curated, through web-based databases including NCBI-GEO, http://www.ncbi.nlm.nih.gov/geo/ and EBI-ArrayExpress, http://www.ebi.ac.uk/microarray-as/ae/. These databases can be searched and microarray data can be downloaded and analyzed according to user determined preferences. Once the data is formatted into a JMP-readable form, then it is a matter of buttons before a joint database of genes shared among the two datasets is constructed and further analyses can be done such as a comparison of differentially regulation. For this analysis, the data, titled Multipotent neural progenitor cells from rat hippocampus: GDS1396 (Muotri, Chu et al. 2005) from NCBI-GEO, was downloaded and opened with Excel. Then the sub-groups, titled Multipotent NPCs (GSM47547-GSM47557) and Neuron Derived from NPCs (GSM47557-GSM47560), were analyzed using a 2-tailed, unequal variance, t-test without normalization. Those genes with p-values of <0.01 were selected and joined with the ND1vND5 mouse-able genes dataset. The prime force behind such analysis was to compare this NPC dataset with others NPC datasets.

Finally, as a last note: the analysis of the microarray data would not have been possible without the assistance of Tim Tully of Dart Neuroscience, Inc., Mohana Gudurvalmiki, and my advisor, Holly Cline.

3.2 Results

3.2.1 Preliminary experiment using RiboAmp HS Plus

Results of the RiboAmp HS Plus experiments show that this amplification protocol does not amplify totRNA with high fidelity. At 5ng starting input (RiboAmp.1dilA-4dilA), the NanoDrop concentration analysis show greater than 20µg aRNA product for all four reactions; 15-20µg of aRNA is required to run standard format chips; however, the Agilent Bioanalyzer trace of the labeled aRNA before fragmentation show the kit preferentially amplified shorter transcripts for the 5ng samples as indicated by the steep slope after the peak at 33secs. At 200pg (RiboAmp.1dilB-4dilB) starting input, the Bioanalyzer trace showed a greater distribution of aRNA indicated by a more gradual slope after the peak at 36secs. However, Nanodrop concentration analysis of the 200pg samples showed that that only 2 out of the 4 amplifications produced enough aRNA to run a standard format chip; this showed that at low concentrations, amplification was inconsistent. The two 200pg samples (RiboAmp.1dilA and 2dilA) which yielded enough aRNA to proceed to chip hybridization and the corresponding two 5ng samples (RiboAmp.1dilA and 2dilA) were hybridized onto standard format *Xenopus* Genome GeneChips 1.0. The first-pass analysis of the results immediately demonstrated the low faithfulness of the low input amplification. Both RiboAmp.1dilA and RiboAmp.2dilA showed 54.3% and 54.4% present calls respectively which are considered an adequate

percentage of probe hybridization. However, RiboAmp.1dilB and RiboAmp.2dilB which should range in the 50% present calls if high fidelity is maintained showed only 29.9% and 34.0% present calls. This indicated that the amplified products of the low inputs were inconsistent. Additionally, it was observed that the amplification product had contaminating precipitate which produced inconsistent probe labeling.

3.2.2 Proof of principle experiment using WT-Ovation Pico Kit

Two GeneChips were run as a proof of principle experiment to access the NuGEN WT-Ovation Pico Kit and FL-Ovation cDNA Biotin Module. Four samples were amplified at the minimum input of 500pg (NuGEN1.1-4). All four samples yielded greater than 5µg of amplified product. Two samples which had the highest quality amplified product were used for hybridization onto *Xenopus* Genome GeneChips 1.0. The visual representation of the microarray chip showed even hybridization across the field indicating that the probes did not clump as it did in the RiboAmp experiment. Also, the first pass GCOS analysis showed greater than 67% present call for both chips. This first experiment with the NuGEN kits was promising enough to warrant further investigations using this kit.

3.2.3 Amplification fidelity experiment using WT-Ovation Pico Kit

The next preliminary experiment done with the NuGEN kits was to check the fidelity of the amplification. This was done using four samples at 50ng (NuGEN2.1dilA-4dilA), diluting the same four samples to 500pg (NuGEN2.1dilB-4dilB) and comparing the microarray results between the two groups. The amplifications of seven of eight samples resulted in sufficient amplified product (4-5µg of a-cDNA); one resulted in only 3.7 µg of a-cDNA; however, all eight samples were hybridized onto *Xenopus* Genome GeneChips 1.0 and all eight chips showed good and equal hybridization. The sample with the lowest input amount was indistinguishable from the rest indicating that inputs as low as 3.7µg can be used in the future.

Comparing the microarray results of the NuGEN2.1dilA-4dilA and NuGEN2.1dilB-4dilB showed little difference as indicated by the plot of means (Figure 3.3-A). The plot showed a correlation of 0.99. This result suggests high fidelity of amplification because both microarray outcomes of the varied input amounts were very highly correlative.

Another comparison done with this set of chip data was to compare brains of stage 43 (NuGEN2.1dilA/B and 2.2dilA/B or collectively NuGEN2.Stage43) and stage 47/48 (NuGEN2.3dilA/B and 2.4dilA/B or NUGEN2.Stage47). NuGEN2.1dilA/B and NuGEN2.2dilA/B were from stage 43 midbrains and NuGEN2.3 dilA/B and NuGEN2.4 dilA/B were from stage 47/48 midbrains; therefore a comparison was made between NuGEN2.1dilA, NuGEN2.1dilB, NuGEN2.2dilA, and NuGEN2.2dilB (stage 43) and NuGEN2.3dilA, NuGEN2.3dilB, NuGEN2.4dilA, and NuGEN2.4dilB (stage 47/48). Again, the plot of the means showed a very high 0.98 correlation between the 2 stages (Figure 3.3-B). Although, this result suggests that there was very little difference between the midbrains as a whole between the two stages, this was in fact unlikely, since other studies indicate that this was a period of significant circuit assembly. This result provided

additional motivation to develop methods to identify and collect a homogenous pool of NPCs for these microarray experiments.

3.2.4 Microarray confirmation of plasmid specificity

Two sets of three technical replicates at the level of hybridization were performed of hand-collected cells expressing the Sox2 reporter plasmid, Sox2/Oct3.mFGF4-Gal4VP16-14xUAS.mFGF4-TurboGFP.NLS (JLO#100). One set of three was PTD1 PTD1 cell-collections and the other set of three was PTD5 PreND5 cell-collections. The chips used for this experiment were the *Xenopus* Genome GeneChip 1.0. The chip analysis was performed using a program developed by DART Neuroscience. Significant genes constituted genes with p-values of <0.01; this raw dataset will be referred to as PreND1vPreND5 for preliminary ND1verses preliminary ND5.

Although this dataset was not rigorously analyzed, a couple of points were drawn from just looking at the raw data. First, both Sox2 and Sox3 were up-regulated in PTD1 compared to PTD5 as expected if PTD1 FP-expressing cells were more NPC-like than PTD5 FP-expressing cells. Other Sox-proteins were up-regulated as well such as Sox-D and Sox-11. Another NPC gene that was up-regulated was PCNA, a marker for dividing cells; in fact it was the third, fourth, and fifth most up-regulated gene in the dataset. The genes that were down-regulated in PTD1 (NPCs) thus up-regulated in PTD5 (neurons) included PSA-NCAM; the immunohistochemical studies above showed a complementary PSA-NCAM staining of neurons relative to the Sox2 staining NPCs. The data taken together gave us more confidence that the reporter plasmid used to select NPCs was functioning to identify NPCs as designed.

3.2.5 Final microarray experiments

The final microarray experiments consisted of fifty-five *X. laevis* GeneChip 2.0 microarray chips and six raw datasets from six comparisons. What is presented here is less than a month's worth of analysis by four people which barely scratched the surface of the datasets; still, much was learned from the initial analysis revealing several promising results.

Before the pathway analysis could be analyzed with Ingenuity, we conducted a Monte Carlo experiment, which was first considered to address the issue of false positives in the data input from JMP. We used a p-value of 0.01 to identify genes that were significantly differentially regulated. Base on this p value, we would expect 335 out of 33,442 represented genes to be the false positive rate of the microarray experiment. Because the poor degree of annotation of *Xenopus* database, we were only able to input 11,972 mouse homologs in the Ingenuity Pathway Analysis program. Therefore, we would expect 120 genes of this dataset to be falsely positive. Then we entered 120 random genes into the pathway analysis program to determine the number of genes that would be connected into a pathway. We found that the maximum number of genes involved in a pathway ranged from 18 to 25 with 23 being the average. This means that pathways indentified by Ingenuity with less than 23 genes, or 25 genes if being conservative, are not likely to be true network hits; however, it did not mean that a particular network with less than 23 gene were absolutely false.

With this in mind, we first looked at the Ingenuity analysis for ND1vND5 to validate the merit microarray experiments. The input consisted of 1,610 genes of which 1,202 were network eligible and 1,065 were function/pathway/list eligible. The actual input number of genes may be reduced because some may be duplicates, while others are simply not currently connected to any network or pathway in the Ingenuity database. Nevertheless, we saw 26 networks out of 50 represented in the program; that included more than 23 genes and 25 networks with more than 25 genes from the input list (Example Network Combining MCM7 Figure 3.4-A). It was interesting to see that several of the networks were NPC relevant pathways, such as cell cycle, cellular growth and proliferation, cancer, embryonic development, and DNA replication and repair. The three topmost functions that the networks were most involved with were cellular growth and proliferation, cell death, and cell cycle. The topmost three canonical pathways were polyamine regulation in colon cancer, protein ubiquitination pathway, and cell cycle: G2/M DNA damage checkpoint regulation (Figure 3.4-B). The diseases and disorders that the Ingenuity program identified included cancers, GI diseases, genetic disorders, neurological diseases, and skeletal and muscular disorders. The results (Figure 3.4-C) indicated that many of the genes that were differentially regulated were what might be expected from a comparison of a proliferative cell (NPC) and a differentiated cell (neuron).

In comparison, we looked at the Ingenuity output of ND1vSMC. These two sets are NPC but from different times in development; one from early stage 48 and the other late stage 48. There were no real noticeable differences in the pathways involved: cell cycle, DNA damage and repair, and developmental and embryonic function. The only slight difference was that pathways involved in cell growth and proliferation were ranked lower in ND1vSMC than ND1vND5 Ingenuity analysis. In contrast, pathway functions ranked in the topmost three were genetic disorders, neurological diseases, and skeletal and muscular disorders. Cell death, cellular development, and cellular growth and proliferation functions ranked 4, 5, and 6 respectively. Of the topmost three canonical pathways was cell cycle G2/M DNA damage checkpoint regulation, Huntington's disease signaling, and axonal guidance signaling. These results correlate with the previous observation of Pranav Sharma of the tendency of NPCs in older tadpoles to have decreased XdU incorporation. The pathways of the differentially regulated genes have moved away from genes involved in proliferative cell-cycle control and cancer as highlighted in the ND1vND5 pathway analysis and move towards genes that may be involved in cell-cycle exit and development of organ systems indicated by their functions in neurological, skeletal, and muscular organs. This suggested that the genes that were differentially regulated between ND1vSMC were not related to stem cell biology per se but may be related to pathways that may explain why SMC NPCs (late stage 48) had a decreased proliferative capacity than ND1 NPCs (early stage 48).

Once we were satisfied that the ND1vND5 and ND1vSMC demonstrated some validation of the hypothesis that the PTD1 cells were NPCs, other analysis was done to choose candidate genes for the imaging experiments that were to follow. At this point the JMP comparisons and raw dataset scanning began in earnest. Fifteen out of sixteen candidate genes were extracted from these analyses. The exact process by which these

particular fifteen were chosen will be discussed below in the section entitled Morpholinos (Section 4.1.2). I will give a general overview of the various analyses done so far in this result section.

The largest differences in expression were in a gene called GST-Pi (AKA GSTP1) which was a call in five of the six raw datasets; there were five probe sets for GST-Pi on this microarray. For ND1vND5 and ND1vSMC, all five probes were differentially regulated with a p-value <0.01. The fold changes for ND1vND5 ranged from 2.13 to 4.56 up-regulated in ND1 in comparison to ND5 and ND1vSMC ranged from 1.34 to 1.56 up-regulated in SMC in comparison to ND1. For DD1vLD1, three probe sets were differentially regulated with a p-value <0.01. The fold changes were 1.16 down-regulated and 2.15 and 5.27 up-regulated in DD1 in comparison to LD1. Three probes were differentially regulated in CPG24vCMo24; they were up-regulated by 0.48, 0.79, and 0.89 in CPG15 control cells than in CPG15 morpholinos cells. Only one was significant in CPG12vCMo12 comparison; 0.73 up-regulated in CPG15 control compared to morpholino. There was no significant differential regulation of GST-Pi in the DD5vLD5 dataset. This indicates that GST-Pi was a protein that was comparatively most heavily expressed in older neural progenitor cells (SMCs), comparatively slightly less expressed in younger proliferative cells (ND1 and DD1), and comparatively even less in differentiating or differentiated cells (LD1 and ND5) suggesting a temporal expression pattern.

In analyzing the JMP 2-way comparisons, we found the ND1vND5/DD1vLD1 filtered data set has shared 122 significant genes with p-values <0.01. Of those, 63 genes (52.2%) were regulated in the same direction, suggesting their transcription was similarly (up or down) regulated in active progenitors (ND1 and DD1). The ND1vND5/DD5vLD5 filtered dataset shared 284 genes with p-values <0.01 and 154 (53.2%) were regulated in the same direction, possibly identifying transcripts preferentially expressed in differentiated neurons (ND5 and LD5). DD5vLD5/CPG24vCMo24 had 185 genes with p-values <0.01 and 91 (49.2%) were regulated in the same direction. The ND1vND5/ND1vSMC filtered dataset had 803 shared significant genes with p-values <0.01 of those 707 (88.0%) were regulated in the same direction. This may be likely because the ND1 dataset was used in both comparisons, so this dataset may have more false positives than other 2-way comparisons that don't share a dataset. The JMP 3-way comparison between ND1vND5/ND1vSMC/DD1vLD1 showed 30 shared significant genes and 13 genes (43.3%) regulated in the same direction in all three raw datasets. These hits from the 3-way are most likely to be significant because of the virtual p-value being $< 0.01^3$ or 0.00001. The 2-way "not" comparison which identified significant genes in DD1vLD1 but not significant in ND1vSMC showed 548 genes with p-values <0.01. The large number of genes in this set may be likely due to the "not" comparison which does not enhance our statistical power the way the "and" comparisons do; we can set the p-value lower to compensate for this in future analysis.

The Ingenuity generated analysis of ND1vND5/ND1vSMC filtered dataset with only the genes regulate in the same direction to identify stemness genes that are involved in maintaining proliferative capacity. There were 707 genes in this filtered dataset with only

303 corresponding mouse genes of which 250 genes were network eligible and 222 genes were functions/pathways/list eligible. The networks that were prominent were protein synthesis and gene expression, DNA replication, recombination, and repair, and cancer, cell cycle, and reproductive disease. The more interesting results were the network molecular and cellular functions; presenting them from the top were cancer, cell cycle, and cellular growth and proliferation. Genetic disorder and neurological disease came in 4 and 5. Of the canonical pathways were cell-cycle G2/M DNA damage check-point regulation, mitotic roles of Polo-link kinase, and Huntington's disease signaling. The Ingenuity analysis highlighted pathways such as cell-cycle control, DNA modeling and remodeling, and cell growth and proliferation, the results correlated with the assumptions made for this comparison as explained in (Section 3.1.5.2; *ND1vND5 and DD5vLD5 same*). Further analysis of the pathways and the individual genes may result in the identification of genes that may be involved with maintaining a high proliferative capacity.

The Ingenuity pathway analysis of DD1vLD1/ND1vSMC/not, which was a comparison done to highlight genes that were activity-dependent regulators of differentiation also showed some interesting results. The input dataset was only 208 mouse representable genes. Only 172 genes were network eligible and 152 were function/pathway/list eligible. The three topmost networks identified were cell morphology, DNA replication, and cellular assembly and organization. The next three included cellular development, cancer and cell-to-cell signaling. The molecular and cellular functions these networks serve were cellular assembly, DNA replication, and cardiovascular system development. Organ development, cell morphology, and cell-to-cell signaling and interaction came in 4, 5, and 6. In the list of relevant canonical pathways were NRF2-mediated oxidative stress response, antigen presentation pathway, and Ephrin receptor signaling. Also in the list were tight junction signaling, Notch signaling, dendritic cell maturation and axonal guidance signaling. An example of a network diagram for this Ingenuity analysis is in (Figure 3.5) which highlighted the involvement of the Ephrin pathway through the differential expression of EfnA1 and EfnB1. This comparison was done to identify genes that may be involved in activity dependent differentiation signals and accordingly, many pathways potentially involved in neuronal processes were alluded to such as cell-to-cell signaling, Notch signaling, dendritic cell maturation, and axonal guidance signaling in the analysis. The involvement of NRF2-mediated oxidative stress response, a response to external insults to the cell, suggested that external stimuli initiated cascades were activated; this can be extrapolated to be related to activity dependent mechanisms. This particular analysis illustrates that Ingenuity could become increasingly valuable in this field as more neuroscience-relevant signaling pathways are added to the database and more neuro-specific results can be generated from the data.

The Ingenuity analysis for the CPG15 morpholino experiments showed that at 12hrs there was activation of a signaling pathway involved in nervous system development and function. There was only one significant pathway due to the small number of input genes; there were only 72 genes with p-values <0.01 in the input for CPG12vCMo12 of which 61 were network eligible and 55 were function/pathway/list eligible. This pathway

involved MAPK/ERK activation by FGF13 and MMP7 and the eventual activation of ELK4. The molecular and cellular functions activated by all the analysis pathways were in cardiovascular disease, organ morphology, and organismal injury and abnormalities as well as post-translational modification, protein degradation, lipid metabolism, and neurological development and disease. The top canonical pathways were phenylalanine metabolism, mitochondrial dysfunction, and oxidative phosphorylation. The Ingenuity Pathway Analysis results for the 24hr CPG15 harvest were markedly different from the 12hr CPG15 harvest, illustrating how quickly CPG15 functions in the cells; the pathway analysis showed that activation of cell death occurred between 12 and 24hrs of CPG15 functional knockdown. The top associated networks were skeletal and muscular disorders involving amino acid metabolism, immunological disease and DNA replication and recombination. Cell cycle and cancer came in fourth. Of molecular and biological functions were cell death at the top followed by gene expression, cellular growth and proliferation, cellular development, and cellular function and maintenance. Top canonical pathways were NRF2-mediated oxidative stress response pathways, glucocorticoid receptor signaling and growth hormone signaling. There were 418 genes with p-values <0.01 for CPG24vCMo24 input of which 322 genes were network eligible and 303 genes that were function/pathways/list eligible. The CPG15 morpholino experiments were to access how CPG15 protein may play a role in NPC survival and possibility in activity-dependent neurogenesis. Correlating with CPG15 role in NPC survival, the functional knockdown of CPG15 resulted in activation of many cell death pathways including metabolism of many cellular components such lipids, amino acids, and proteins. Canonical pathways such as mitochondrial dysfunction and oxidative phosphorylation also suggested activation of apoptotic signaling cascades.

The literature comparisons done showed many similarities between mouse and rat neural progenitor cell microarray datasets. The Easterday, Dougherty *et al.* 2003 reported two datasets comparing neurosphere-generating neural stem cells and differentiation-induced neurons. One dataset contained genes which *in situ hybridizations* of E13, E17, and P1 were performed and rated, and the other dataset contained the genes in the experimental dataset, which were shared among mouse embryonic stem cells and human embryonic stem cells; these two sets identified neural progenitor specific genes and stemness genes respectively. Comparing the neural progenitor specific gene dataset, there were 16 genes out of 48 annotated genes shared with the complete raw datasets of PreND1vPreND5 and ND1vND5. Of those, 2 of 5 genes were restricted to the germinal zone, 6 of 8 genes were localized to the germinal zone, 5 of 12 genes were generally localized to the germinal zone, and 7 of 16 were not localized to the germinal zone. Comparing the stemness gene dataset, 15 of 69 annotated genes were shared with this dataset.

When the dataset of Muotri, Chu *et al.* 2005 was compared to ND1vND5 mouse-able gene dataset with p-values <0.01 (1,251 genes), there were also many similarly expressed genes. There were 76 genes that were shared out of the 365 genes with p-values <0.01 that were differentially regulated in the Muotri, Dhu et al. dataset. Of those, 50 genes out of the 76 shared genes were similarly regulated. That is 66% of the shared genes were also regulated in the same manner. Ingenuity Pathway Analysis of the 76 shared genes of

which 74 genes were network eligible and 73 were functions/pathways/list eligible showed networks associated with cellular assembly, organization, and cell death and cell morphology and signaling in nervous system development. Molecular and cellular functions involving the pathways were cellular compromise, DNA replication and repair, and cell death. It appears the shared dataset between ND1vND5 and the Muotri, Chu *et al.* 2005 datasets highlights processes of proliferative cells.

3.3 Conclusion

3.3.1 Resolving the methodological considerations of *X. laevis* microarray

This project had a number of unique technical issues that needed to be resolved even before the planning of the experiments itself. We were interested in collecting a relatively homogeneous population of progenitors from an identified region of the CNS. This has not been done in other animals. The small size of the animals and the lack of targeted transgenics meant only a small number of homogenous cells can be isolated resulting in a small amount of isolatable totRNA. Additionally, the only available microarray format for *Xenopus* was the standard format chip which required 5μg of product a- cDNA or 15-20μg of amplified aRNA, this amount could not be sufficiently amplified by using a single cell amplification protocol. Therefore, miniaturizing the microarray process was an undertaking that lasted more than a year. Everything from the isolation to the hybridization was optimized and ironically, the final experiment of fifty-five chips took no longer than 3 months. What was learned was that hand-picking cells of interest was not only possible, but the preferred method of collecting tissue, because acutely isolated cells do not have *in vitro* artifacts as would cells grown or induced in culture; although, even acutely isolated cells, whether it is by hand or by FACS, may have immediate early gene artifacts that result from the sorting process. In this light, the sorting process would greatly benefit from a more sensitive amplification process so hybridizing the chips would require fewer harvested cells. Also, as noted before, this would not only decrease harvest time but also decrease the odds for contamination from other cell-types, and will also facilitate doing biological replicates, which will serve to statistically strengthen the microarray comparisons.

Once the cells are harvested, the very small amount of totRNA in the picograms range had to be efficiently and consistently isolated. There are several kits and methods. The two kits tried where of the two basic types: a column based method and a purely buffer based method. Although, technically, the buffer base method should yield more and higher quality RNA, just like the Cesium DNA isolation protocol always yields more and cleaner DNA than any column commercially available today, practically, what you cannot see can be pipetted away in a blink of an eye. Therefore, column based method was preferred for this experiment.

Improved cell collection and RNA processing would make replication of the experiments feasible. This was critical because of the false positive rates in the microarray data. For instance, when PreND1vPreND5 and ND1vND5 raw datasets were compared, relatively few genes were similarly regulated genes. A clear example was the stem cell markers discussed above: in PreND1vPreND5 there are many Sox-genes that

were differentially regulated but in ND1vND5 there were only one Sox gene differentially regulated. Additionally, NCAM which appeared in the PreND1vPreND5 raw dataset did not appear in ND1vND5. This may be the result of the difference in workflow which differed in the totRNA isolation step. The totRNA for the three replicates that constituted the PreND1vPreND5 chip dataset was isolated using one column, while totRNA for the four/five replicates of ND1vND5 was isolated using five separate columns. It is postulated that the variation introduced by the column drowned out significantly regulated genes. But, technology is still moving forward to favor small inputs. Better isolation methods such as the *in situ* totRNA extraction method that has already been commercialized and the adaptation of the TRAP method of cell-type specific mRNA isolation may decrease the variability seen in these experiments and improve collection from small samples.

Finally, once the RNA was in hand, it needed to be amplified with consistency, efficiency and fidelity. Three commercially available kits were tested for this purpose. The RiboAmp HS Plus kit did not meet the standard of consistency and fidelity for small amounts of input. The TargetAmp Pico Kit did not work in my hands at all. I decided to use the NuGEN kit. This was partly due to the unique single-round amplification step that produced the more stable a-cDNA instead of the two-round amplification step of the other two kits that produced the more labile aRNA. Additionally, the NuGEN kit took one day, albeit a long day, to obtain a product where as the other two required a minimum of a day and a half. In agreement with my finding was also a recent study that tested four amplification kits, Affymetrix One- and Two-round Amplification Kit, Molecular Devices RiboAmp HS, Ambion MessageAmpII, and NuGEN WT-Ovation Pico Kit. The NuGEN pico-system appeared more suitable for the amplification of picograms of RNA because it provided consistent high quality expression profiles and was reproducible across laboratories and operators despite the inevitable variability introduced by the changing of hands (Clement-Ziza, Gentien et al. 2009).

3.3.2 GST-Pi: A gene up-regulated in NPCs in *X. laevis*

Glutathione S-transferase Pi (GSTP1) has been studied in the context of cancer biology as a cancer susceptibility gene and associated with cancer drug resistance. Its expression was shown to be correlated with proliferative activity in various cancers including oral cancers (Silva, Ribeiro et al. 2007). It also plays an important role in the detoxification of xenobiotics such as carcinogens in cigarettes. The Allen Brain Atlas shows its mRNA is expressed broadly throughout the adult mouse brain with significantly higher expression in the hippocampal neurogenic niche (Figure 3.6-A). GeneCards entry shows it is expressed in tissues throughout the body both during normal conditions and cancer conditions (Figure 3.6-B). Its expression has been shown to be neuroprotective against MPTP induced neuronal death (Castro-Caldas, Neves-Carvalho et al. 2009). Due to its ubiquitous expression throughout the body and in the brain, it may not be a good candidate for use as a NPC marker; however, it may be involved in the regulation of proliferation as suggested by the cancer biology data or cell survival as indicated by its cell protective role. Its high expression in NPCs makes it an interesting candidate gene.

3.3.3 Ingenuity analysis was useful in identifying genes and pathways of interest

Ingenuity pathway analysis program was useful in identifying several genes of interest. For example, Ephrin-B1 was chosen because it was highlighted in a highly ranked pathway resulting from the ND1vND5/ND1vSMC/same filtered dataset for genes involved in maintaining stemness; additionally, the involvement of various other Ephrins in DD1vLD1/ND1vSMC/not filtered dataset for activity dependent genes suggested that Ephrins may also be an activity dependent maintainer of stemness. The pathway analyses of other candidates are detailed in the next section where the candidates are addressed individually (Section 4.1.2, Morpholinos).

The other valuable feature of Ingenuity was its ability to add key molecules within a pathway even if it was not a gene among the input dataset and display it in such a way to highlight the key molecules. For example, the merged pathway diagram involving two independent pathways sharing the gene, MCM7, a marker for stem cells, highlighted two interesting genes (Figure 3.5): Tenascin C (TNC) and Tumor Necrosis Factor (TNF). These genes were indicated by Ingenuity to be the two key extracellular initiators of the pathway involving MCM7. I discovered TNC was an extracellular matrix protein implicated in guidance of migrating neurons and extending axons in development and plasticity (Joester and Faissner 2001) and highly expressed in NPC niches (von Holst 2008). TNF was a gene studied in cancer biology but the knockout mice displayed neuro-dysfunction which suggested that TNF played a neuroprotective role in the brain (Turrin and Rivest 2006). I would never have considered these two genes to be part of NPC biology but their emphasis in the MCM7 pathway by Ingenuity has brought them into the spotlight. There are currently some interesting ideas concerning their involvement in NPC biology but there are still many open questions to their exact role.

3.3.4 CPG15 functional knockdown by morpholinos activates cell death pathways

CPG15 has been previously studied in the Cline laboratory in the context of activity dependent plasticity. It was a candidate activity-regulated gene even before the microarray experiments were performed because of its various characteristics mentioned earlier (Section 1.3.2.2). The microarray studies confirmed the activation of cell death pathways between 12hrs and 24hrs of its functional knockdown with morpholinos. The results of the 12hr morpholino functional knockdown suggest that cell death was induced by a growth factor (FGF13) related pathway that activates MAPK and ERK. It is yet to be determined how CPG15 functions in the NPC, but the microarray data illustrates the possibility that CPG15 acts indirectly as a cell growth, survival, differentiation factor rather than directly as an anti-apoptotic factor.

3.3.5 Molecular signature of *X. laevis* NPCs is similar to other model systems

The albino *X. laevis* model system is a unique system to study NPCs because it allows an *in vivo* look into neurogenesis; this is a characteristic not shared by mammalian model systems where the neurogenic pools are deep within the CNS. However, the lack of characterization of *X. laevis* NPCs makes it difficult to place the results into context. For this was another purpose of the microarray experiments. It was to not only look for activity-related neurogenic genes but also to introduce the *X. laevis* as a NPC-neurogenesis model system. Although amphibian and fish species have been used

extensively to study cell proliferation and differentiation in the CNS and microarrays have been used to characterize changes in gene expression during early *Xenopus* development, NPCs from *Xenopus* CNS have not yet been characterized extensively. One purpose of the microarray experiments was to characterize *X. laevis* NPCs and to place these cells in the context of stem cells and NPCs from other species. These studies will introduce *X. laevis* as a valuable model system to study NPCs and the regulation of neurogenesis *in vivo*.

When I compared rodent NPCs verses neuron microarrays with our data from *Xenopus laevis*, it showed that the *X. laevis* NPCs have many similarities in gene expression besides those known to be NSC/NPC markers like Sox2. In the Muotri, Chu *et al.* 2005 comparison, many of the shared genes also shared the same differential regulation. Furthermore, Ingenuity comparison analysis of ND1vND5 and the Muotri, Chu *et al.* 2005 shared genes dataset showed shared function in cellular growth and proliferation, cell death, cell cycle, gene expression, and DNA replication and repair. Both datasets shared canonical pathways including polyamine regulation, which has been shown to regulate cell proliferation (Oredsson 2003) and neuronal plasticity (Yoneda and Ogita 1991), and protein ubiquitination pathways.

The Easterday, Dougherty *et al.* 2003 mouse NPCs comparison also showed that there were several similarities between the datasets. Although, the genes were too few to enter into an Ingenuity analysis, shared genes such as cyclins, translation elongation factors, histone H2A, splicing factors, and ubiquitin enzymes suggest involvement of cell cycle, DNA replication, and ubiquitination pathways; all reminiscent of the similarities found with the Muotri, Chu *et al.* 2005 dataset. The other important observation made in the Easterday, Dougherty *et al.* 2003 comparison was that there were many stemness genes that were shared between the two datasets that were also shared by mouse and human embryonic stem cells. Additionally, the Ingenuity Pathway Analysis tool also suggested many overlapping pathways that were involved in cellular growth and proliferation for the ND1vND5 raw dataset. Together, it suggests that there are many NPC genes and pathways that are also part of proliferating stem cells in general. This brings into focus one of the challenges faced by cancer researchers that is now being faced by researchers in the field of therapeutic NSCs/NPCs science: how to target therapies specifically to NSCs/NPCs whether they are endogenous pools or transplanted pools and not to all stem cells of the body. The other more interesting side of the coin is that therapies that have already been established for stem cells in cancer can be "recycled" to be used in NSC/NPC therapies in neurological diseases.

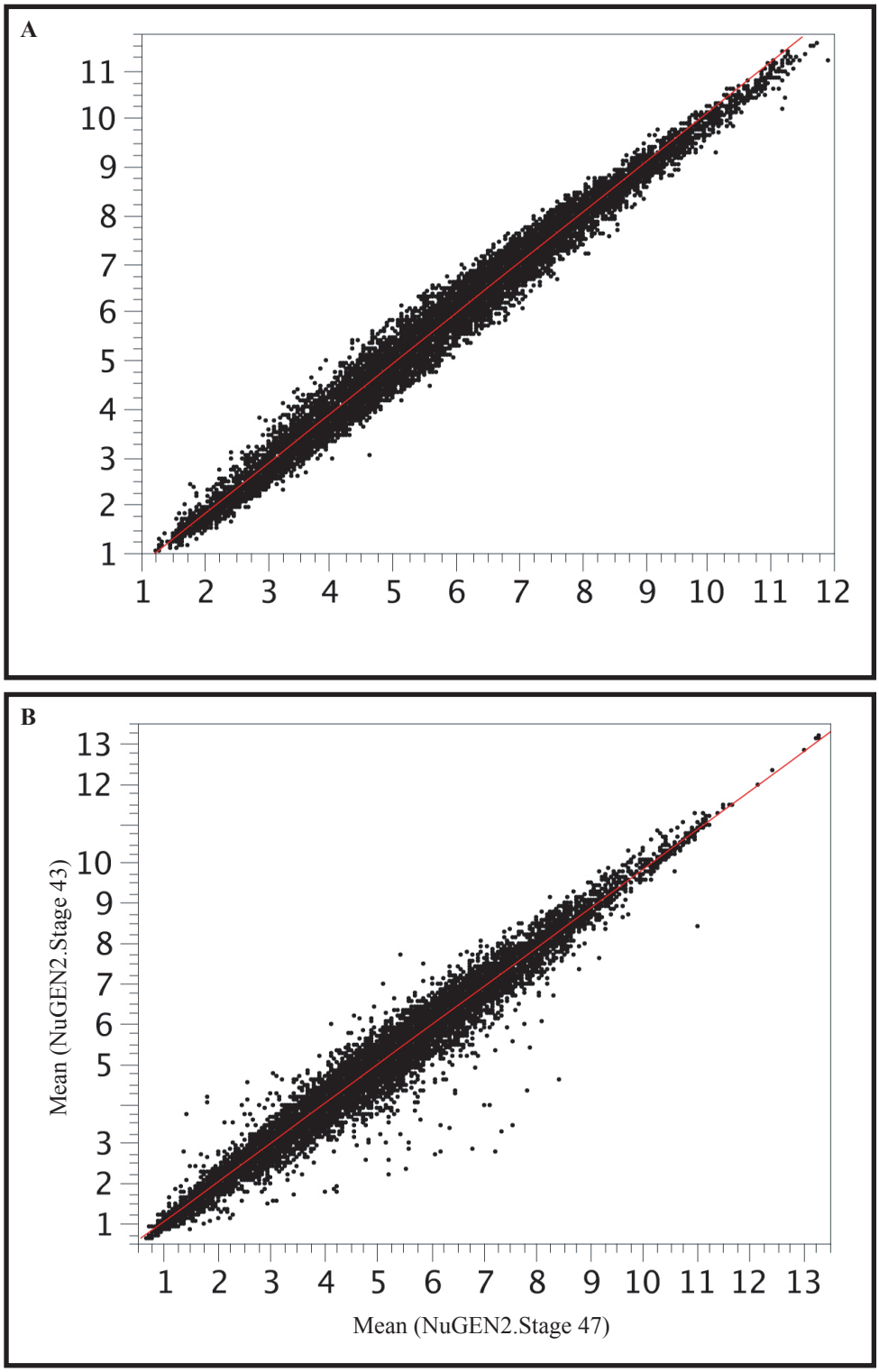

Figure 3.1 | Preliminary NuGene data. Comparison of two different concentrations of staring totRNA using NuGEN kit and comparison of two different stages of tadpoles show no significant difference. Graphs show of the mean value of probe-by-probe signal plotted against each other. **(A)** Mean NuGEN kit amplification of 50ng (dilA) compared with mean of 500pg (dilB). Correlation was 0.99. **(B)** Mean of Stage 43 brains compared with mean of stage 47 brains showed a correlation of 0.98.

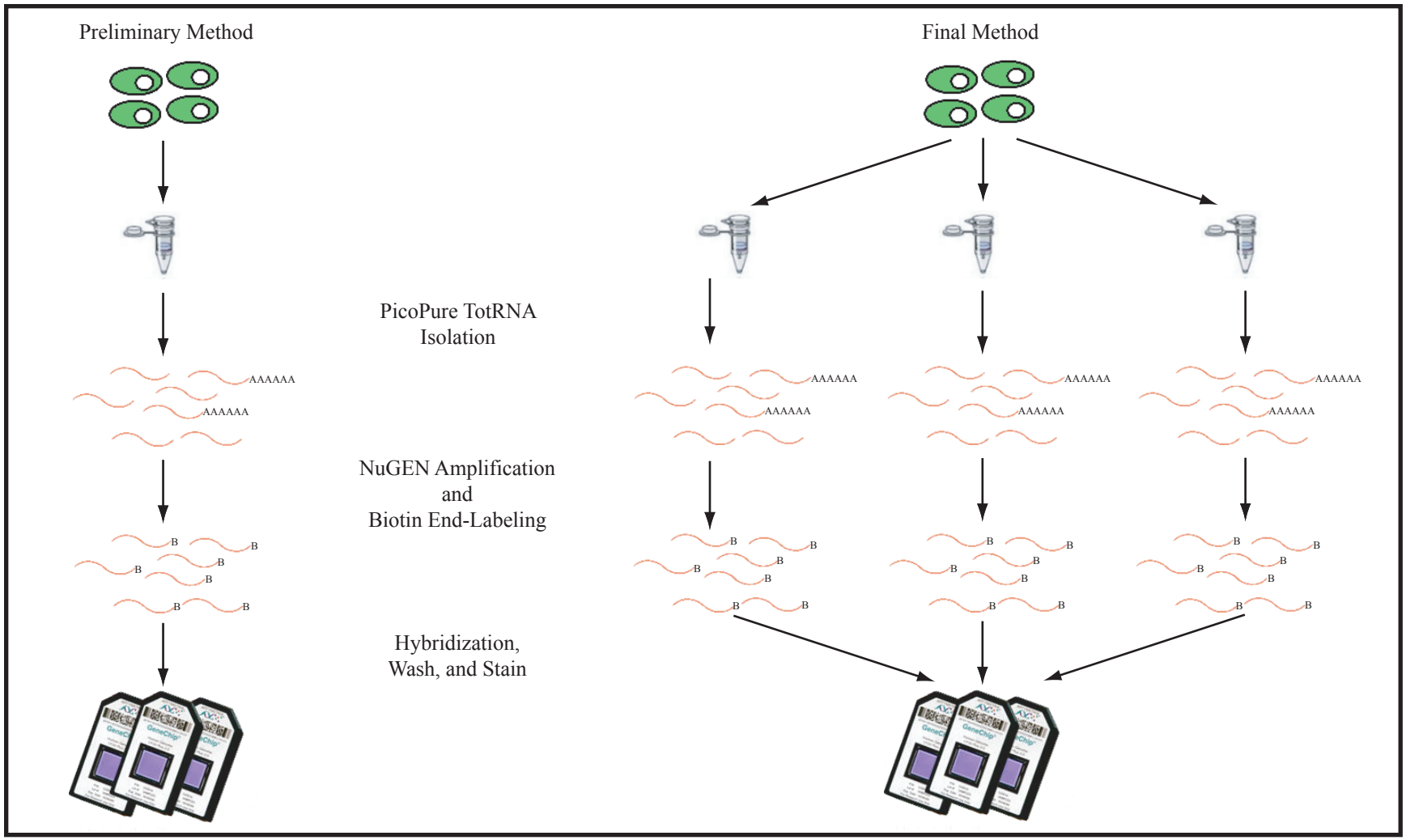

Figure 3.2 | Microarray work flow diagram. PreND1vPreND5 microarray experiment used data from technical replicates at the level of Hybridization, Wash, and Stain. ND1vND5 microarray experiment used data from technical replicates at the level of the PicoPure columns.

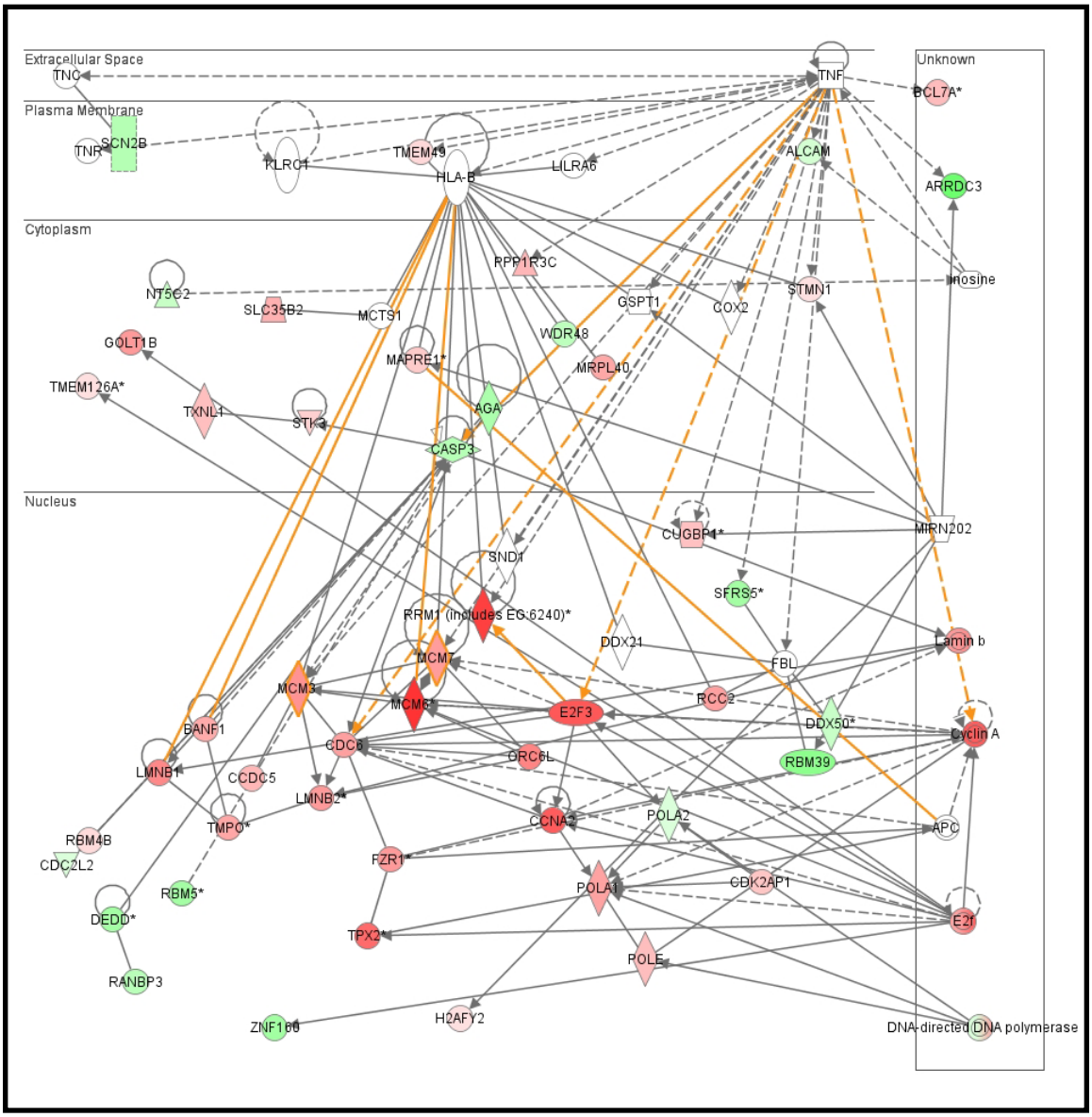

Figure 3.3 | Ingenuity Pathway Analysis merge of MCM7. Two networks which contain MCM7 in the ND1vND5 dataset with differentially regulated genes with p-values <0.01 were merged together. MCM7 is a proliferation marker which showed increased differential expression in ND1 cells. MCM7 is a part of minichromosome maintenance complex (MCM) of proteins and is known to be expressed in cells with proliferative potential. Two networks which contained MCM7 were combined and displayed according the protein location within a cell. Ingenuity displays input genes in networks and adds prominent genes for that network that may not appear in the input dataset. Here TNF and TNC are major extracellular components that drive much of the merged pathway involving MCM7.

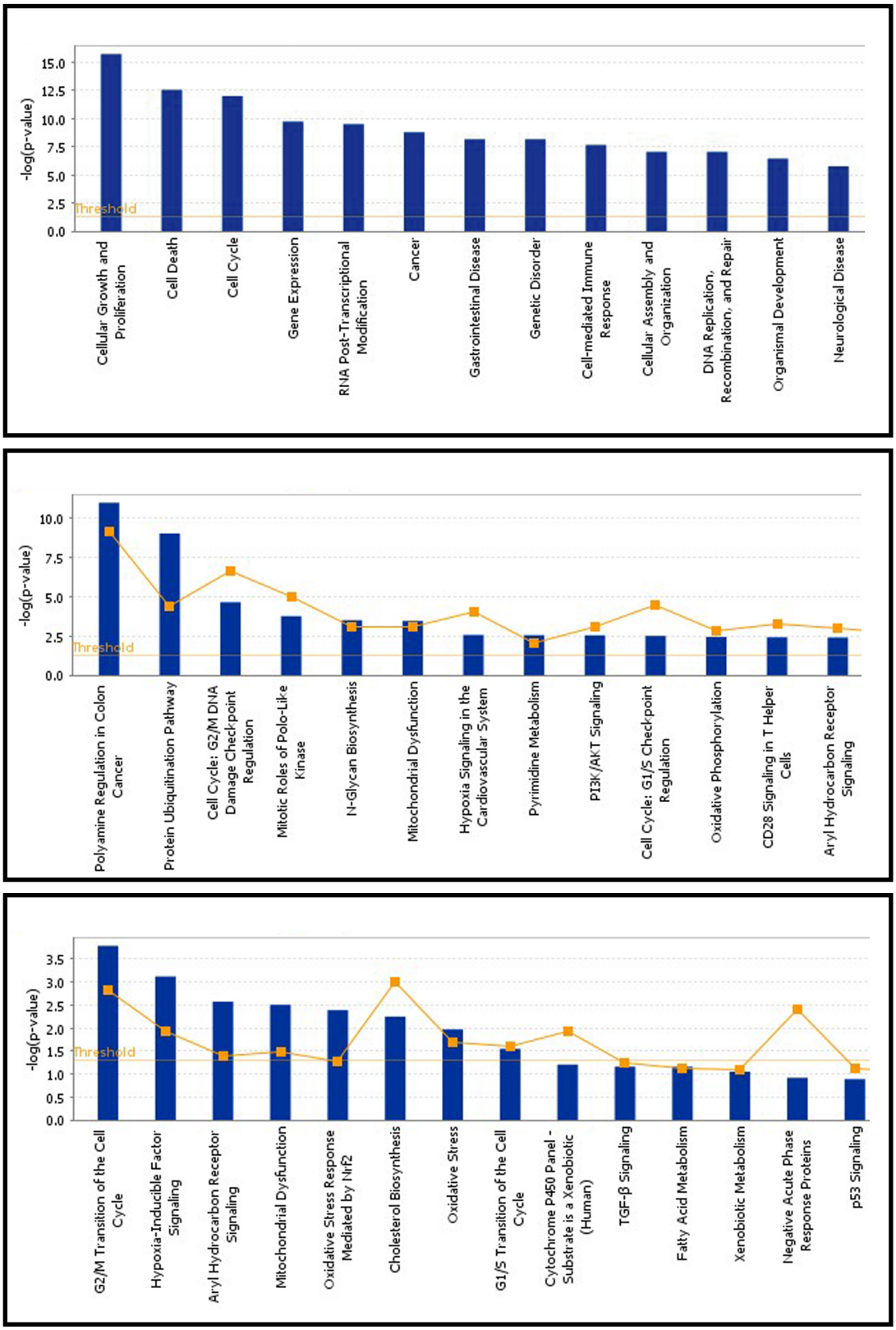

Figure 3.4 | Ingenuity Pathway Analysis for ND1vND5. Pathway overview of functions, canonical cascades, and gene lists. Pathways that were highlighted were those expected in proliferative cells.

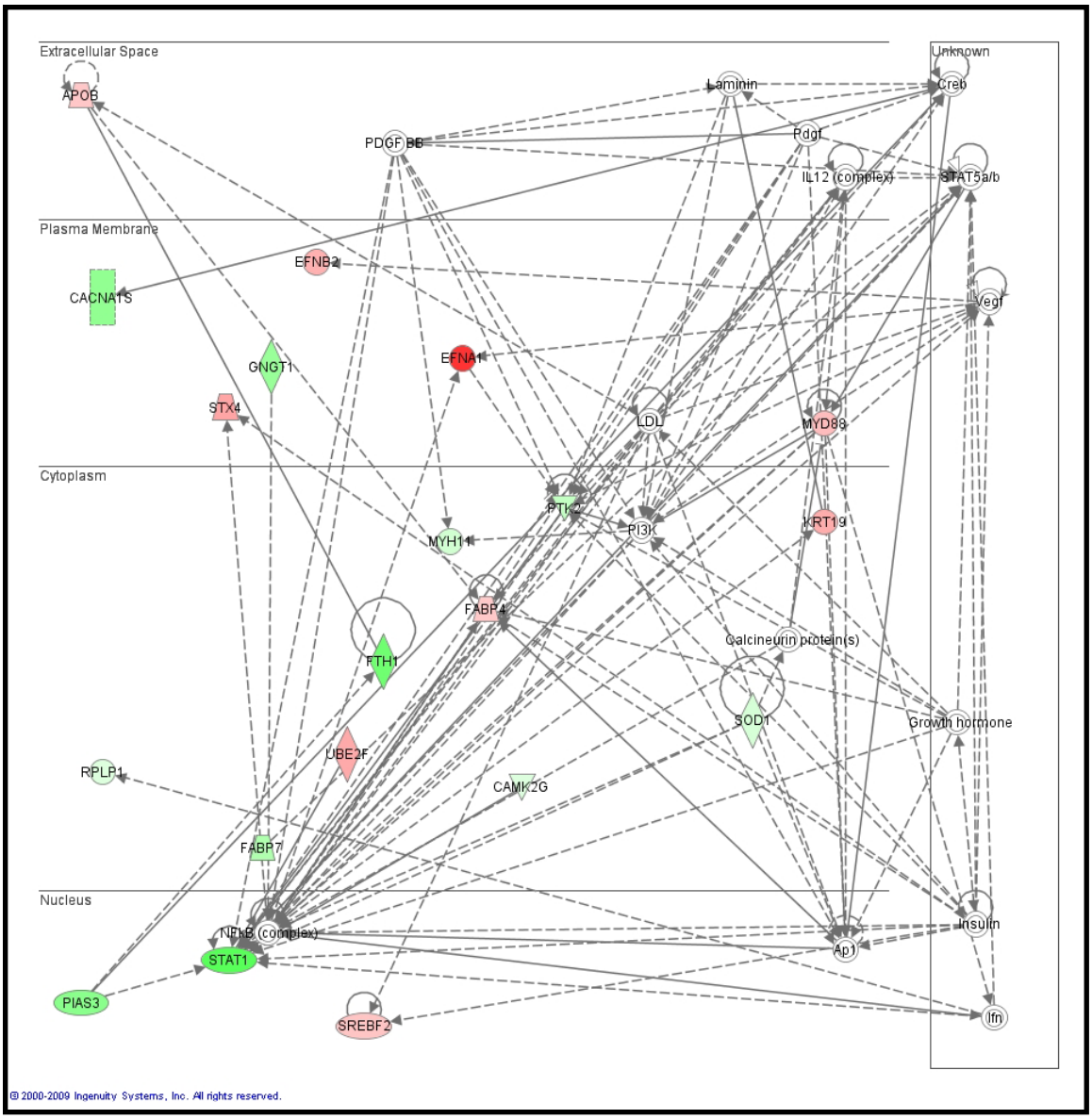

Figure 3.5 │ Ingenuity Pathway Analysis for the DD1vLD1/ND1vSMC/not JMP filtered dataset. This analysis was done to highlight genes that may be involved in activity-dependent differentiation. The pathway shows involvement of Ephrin pathways with the differential expression of EfnA1 and EfnB1.

Chapter 4 Imaging

4.1 Rationale for the imaging experiments

Imaging studies with cortical and hippocampal slice cultures suggest that much can be learned from observing the same proliferating cell over time that cannot be learned from classic BrdU experiments or immunocytochemistry experiments. For examples, much of what is known about symmetrical and asymmetrical division of NSCs/NPCs in vertebrates was discovered with time-lapse imaging experiments of cultured cortical slices (Noctor, Flint et al. 2001; Kosodo, Roper et al. 2004; Noctor, Martinez-Cerdeno et al. 2004; Kosodo, Toida et al. 2008), while most of what is known about activity-dependent regulation of cell proliferation comes from studies in adult hippocampus (Kempermann, van Praag et al. 2000; Lein, Hawrylycz et al. 2007; Buck, Bradford et al. 2008; Fabel and Kempermann 2008) and hippocampal slice cultures (Raineteau, Rietschin et al. 2004; Takashi, Hideki et al. 2007) or the olfactory system (Lledo, Saghatelyan et al. 2004; Ma, Kim et al. 2009). Although there has been *in vivo* studies of activity-dependent migration and integration of NPCs in the rodent olfactory bulb (Mizrahi, Lu et al. 2006), thus far, it has been impossible to address questions concerning how physiologically relevant activity can affect the regulation of neurogenesis at the source in intact mammalian systems. An *in vivo* approach will be extremely valuable to test whether activity-dependent mechanisms regulate neurogenesis. Additionally, the albino *X. laevis* model system can also tackle questions regarding how an *in vivo* change in a cell autonomous and/or cell non-autonomous pathway can acutely affect the physiological output of a NPC.

4.1.1 Screen

Several molecules of interest were extracted from the microarray analysis. I used an imaging approach to screen for the functional output, but not necessarily validate the microarray results of, the candidates. Further follow-up validation experiments using RT-qPCR and immunohistochemistry or *in situ hybridizations* are also necessary. The purpose of the imaging was to observe the immediate physiological output of candidate gene knockdown with respect to proliferation rate and differentiation rate. Consistent with the goal, the GOIs were chosen for their possible connection with regulatory pathways of neurogenesis involved in the switch between proliferation and differentiation.

4.1.2 Morpholinos

A total of 17 morpholinos were designed against 15 candidate genes. The following alphabetical list will briefly review the rationale for their selection as well as a speculation to their output as suggested by targeted literature explorations. There are many resources to search known functions of GOIs besides PubMed, NCBI, and EMBL-EBI, one such recommended resource is GeneCards which combines several public and commercial databases onto one page. As with other online resources, the problem is in its mammal-centric bias; for GeneCards, it is human-centric.

CPEB. Cytoplasmic polyadenylation element binding protein 1 is a sequence specific RNA-binding protein that stimulates polyadenylation and translation in germ cells and

neurons (Groisman, Ivshina et al. 2006). It was chosen because CPEB was present in the PreND1vPreND5 raw dataset along with its associated partner, Maskin. Also, Maskin expression was significantly regulated in the ND1vND5 raw dataset. The CPEB1 morpholino has another advantage: its knockdown effectiveness has already been verified by (Bestman and Cline 2008). It has been shown recently to be involved in the regulation of cell senescence (Groisman, Ivshina et al. 2006). It was believed a knockdown of CPEB according to this study will result in lack of senescence and thus proliferation of NPCs.

CPG15. Candidate plasticity gene 15 has been studied in the Cline Lab for many years. My interest in this gene was because of its various characteristics: it is activity dependent, it was shown to be involved in NPC survival, and it is regulated by dark-rearing. The Ingenuity results suggest that CPG15 is involved in NPC survival with the top network function for the 24hr harvest being cell death pathways. The prediction was that it would cause apoptosis or initiate differentiation in NPCs.

Dio3. Deiodinase, iodothyronine, type III is an enzyme in the thyroid hormone pathway. It is the enzyme which removes iodine from the active form of thyroid hormone (T3) effectively inactivating it. Dio3 was found in the ND1vND5/DD5vLD5/same filtered dataset; it was shown to be increased 0.77 and 1.02 favoring ND1 and DD1 respectively. T3 levels in *X. laevis* are low before the metamorphic stages (stage 52 to stage 63), but the presence of T3 receptors (TR) have been detected in NPCs suggesting that relative changes in T3 levels may have an effect. Increased proliferation correlates with increased thyroid hormone and TR activation in *X. laevis* tadpoles at metamorphic stages (Denver, Hu et al. 2009), therefore, a knockdown of Dio3 which will in effect increase T3 levels also is predicted to increase proliferation in the stages of interest.

Ef1A. Elongation Factor 1α encodes an isoform of the alpha subunit of the elongation factor-1 complex, which is responsible for the enzymatic delivery of aminoacyl tRNAs to the ribosome. It is a housekeeping gene that has been shown to be highly expressed in NSCs/NPCs from mouse ventral mesencephalon (Jung, Hida et al. 2004). It has been shown to be involved in several cellular processes in cancer biology including cell proliferation, survival, and motility (Pecorari, Marin et al. 2009). It was predicted that its functional knockdown will decrease NPC proliferation.

Elk4. Elk4 is a transcription factor in a member of the ternary complex factors (TDFs) which are regulated by extracellular regulated kinases (ERK) as part of the MAPK pathway of growth factor signaling; TDFs are implicated in cell proliferation (Buchwalter, Gross et al. 2004). Two probe sets of ELK-4 (*X. laevis* ELK4A) were seen differentially regulated in the ND1vSMC comparison. ND1vSMC raw dataset was explored to identify genes that may be regulated to cause the ND1 cells (early stage 48) to be more proliferative than SMC cells (late stage 48) as seen in Pranav Sharma's preliminary data. Both ELK4 probe sets were down regulated in ND1 by 1.03 and 3.04. There was not much literature on ELK4, which made it an attractive candidate; one of the applications of microarrays was to discover new genes of interest. What is more, ELK1 who shares regions of homology with ELK4 has been shown to interact with BRCA1 isoforms and its repression by BRCA1 genes have been shown to have anti-proliferative

activity in breast cancers (Maniccia, Lewis et al. 2009). Also, ELK1 has been shown to be repressed by Ndrg4 and its suppression is thought to support neuronal differentiation in PC12 cells (Hongo, Watanabe et al. 2006). Based on what little is known about ELK4 and its homology to ELK1, it was hypothesized that morpholino knockdown of ELK4 will result in decreased proliferation possibly by increasing differentiation.

MGC82106. This protein is thought to be an isoform of ELK4. This particular isoform was shown to be significantly regulated in the ND1vND5/ND1vSMC/same filtered dataset. It was decreased by 2.45 and 3.04 in ND1 cells agreeing with the above data for ELK4.

EphB1. Ephrin-B1, also known as Elk, is a type I membrane protein and a member of Eph-related receptor tyrosine kinases; it binds Ephrin-B family of ligand. EphB1 may play a role in cell adhesion and function in the development or maintenance of the nervous system. The ephrin family of genes such as EphA1 and EphB2 were represented in several of our analysis suggesting that ephrin mediated cascades are prominent in progenitor cells. EphB1 was found in the ND1vND5/ND1vSMC/same filtered dataset for searches of genes involved in maintaining stemness; it was upregulated 0.38 in ND1vND5 and 0.79 in ND1vSMC to favor ND1 cells. Additionally, EphB1 involvement in the growth factor receptor tyrosine pathway also enhanced its candidacy. Ephrin-B receptors have been implicated in NPC proliferation, migration, and polarity in the adult hippocampus (Chumley, Catchpole et al. 2007). Since many times, signaling pathways are shared between neurogenesis in the adult and during development, it was speculated that a knockdown of EphB1 would result in decreased proliferation.

Fmr1A. Fragile-X mental retardation protein 1 binds the RNA and is associated with polysomes. It is thought to be involved in mRNA trafficking from the nucleus to the cytoplasm. FMR1 was differentially regulated in the PreND1vPreND5 microarray which showed 0.42 decreases in pND1. Additionally, a protein similar to 82-kD FMRP Interacting Protein, proliferation-inducing gene 1 (AKA nuclear Fragile-X mental retardation protein interaction protein) was seen in the PreND1vPreND5 raw dataset as well as in the ND1vSMC raw dataset; PreND1vPreND5 dataset showed 0.73 decrease in pND1, ND1vSMC showed 0.49 decrease in ND1. The interest in Fragile-X mental retardation syndrome and all its related genes was because their role in neuronal proliferation was still controversial. One study showed that FMR1 increases NPC proliferation and alters its differentiation (Castrén, Tervonen et al. 2005) while another showed that FMR1 only alters NPC differentiation (Bhattacharyya, McMillan et al. 2008); the possible discrepancy to these studies is that each of the studies uses a different source of *in vitro* cells. An *in vivo* study may elucidate the role of FMR1 and related genes in proliferation of NPCs.

FXR1. Fragile-X mental retardation, autosomal homologue gene interacts with the functionally-similar proteins FMR1 and FXR2. Interestingly, it appeared in the filtered dataset for DD5vLD5/CPG24vCMo24/opposite for genes are may be involved in a CPG15 signaling in NPCs. It was up-regulated 0.48 in DD5 and was down-regulated 0.40 in CPG24. It was difficult to predict what the Fragile-X mental retardation proteins would

do in the morpholino knockdown experiments because of the conflicting data but according to the microarray data, it was predicted to increase proliferation by inhibiting differentiation.

GST-Pi. Glutathione S-transferase Pi 1 (GSTP1) is a member of the Glutathione S-transferases (GSTs); they are a family of enzymes that play an important role in detoxification by catalyzing the conjugation of many hydrophobic and electrophilic compounds with reduced glutathione. It is thought to GST-Pi is thought to play a role in the susceptibility to cancers. Clearly, GST-Pi is a much regulated gene that deserves to be among the candidate genes simply because it is the most prominent feature in the entire experiment. In general, GST-Pi was up-regulated in NPCs thus it was predicted that GST-Pi morpholino knockdown would result in decrease proliferation.

HDAC6. Histone deacetylases are responsible for the deacetylation of histones; epigenetic changes in chromosomes are involved in transcriptional regulation, cell cycle progression and developmental events. A unique role for HDAC6 in particular, is its role in microtubule-dependent cell motility via deacetylation of tubulin. HDAC6 is differentially down-regulated in ND1vND5, ND1vSMC, and DD1vLD1 by 0.40, 0.57, and 2.27 respectively; it appeared in the 3-way JMP comparison. HDAC6 expression has been correlated to estrogen response in breast cancers (Azuma, Urano et al. 2009), EGF signaling cascades in tumors (Kamemura, Ito et al. 2008), and thought to be a player in coupling cell cycle exit with neuronal differentiation and migration (Ajamian, Suuronen et al. 2003). According to the literature and microarray data which favors its expression in older NPCs (SMC) and non-proliferative cells (ND5 and LD1), HDAC6 knockdown was predicted to increase proliferation and/or decrease differentiation.

HSPA5. Heat shock proteins are a class of functionally related proteins whose expression is increased when cells are exposed to elevated temperatures and other physiological stress as part of the stress response. Its expression is transcriptional regulated via various activation pathways that detect changes in the environment as well as changes within the cell. It also has a role in normal cells as part of the proteasome pathway. HSPA5 is a member of the heat-shock protein-70 (HSP70) family regulated by glucose levels and is also known as glucose-regulated protein 78 (GRP78). It was represented in the 3-way filtered dataset. It increased in ND1 and DD1: ND1vND5 1.03, ND1vSMC 0.30, and DD1vLD1 0.24. There was nothing of note in the literature concerning HSPA5 involvement in neurogenesis, proliferation, or differentiation. However, there is some literature relating HSPA5 to cancer and cancer therapy as reviewed by (Lee 2007) suggesting a stem cell role that may translate similarly to NPCs. This candidate gene was chosen for its exploratory value in investigating how stress related pathways can affect NPCs. In light of the microarray data, it was predicted that HSPA5 knockdown will result in decreased proliferation.

MMP9. Matrix metalloproteinase (MMP) family are involved in the breakdown of extracellular matrix. They are involved in normal physiological conditions involving development and tissue remodeling as well as in disease processes particularly in metastasis of cancers. MMP9 is a TypeIV collagenase. It was another candidate gene

taken from the 3-way filtered dataset and it was down-regulated in ND1 and DD1: ND1vND5 by 3.2, ND1vSMC by 4.95, and DD1vLD1 by 3.26. MMP9 has been shown to be expressed in dividing granule cells in the adult monkey hippocampus after an ischemic attack and is thought to play a role in neurogenesis. (Buck, Bradford et al. 2008). Another study showed an up-regulation of MMP9 in response to retinoic acid in neuroblastoma SKNBE cell line also suggesting a role in differentiation of NPCs (Chambaut-Guérin, Hérigault et al. 2000). It was predicted that the knockdown of MMP9 will delay differentiation signals and thus increase proliferation.

PMR1. Polysomal ribonuclease 1 is a 60 kDa endoribonuclease from *Xenopus* liver polysomes; it was identified as a ribonuclease involved in the estrogen-regulated destabilization of serum protein mRNAs. PMR1 was differentially regulated in DD1vLD1, ND1vSMC, CPG12vCMo12, and CPG24vCMo24 in the same direction: 3.05 up in DD1, 3.97 up in ND1, 1.49 up in CPG12, and 3.23 in CPG24 respectively suggesting a role in the proliferation or cell-death pathway. The literature was very limited in this gene which was identified originally in *Xenopus* oocytes and liver; there is some homology to other peroxidases such as lactoperoxidase, myeloperoxidase, and eosinophil peroxidase. Nevertheless, its prominent regulation in four of the six raw data sets warranted an investigation.

PRKACA. CyclicAMP-dependent protein kinase catalytic subunit alpha is one of the enzymatic subunits of cAMP-dependent protein kinase (PKA). The inactive kinase holoenzyme is a tetramer which has two regulatory and two catalytic subunits. cAMP binding causes the dissociation of the inactive form into a dimer of regulatory subunits bound to four cAMP and two free monomeric catalytic subunits which catalyses various targets. It was identified in the ND1vND5/DD1vLD1/same filtered dataset: 0.47 up in ND1 and 0.36 up in DD1 suggesting PRKACA and the PKA pathway may be involved in NPC stemness state. The PKA pathway is a signal transduction pathway involved in many signaling cascades thus its knockdown was difficult to predict. However, according to the microarray data, its knockdown should decrease proliferation and increase differentiation.

Wnt7B. Wingless-type MMTV integration site family, member 7B is in the Wnt family of genes. The Wnt genes are ligands that bind members of the frizzled family of seven transmembrane receptors and together the Wnt/Frizzled pathway has been implicated in patterning and proliferation of NPCs. Wnt7B was differentially up-regulated by 0.7 in ND5 in the raw dataset for ND1vND5 suggesting its involvement in pathways of neurons. Wnt7B was found to regulate epithelial and mesenchymal proliferation and vascular development in the lung (Rajagopal, Carroll et al. 2008) and found to be differentially regulated in human breast tissue (Rajagopal, Carroll et al. 2008). Additionally, Wnt7B was found to stimulate proliferation of embryonic mouse cortical progenitors and increased the number of cells that can generate primary neurospheres (Viti, Gulacsi et al. 2003). Given Wnt7B involvement in the proliferation of various tissues, it was predicted that a functional knockdown would decrease proliferation in the brain.

Control morpholino. The control morpholino used in these imaging experiments was specifically designed against the CPG15 gene sequence. It was a miss-match control for the CPG15 morpholino but GeneTools representatives suggested that it could be used as an initial control for any morpholino. If further investigation of a morpholino other than CPG15 is carried out, sequence specific control morpholinos will be used to verify the initial results.

4.2 Methods

This section of the thesis was newly developed with the assistance of Jennifer Bestman. She has collaborated with me on all parts of the imaging project presented here from optimization of WBE protocol to the final analysis. Her expertise in *in vivo* imaging and imaging analysis was essential to this project.

4.2.1 Whole brain electroporation

Bulk tectal cell transfections of plasmid DNA and morpholinos (WBE) were accomplished by whole brain electroporation (Haas, Jensen et al. 2002). Briefly, a glass pipette (World Precision, Instruments, Sarasota, FL, Cat.#MTW100F-3) was made using a Sutter P-97 (Sutter Instruments,) puller and Pipette Cookbook protocol for Xenopus microinjections. It was filled with DNA (2-5µg/µl) and/or morpholino (1mM) solution with 0.01 % Fast Green (Sigma-Aldrich, Cat.#F7252) and inserted into the ventricle of the anesthetized st47 tadpole. The DNA was pressure injected into the ventricle with a picospritzer (Picospritzer II, General Valve Corporation, Fairfield, NJ). A custom made platinum electrode with two parallel plates was placed on either side of the tectum, and brief stimulations (five exponential decay pulses, 45-47 volts, 1.6 ms duration, 1 sec of interval, 1Hz, field strength 200 V/cm at peak, time constant of 70 ms, generated by a SD9 Stimulator (Grass Instruments, Quincy, MA or Grass Technologies, Warwick, RI) was delivered across the whole tectum between the platinum plate electrodes. The polarity of the pulses was switched to electroporate the other side of the brain. This method provides high efficiency delivery of genes of interest and morpholinos into multiple neurons in tectum. Tadpoles recovered from anesthesia within 10 minutes, and were returned to the 12-hour light/12-hour dark cycle incubator. Experiments were 24hrs to 36hrs after electroporation at stage 48.

4.2.2 Imaging protocol

The imaging protocol took into account many factors and many permutations were made to optimize it. Such factors such as the unanticipated behavior of Kaede fluorescent protein in *X. laevis* and the interference of red-lissamine tagged morpholino during imaging had to be dealt with multiple trouble-shooting experiments not detailed below. Thus as a reminder note: the protocol presented here is the final version and in comparison to the work it took to obtain the images, the work done in developing it was far greater.

4.2.2.1 Experimental Set-up

Animals used for the imaging protocol were electroporated by WBE with two plasmids: Sox2/Oct3.mFGF4-Gal4VP16-eGFP (JLO#87) and 14xUAS.mFGF4-Kaede plasmid (JLO#123) each at the final concentration of 0.5µg/µl. The plasmid

concentrations were determined by electroporation by WBE of various combinations of serial dilutions of the two plasmids; concentrations between 0.1µg/µl and 2µg/µl were tested and the resultant concentration of 0.5µg/µl was decided to be optimal. Morpholinos were electroporated at the final concentration of 0.1mM. This concentration of morpholino was chosen because it was the lowest concentration that could produce an effect according to (Falk, Drinjakovic et al. 2007) but also was just enough to image the red-lissamine at full 100% laser power. Since, the Kaede-red was imaged at laser powers at the lower end of the spectrum (2-30%) the morpholino was minimally detected during the imaging of the Kaede-red. The three day or the 2hr time-lapse imaging protocol began 24hrs to 36hrs after WBE. Animal husbandry prior to the experiments was performed according to (Methods 2.2.3).

Laser and microscope set-up. For daily experiments, animals were anesthetized, placed in a sylgard chamber, imaged, and placed in a 6-well plate to recover. For 2hr time-lapse experiments, 6-7 animals were placed in a specialized imaging chamber constructed by myself and Jennifer Bestman (Methods 4.2.2.2); 2hr time-lapse images were taken without anesthesia. All animals were imaged using a PerkinElmer UltraVIEW VoX spinning disk confocal system with FRAP PhotoKinesis device set-up on an Olympus Ix81 upright microscope. Confocal system included the CSU XI A3 scanner unit equipped with multiple filter sets for ultra-fast scanning (Yokogawa Electric Corporation, Newnan, GA), EM-CCD Camera (Hamamtsu Photonics, Bridgewater, NJ, Cat.#C9100-02), ASI xy-motorized & z-Piezo stage (ASI Instruments, Warren, MI), and four lasers. The four lasers consisted of a UV-405nm 50mW laser for photo-conversion, diode laser for 488nM excitation of Kaede-green, 561nm 50mW laser for excitation of Kaede-red, and 640nm 40mW laser not used in this study but would excite far-red fluorescent proteins. The software interface for image acquisition was PerkinElmer Volocity Acquisition and Image Analysis Software by Improvision.

Photoconversion. Kaede-green expressing cells were photo-converted using the 405 laser either by using the FRAP PhotoKinesis device or by opening the confocal shutter. If single cells were being photo-converted, a ROI was drawn within the cell body and photo-converted at full power 405nm laser and at 50-100cycles per PhotoKinesis initiation; 1-5 initiations were required for full conversion (Figure 4.1-A to F). Full conversion was defined as Kaede-red intensity change was no longer detected by the program with subsequent initiations; care was taken not to photobleach the converted Kaede-red with over-exposure. If all the cells in the tectum were being photo-converted, the tectum was exposed to full power 405nm laser by opening the laser shutter for 1-to-4 30sec sessions; the piezo stage was moved manually during the 30sec session to assure deeper cells were also exposed to the laser. If morpholinos were used in the experiment, an image prior to photo-conversion was taken using optimal imaging settings for both green and red channels.

Daily imaging. Imaging the photo-converted Kaede-red was optimized for each tecta of each animal on the first day of imaging. Laser power, imaging times, and/or camera sensitivity settings were changed to allow for the full range of intensity recordings without any saturated pixels for Day1 images and were kept the same for subsequent

imaging sessions; imaging conditions were set with the knowledge that Kaede-red will intensify slightly over time (personal experience). The Kaede-green channel was set at a very low setting (2-4%) laser power and had the same imaging times and camera sensitivity settings as Kaede-red channel; Kaede-green was kept low because Kaede-green was still being produced by these cells and the green channel became over-saturated over the 24hr interval using any other settings. Having the same channel settings for both Kaede-red and Kaede-green allowed for red to green ratio comparisons over all three days of imaging. Tracking of photo-converted Kaede was shown to be able to follow division events. (Figure 4.1-G to I)

2hr time-lapse imaging. Both channels were optimized across all animals avoiding any over-saturated pixels for the first day of imaging and taking into account the changes in Kaede-red and Kaede-green. The imaging protocol was programmed into the Volocity software to acquire data every 2hrs over days; it controlled the stage position in x, y, and z-axis, the objective position for each points of interest, the channel conditions, the laser shutter, and the camera. The animals were placed in the multi-tadpole chamber and perfused with Steinburg's solution using a peristaltic pump (Rainin, Oakland, CA, Cat.#7103-054) at approximately a drop per 2-3 seconds. First an initial image was taken. Then using the PhotoKinesis device, some cells of interest were photo-converted as described above. After which, the control of the imaging session was taken over by the Volocity program and manually checked every 8-10hrs. Only some animals survived for multiple days of imaging while some did not even survive 2hrs; the maximum imaging time was over 4days.

4.2.2.2 Construction of multi-tadpole chamber

The multi-tadpole chamber was constructed onto Nunc MiniTrays (Thermo Fisher Scientific, Rochester, NY, Cat.#163118 or Cat.#163118). A low temperature glue-gun was used to make channels between the wells where the tadpoles were to be placed. A nylon hammock was fashioned to suspend the tadpoles in the space between four miniwells; the tadpoles' respiratory apparatus is on the underside of the animal so suspension of the animal decreased the likelihood of suffocation. The 60μm hydrophilic nylon mesh (Millipore, Billerica, MA, Cat.#NY6000010) was cut into a rectangle, slung across the space and tacked down onto the four corner wells using a dab of hot-glue into each well; a pocket for the tadpole was maintained by pressing a cut p200 micropipette tip into the center while the corners were being secured. One 16g syringe needle was bent and placed in one of the channels to act as an output source. Then a No.1 24x60mm cover glass (Corning, Lowell, MA, Cat.#2935-246) was placed so that the tadpoles' mouths were exposed, the tectum was covered, and the syringe needle was under the glass; this immobilized the tadpoles while minimizing suffocation. Then using hot-glue all spaces not covered by the cover glass was filled such that the perfusion solution may only enter through the top of the cover glass where mouths are located and exit through the syringe needle located under the cover glass; this created a flow of solution from the mouth of the tadpole to the tail. The perfusion solution input was fashioned using a cut and bent p200/p1000 micropipette tip. Two binder clips were glued on the plate walls to hold down the cover glass. Then the entire MiniTray was glued on to a Nunc rectangular dish (Thermo Fisher Scientific, Cat.#267060) and a back-up output, a cut and bent p1000

micropipette tip, was secured with hot-glue. The tubes to the peristaltic pump for the input and the back-up output were a larger gauge than the tube for the output located under the cover glass; the overflow of the MiniTray was preferred than the situation where the MiniTray is sucked dry by lack of input (Figure 4.2).

4.2.2.3 Experimental conditions

Animals were reared under normal 12h light/12h dark conditions until stage 46 when experiments started. Three different experimental conditions were used for the imaging experiments as explained in detail below. The visual-deprivation protocol was the control baseline condition. The visual-stimulation protocol was used to test the effects of the visual experience or brain activity paradigm. The cell-division inhibitor drug treatments were used to test whether we could identify cell proliferation events in the imaging assay.

Visual-deprivation. Animals were deprived of visual stimulation by wrapping tadpole dishes with aluminum foil after WBE and after each 24hr imaging session. This served two purposes. One was to keep Kaede-green from photo-conversion by natural and incandescent light; only filtered light using a UV-blocking film prevents Kaede photo-conversion. Second, since previous experiments showed that light deprivation resulted in increased proliferation, we anticipated that changes in cell proliferation would be easier to detect under baseline conditions in which proliferation rates were increased. This will be referred to as the "control" experimental condition.

Visual-stimulation. Animals for visual stimulation treatment were taken from the dark, imaged on Day1 after photo-conversion of Kaede, and placed back in the dark. On Day2, they were imaged and placed in a chamber with flashing green LEDs (light-box) for 12-18hrs before the final Day3 image. In this way, proliferation rate for the first 24hrs can be compared to proliferation rate for the second 24hrs, to test whether visual stimulation decreases cell proliferation as seen in preliminary experiments by Pranav Sharma with BrdU labeling.

Cell-division inhibitor drug treatments. Two cell-division inhibitors and their application protocol were used according to (Caron, Prober et al. 2008). Tadpoles were incubated in a mixture of 2% DMSO (Sigma, Cat.#D8418), 20 mM hydroxyurea (Sigma, Cat.#H8627) and 150 µM aphidicolin (Sigma, Cat.#A0781) 6 hours before the imaging session on Day1. This was done because the drug, aphidicolin, inhibits cell division by blocking DNA replication during (S-phase) and the suspected cell-cycle time for *Xenopus* cells was thought to be 8-12hrs from BrdU experiments. If a cell enters the cell cycle just prior to the D1 imaging session, it may be recorded as a division event for D2. One set of animals was kept in the proliferation-blocking drug in DMSO solution (Drug-treated) or DMSO-only solution (DMSO-treated control) throughout the Day1, Day2, and Day3 imaging sessions. The second set was placed back in Steinburg's solution after the Day2 imaging session to test whether cell proliferation increased following the wash-out of the proliferation-blockers. For both sets of experiments a control set of animals in only 2% DMSO was also imaged along side the experimental animals.

4.2.3 Imaging analysis

The analysis of the images was done by eye, comparing images over three days. Because the field of view can change along the x, y and z dimensions for each of the days of imaging, data sets were first reviewed to identify regions of the tectum that were within the field of view over the 3 days. Cells in these regions were identified in the first image and were followed in subsequent images (as either present or absent) and all additional cells were identified in the day 2 and day 3 images using both red and green channels; green only cells were omitted from the count. All 2-D image analysis should be confirmed by 3-D image analysis as explained in detail below.

All two-dimensional cell counts were analyzed in Excel spreadsheet. Normalized changes over Day2-Day1, D3-D2, D3-D1 were calculated by first taking the difference of cell numbers over the days in question then dividing by the initial day cell count; the resulting value is the normalized change in the number of cells per cells present on the initial day in question. The normalized change in cell number was multiplied by 100 to represent the value as normalized percent change. A Mann-Whitney test was performed between experimental groups and a Wilcoxen paired-test was performed within experimental groups. When three groups were considered, a 1-way Anova test between all pairs was performed using Tukey error correction.

All data analysis in which cell counts were determined from three-dimensional image sets was performed by Jennifer Bestman. The software, Volocity, was used for the measurements.

4.3 Results

Only a portion of the data was analyzed to date. The comparisons done were the control experiments: Drug-treated verses DMSO-treated control and control (visual deprivation) and control verses control morpholino (CMo). The experimental conditions that were analyzed are: Visual stimulation, CPG15 morpholino verses CMo, and Dio3 morpholino verses CMo.

4.3.1 Control experiments

A three-way comparison was done between drugs treatment groups (n of 9 tecta) and control groups (Figure 4.3), both untreated controls n of 9 tecta and DMSO-treated controls n of 9 tecta using a 1-way Anova test. Between D1 and D2, the animals were exposed to cell-division inhibiting drugs in DMSO or DMSO only, and between D2 and D3, the animals were placed in Steinberg's solution to recover (Figure 4.4). The average normalized percent change between Day1 and Day2 of drug-treated experimental group was -2%, DMSO-treated control group was 13%, and untreated control group (dark-deprived control) were 15%. The average percent change between Day2 and Day3 of Drug-treated was +2%, DMSO-treated was -1%, and untreated was +6%. The exposure to cell-division inhibiting drugs caused a significant arrest of cell proliferation between Day1 and Day2 (p-value <0.01). By contrast, there was no difference in proliferation between Day2 and Day3. There were no significant differences between the untreated control and DMSO-treated control between Day1 and Day2 or Day2 and Day3 (Figure

4.7-A). There were no significant differences between control and CMo between Day1 and Day2 or Day2 and Day3 (Figure 4.6-G to I).

4.3.2 Experimental conditions

For the visual-stimulation experiment (Figure 4.5), changes in cell numbers over the first 24h interval, during which animals were kept overnight in the dark, were compared to changes in cell numbers over the second 24h interval, when the animals were exposed to 16hrs of visual stimulation (D2-D1 verses D3-D2); 9 tecta were analyzed. The normalized percent change between Day1 and Day2 was +18% and between Day2 and Day3 was -5%. Light-stimulation caused an arrest of proliferation between the Day2 and Day3 as compared with a Wilcoxen paired test (p-value of 0.01). A Wilcoxen paired test of control animals resulted in no significant changes between the same two days.

The morpholino experiments showed that CPG15 morpholino decreased the number of Sox2 FP-expressing cells over the three days of imaging (Figure 4.6-A to C). Between Day1 and Day2 of imaging, cell numbers decreased by an average -3% in CPG15 morpholino-treated animals, compared with an average increase of 8% in the animals treated with control morpholinos resulting in a significant difference using the a Mann-Whitney test (p-value <0.01, Figure 4.7-C). Although relative changes in cell numbers were not significantly different between the two groups between D2 and D3, comparing cell numbers over the three imaging sessions, shows a significant decrease (p-value of 0.01).

The Dio3 morpholino experiment showed increases in average difference by 7% between D1 and D2, 12% between D2 and D3, and 19% over all three images (Figure 4.6-D to F). These values are comparable to changes in cell numbers in control morpholino-treated animals (Figure 4.7-D). The 3D analysis of the Dio3 morpholino done by Jen Bestman agreed with the 2D data presented over the two days.

4.4 Conclusion

4.4.1 Candidate genes were chosen using various filtering methods

The candidate genes were chosen for their involvement in mechanisms that govern proliferation and differentiation in NPCs as suggested by the microarray data; there was a particular bias toward genes that may be regulated by activity. The JMP analysis done to filter the raw datasets such as ND1vND5/ND1vSMC was aimed at filtering out genes involved in proliferation while ND1vND5/DD1vLD1 and ND1vND5/DD5vLD5 were aimed at filtering out stem cell genes that are activity dependent; this JMP results still returned datasets in the hundreds of genes. Ingenuity analysis of these JMP filtered dataset, DD1vLD1/ND1vSMC and ND1vND5/ND1vSMC confirmed that many of these genes were indeed involved in pathways relevant to regulation of stem cells such as pathways and functions involved in proliferation, growth, DNA replication and repair, cell morphology, Notch signaling, cell death, and organ development, to name just a few of the results presented fully in the Microarray Results Section (Section 3.2.5).

The 3-way JMP filter of ND1vND5/ND1vSMC/DD1vLD1 was aimed at highlighting genes that may be involved in both activity regulation and proliferation. The

pared down dataset consisted of 30 genes. Another approach to discovering activity regulated proliferation genes was to use the raw dataset resulting from the CPG15 morpholino microarrays. The filtered dataset returned by the ND5vLD5/CPG24vCMo24 JMP comparison was to highlight genes that may be regulated by CPG15, which is, itself, an activity regulated gene; this filtered dataset resulted in 185 genes. All these JMP analysis and Ingenuity pathway analysis highlighted many genes with great biomedical promise. Although only fifteen genes were initially chosen for imaging analysis, additional genes from the dataset are worth pursuing for future experiments.

4.4.2 Kaede can be used to observe dividing cells *in vivo* using a 24hr time interval

Photo-converted Kaede was intended to be used to label single cells in the sea of cells electroporated by WBE in the brain so that their proliferation and differentiation could be imaged over time; however, we abandoned this strategy because of the concern that selecting the cells for the imaging experiments would bias the results. In most experiments, all Kaede-expressing cells were photo-converted. The photo-conversion of Kaede was used to mark all the cells on the first day of imaging (Day1); it assures us that the cells that are being counted for the analysis were present on the first day of imaging. Therefore, Kaede-red cells on Day2 and Day3 were either cells that were present on PTD1 or cells that were daughter cells of cells that were present on PTD1. The origin of green-only (non-converted Kaede) seen in Day2 and Day3 images is unknown. There are several speculations to their origins. They may be cells that had such a low expression of Kaede that they were non-detectable on Day1 but their continued expression of Kaede-green allows them to be detectable on Day2 or Day3. Green-only cells may have only begun to express Sox2/Oct3 after PTD1. They can be cells with leaky eGFP. The leaky eGFP can be from the driver construct which has Sox2/Oct3.mFGF-Gal4VP16-eGFP. Technically, there should be no expression of eGFP because the Gal4VP16 has its own poly-A tail and stop codon, but preliminary experiments with this driver plasmid construct alone showed the eGFP eventually visibly expressed by PTD3. In any case, because we cannot be sure of the origins of the green-only cells, they were omitted from the analysis. Despite the unknown origins of the green-only cells, the preliminary time-lapse experiment (Figure 4.1) showed that dividing cells can be observed using a 24hr time interval using Kaede to mark cells on the first day of imaging.

4.4.3 Sox2 reporter labels proliferative cells

Two control experiments were done to test whether the cells labeled by the Sox2 reporter were proliferating brain cells (NPCs) whose proliferative activity can be inhibited by cell division blocking drugs and whether the labeled cells were not affected by the morpholino electroporation method by using a control morpholino against CPG15. The drug treatment experiment was done to test that Sox2 labeled cells were proliferating cells NPCs. The Sox2 labeled cells were exposed to cell-division inhibitor drugs between the D1 and D2 imaging sessions; thus blockage of proliferation events was tested between D1 and D2 images. Between the imaging session Day2 and Day3, the animals were removed from the drug treatment placed in Steinberg's solution to test whether the Sox2 labeled cells would recover from the cell-division blocking drug. The data shows that there were significant reduction of cell-division between Day1 and Day2 but no significant difference in cell-division between Day2 and Day3. Another cell division

control was done where drug was applied for both D2 and D3 images, but that data has yet to be analyzed; a first glance impression of this dataset shows inhibition of proliferation between D1 and D2 images and some noticeable cell death in D3 images. This may be because proliferative cells arrested in cell-cycle may be forced into an apoptotic pathway. This characteristic, if true, may be another screening application of the albino *X. laevis* model system: drugs that may affect cell division for cancer therapy purposes can be bath applied to these animals and screened for cell death inducing characteristics in the brain and/or other visible organ systems.

The second control experiment was designed to test whether the delivery and presence of control morpholinos affected cell proliferation and health. The control animals not electroporated with morpholinos verses CMo showed no significant difference in percentage of normalized cell-number change between D1 and D2, D2 and D3, and D1 and D3. However, I noticed that the p-value decreased between the D1-D2 and D2-D3 foreshadowing a possible late off target effect on D3-D4. This may also be due to the small sample size. Both the control experiment with division-blocking drugs and the CMo experiment showed that reporter labeled cells were proliferating cells; both sets of data show increases in percentage of normalized cell count over all three days. This data taken together with the proliferation inhibiting drug data, shows further evidence that the reporter was functioning as designed to label proliferating NPCs.

4.4.4 Visual experience inhibits proliferation

Visual experience experiment was to test whether exposure to flashing LED lights would alter the proliferation properties of Sox2 labeled cells in tecta. Data showed an increase in percentage of normalized cell-count between D1 and D2 images during which time the animals were kept in the dark but a decrease in cell count between D2 and D3 images during which the animals were exposed to light activity. This agreed with Pranav Sharma's unpublished halogenated deoxyuridine (XdU) data which showed increases in proliferation rate of XdU-labeled cell with visual-deprivation compared to the proliferation rate of Xdu-labeld cell with visual experience. I made an additional observation made with this *in vivo* imaging dataset that would not be possible with XdU experiments: I noticed there was a decrease in cell count because of cell death. This was evident by the presence of cellular debris or loss of newly born cells on D3 images where the cells were exposed to visual activity. This may be due to visual-activity inducing mechanisms which resulted in death of newly born cells.

Several studies have suggested a role for activity in neuronal survival and differentiation. It has been shown in the rodent olfactory bulb physiological activity regulates the survival of newly generated neural cells from the subventricular zone. Additionally, it has been shown the blockade of NMDA receptor activity increases developmental apoptosis in granule neurons of the rodent cerebellum. I hypothesize that the default state of NPCs is proliferative and activity is directive of differentiation. In this way, activity may be required not only for the proper wiring of the visual network of the *X. laevis* tadpoles but also for the proper regulation of brain development.

4.4.5 CPG15 morpholinos causes cell death

I had found that animals transfected with CPG15 morpholinos caused increased cell death during the microarray harvesting experiments. The brains of animals who were transfected with CPG15 morpholinos showed cellular debris by PTD5 and when cells were triturated for the cell picking process, the Sox2 labeled cells did not contain red lissamine labeled CPG15 morpholino suggesting that those cells that contained CPG15 morpholinos did not survive. This prevented me from harvesting PTD5 for the microarray experiments. The numbers of labeled cells decreased significantly between Day1 and Day2 images. The decrease during D2 and D3 was not significant. The decrease insignificance in cell death rate between D2 and D3 may have two reasons. One reason may be due to the slight decrease in control morpholino cell count which offsets the significance between the two data sets. The other reason may be due to the fact that the remaining cells after D2 are not NPCs and therefore is not affected by CPG15 knockdown in the same manner. The surviving cells at D3 tend not to have radial glial morphologies and appear to be neurons with elaborate dendritic arbors. The hypothesis is that CPG15 is a cell survival factor for NPCs as seen in (Putz, Harwell et al. 2005) but in the differentiating NPCs and differentiated neuron, CPG15 is a differentiating factor (Cappelletti, Galbiati et al. 2007) and neurite outgrowth promoting factor (Tadahiro, Zhen et al. 2008). The CPG15 knockdown experiment confirms *in vivo* what has been found using *in vitro* tissue culture experiments: CPG15 absence results in NPC death. To investigate further, it would be interesting to study the role of activity in NPCs with CPG15 knockdown because it is still not clear if CPG15 is activity dependent in NPCs. If CPG15 is indeed an activity up-regulated gene in NPCs, then it would be interesting to speculate on how its cell survival or anti-apoptotic role correlates with the cell death results seen in the activity stimulation imaging experiment above. Even more interesting would be to functionally knockdown genes shown to be differentially regulated in the CPG15 functional knockdown microarray experiments to tease out the pathways which involve CPG15 to determine if CPG15 is more closely associated with NPC survival, growth, and differentiation or NPC death.

4.4.6 Dio3 may increase NPC proliferation

The Dio3 morpholino experiment is by far the most interesting one. This is not because there were significant differences between Dio3 knockdown and CMo. It is because the problem must be more complex than originally postulated and the actions of Dio3 are not so easily discernable. It was hypothesized that Dio3 would increase cell proliferation because studies using thyroid hormone showed increases in cell proliferation in *X. laevis* brain cells (personal communication, Hollis Cline). This suggests that the mechanisms for thyroid hormone response are in place in NPCs at the stages of interest. Although there was an upward trend of cell count, the difference was not statistically significant because of the large heterogeneity in the Dio3 samples. One possible reason for the variance in the Dio3 data set is that compensatory mechanisms may be at play. Another reason is that the Dio3 morpholinos were tested in animals that were deprived of visual experience for 24hrs or more over the course of the experiment. Consequently the proliferation rate of the NPCs may already be at a ceiling in the visually-deprived control animals. Therefore, any further stimulation of proliferation due to the functional knockdown of Dio3 may not be detectable in the visually-deprived control animals. A

follow-up experiment where Dio3 morpholino animals were kept in the dark between D1 and D2 imaging sessions and were provided with visual stimulation between D2 and D3 imaging sessions was performed to test this hypothesis but this data have not been analyzed yet. I expect that Dio3 morpholinos will show increased proliferation during the D2-D3 interval when compared to animals treated with control morpholinos.

4.4.7 Observation of Sox2+ NPCs showed both symmetrical and asymmetrical events in the *X. laevis* tectum

Both the 24hr-3day imaging protocol and the 2hr-3day imagine protocol captured several division events. Some division events seemed to be symmetrical. In those cases, the red-to-green ratio was similar in the two daughter cells suggesting equal distribution of cellular components associated with symmetrical division patterns. Other division events were clearly asymmetrical where one daughter cell distinctly had a different morphology than the other. In the asymmetrical cases, I observed that the red-to-green ratio was different in the resulting daughter cells suggesting unequal distribution of cellular components associated with asymmetrical divisions; however, a more quantitative analysis of the red-to-green ratios of Kaede fluorescence in NPCs and progeny is necessary to confirm the qualitative observations.

Figure 4.1 | Photo-conversion of Kaede. One cell expressing only Sox2 reporter constructs, i.e. no morpholinos, was photo-converted using the FRAP photokinesis module on the Perkin-Elmer Confocal set-up. **(A-F)** Time-lapse images of photo-conversion using both green and red channels the cell marked by arrow before the photo-conversion (A) and after photo-conversion (B-F). Astrisk marks the relative size and placement of the photokinesis module. Notice the Keade-red spread throughout the cell leaving two green halos indicating the location of the two cell bodies (F). These images were taken at the maximum continuous speed using 2micron slices of a 20micron section. **(G-I)** These images are through 1micron slices of a 40micron section after fully photo-converting Kaede on Day1 (G), Day2 (H), and Day3 (I). Images show a close-up of the photo-converted cell appearing to cycle through a cell division event. The daughter cells have unequal distribution of Kaede-red. The dimmer cell is below the brighter cell and the brighter cell appears to be dividing again (H).

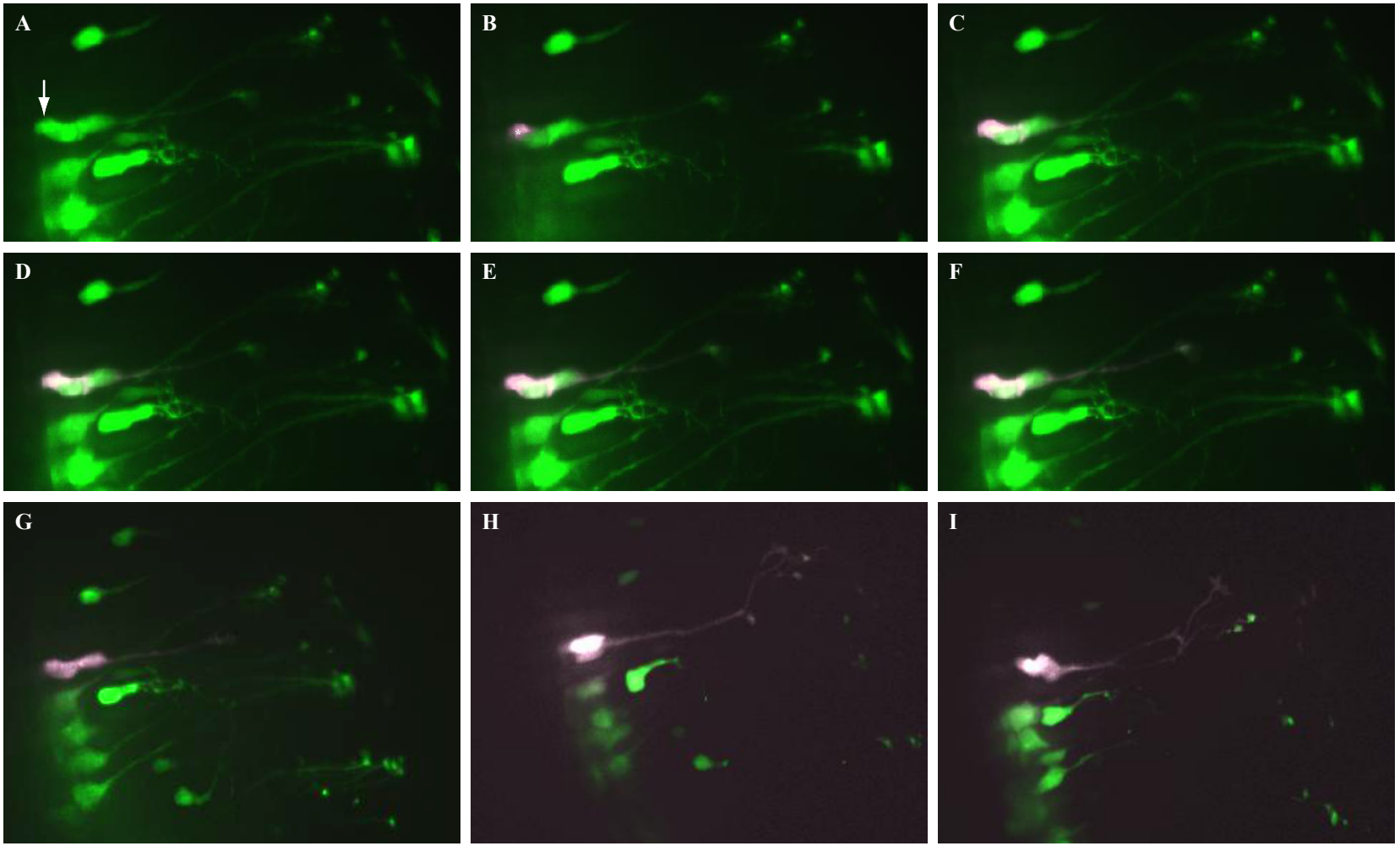
A
B
C
D
E
F
G
H
I

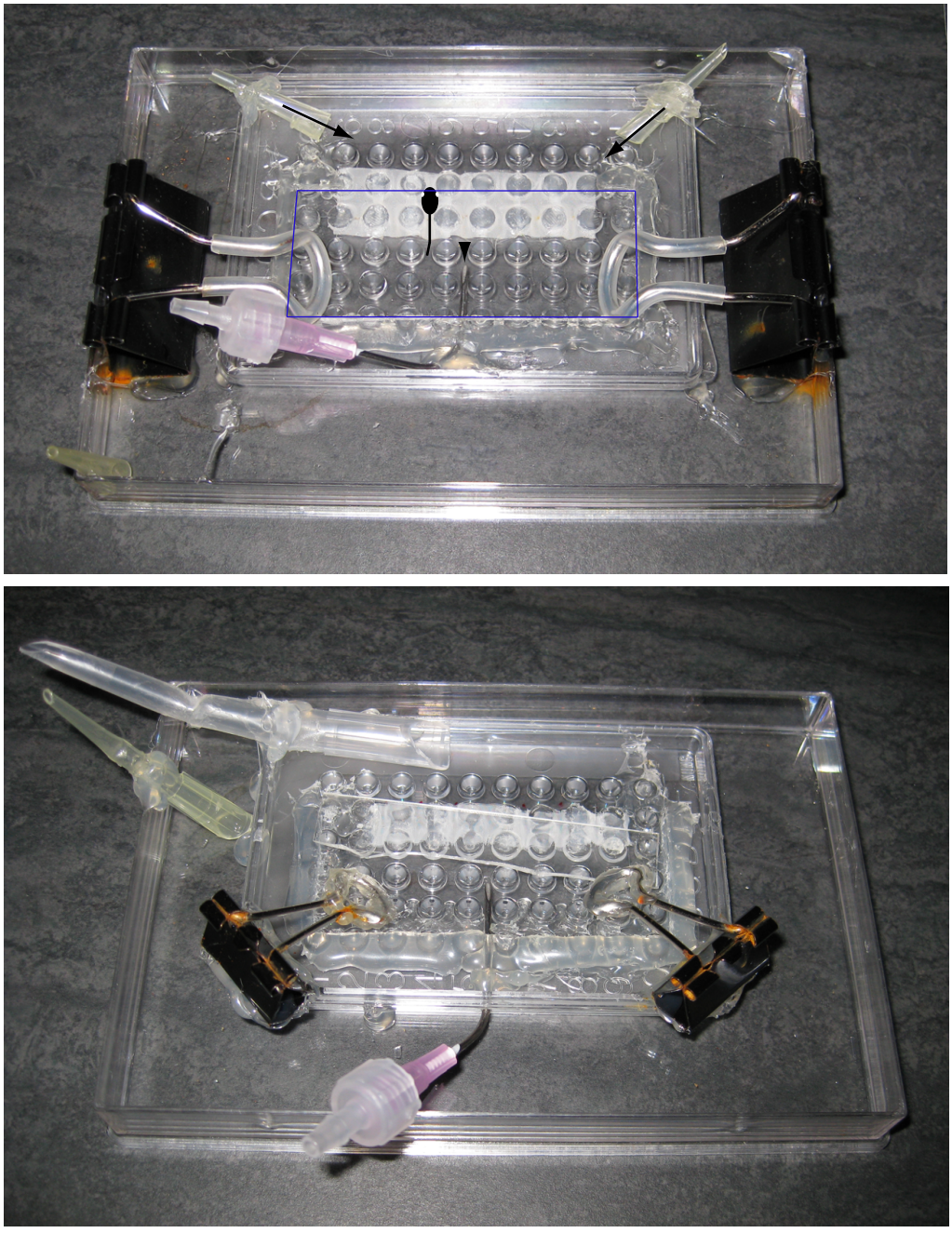

Figure 4.2 | 24hr Imaging chambers. Two different versions of the 24hr imaging chambers/ Top chamber shows a cartoon of tadpole positioned on the hammock. The blue outline shows cover glass position. Arrow show Steinberg's solution outtake source from the peristaltic pump and arrowhead shows Steinberg's solution intake source back to the peristaltic pump.

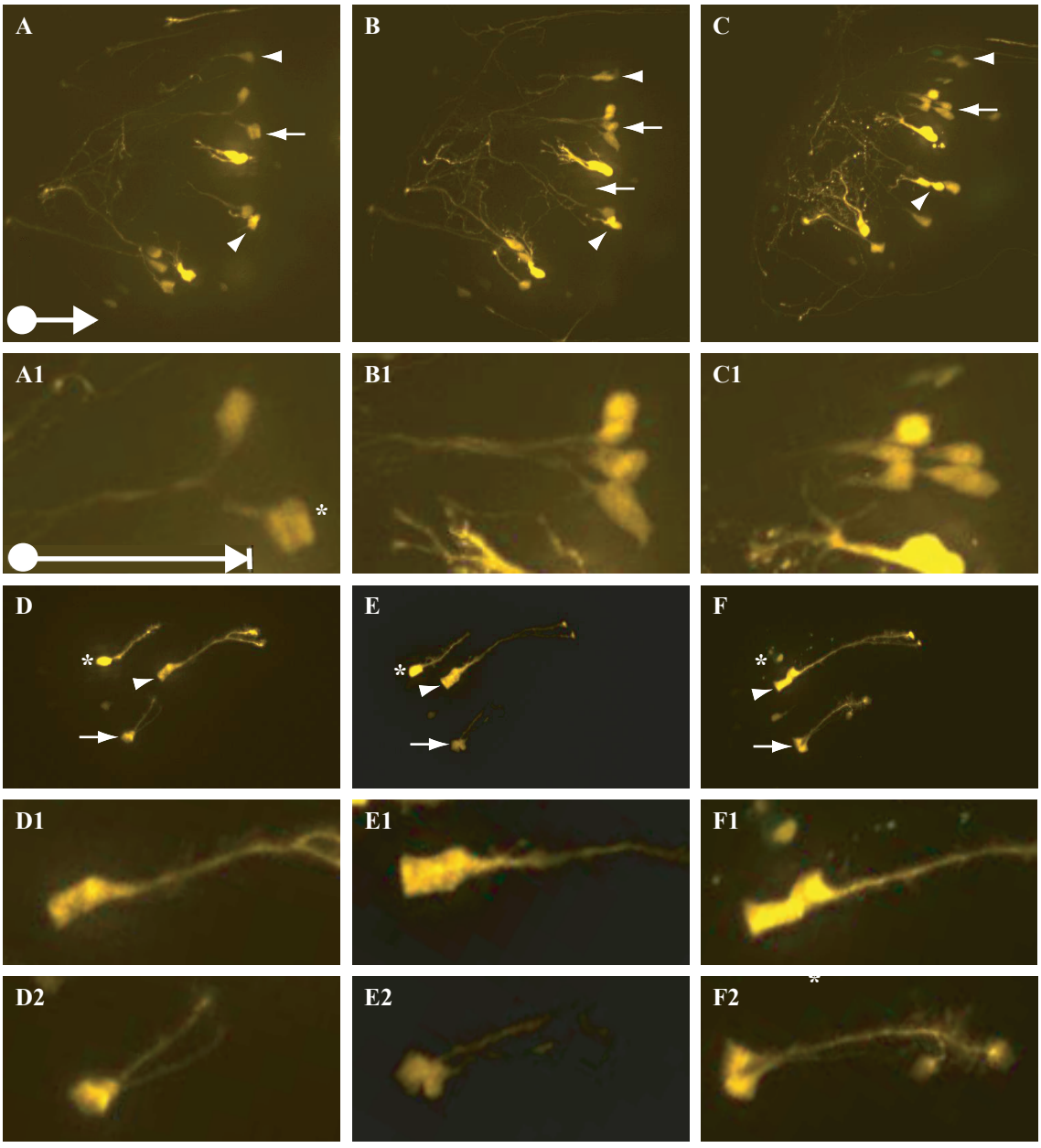

Figure 4-3 | Control brains. These cells were transfected by WBE and imaged over three days while being dark reared. **(A-C)** Images show multiple division events over (A) Day1, (B) Day2, and (C) Day3. Arrowhead and arrows show cells that appear to undergo cell division. **(A1-C1)** Images show two cells with arrows that go through cell-division over three days. One cell marked with asterisk undergoes cell-division twice. **(D-F)** Another set of images of cells in another animal with (D) Day1, (E) Day2, and (F) Day3. Two cells undergo division marked by arrowhead and arrow. Also, notice the cell that undergoes cell-death and the debris that results: asterisks over three days. **(D1-F1)** Cell with arrowhead. In (F1) the axis of division is nearly visible. **(D2-F2)** Cell with arrow. The scale bar for both magnifications are 70microns.

Figure 4.3 | Cell division inhibitor drugs. There are two image sets: one from control-treated group and the other from drug-treated group. **(A-C)** Images of control-treated group (DMSO-only) show cell (1) that fit the criteria for a basal progenitor cell undergoing cell-division. Cell (2) shows radial glia morphology undergoing interkinetic nuclear migration over Day2 and Day3 images **(B2-C2)**. Cells (4 and 5) show division events between Day2 and Day3 **(B3-C3)**. Cell (4) is located behind the cells marked with arrowheads on Day1 **(A3)**. The cells marked by asterisks are the same cell that migrates over three days. The red and green channels along with the 3-D view of the x, y, and z-axis confirm the division events. The shape of the radial glia process along with the relative positions of the cell bodies identifies the same cells over three days. **(D-F)** Images of drug-treated group show one division event (arrow). Note this division event takes place during the second 24hr after drug washed out. **(D1-F1)** Enlarged set. The scale bar marks 70microns. The sections were 1micron slices of a 180micron section.

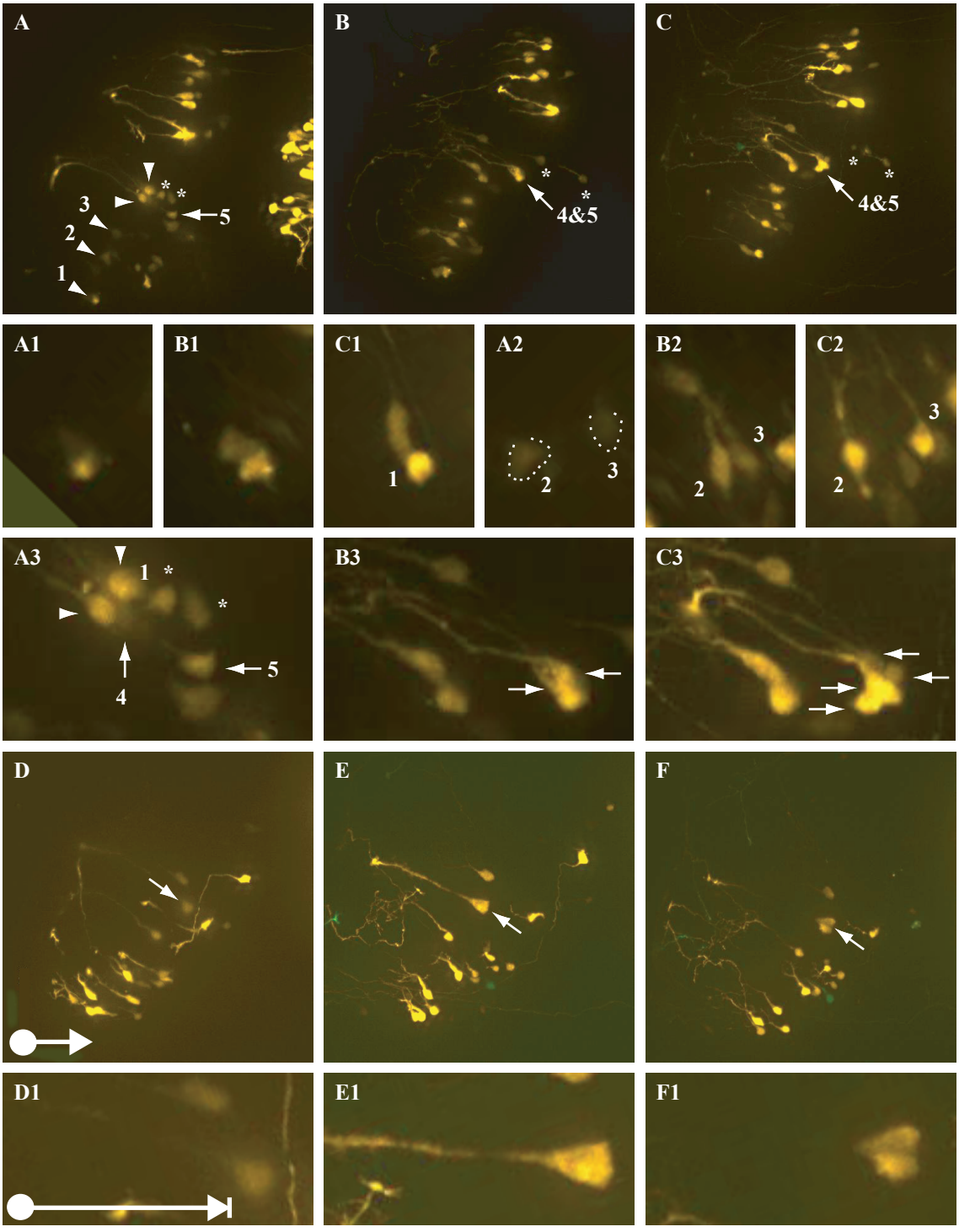
A
B
C
3
2
1
5
4&5
4&5
A1
B1
C1
A2
B2
C2
1
2
3
2
3
2
3
A3
B3
C3
1
4
5
D
E
F
D1
E1
F1

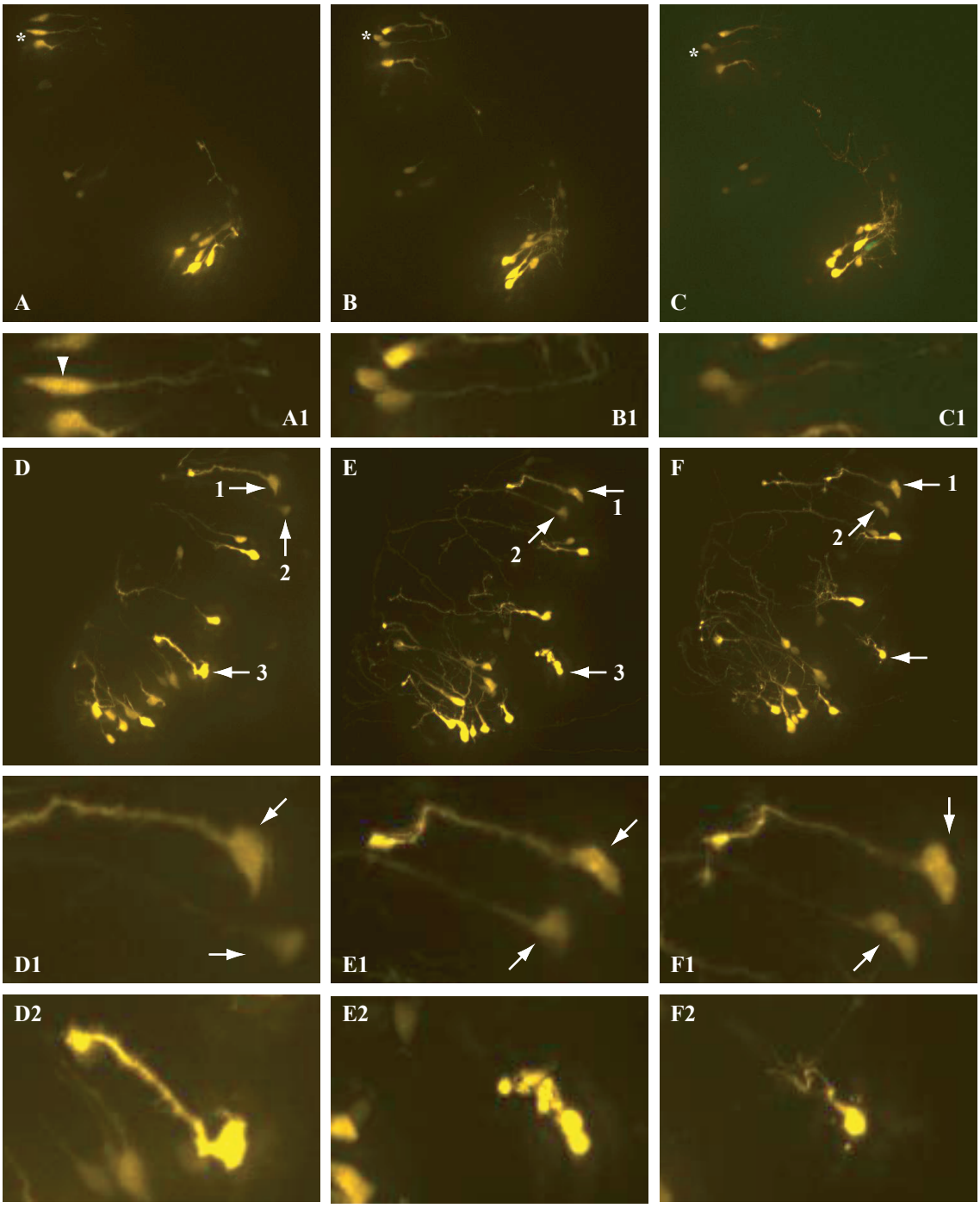

Figure 4.5 | Visual stimulation. Two sets of images of two different tecta. **(A-C)** The asterisk marks the cell that appears to have started its cytokinesis at Day1 and completes by Day2. **(A1-C1)** Notice the dark shadow/contrasting line horizontal to the ventricular plane indicating that plane of division indicated by arrowhead (A1). **(D-F)** Cell (1 and 2) show division plane on Day2 **(E1)** and completes division on Day3 **(F1)**. Cell (3) shows a retraction of radial process and concurrent cell division on Day2 **(E2)** but only one cell appears to have survived to Day3 **(F2)**. The sections were 1micron slices of a 180micron section.

Figure 4.6 | CPG15, Dio3, and ConMo functional gene knockdown. There are three sets of images of CPG15 morpholino, Dio3 morpholino, and control morpholino. **(A-C)** Tectum that has been electroporated with CPG15 morpholino showing cell death marked by asterisk on Day2 (B) and the inability to sustain a newly born cell on Day2 (B) indicated by the disappearance of a new cell on Day3 (C). **(A1-C1)** Images shows close-up of cells in (A-C). **(D-F)** Tectum has been electroporated with Dio3 morpholino. The image series shows cell division events marked by arrow which is enlarged in **(D1-F1)**. **(G-I)** Tectum has been electroporated with control CPG15 morpholino. This image series contains 2 visible division events beginning on Day2. **(G1-I1)** Enlarged image sets show close-up of the division event marked by arrow. A division event of a basal progenitor like cell with multiple processes is indicated by asterisk. The scale bar marks 70microns. The sections were 1micron slices of a 180micron section.

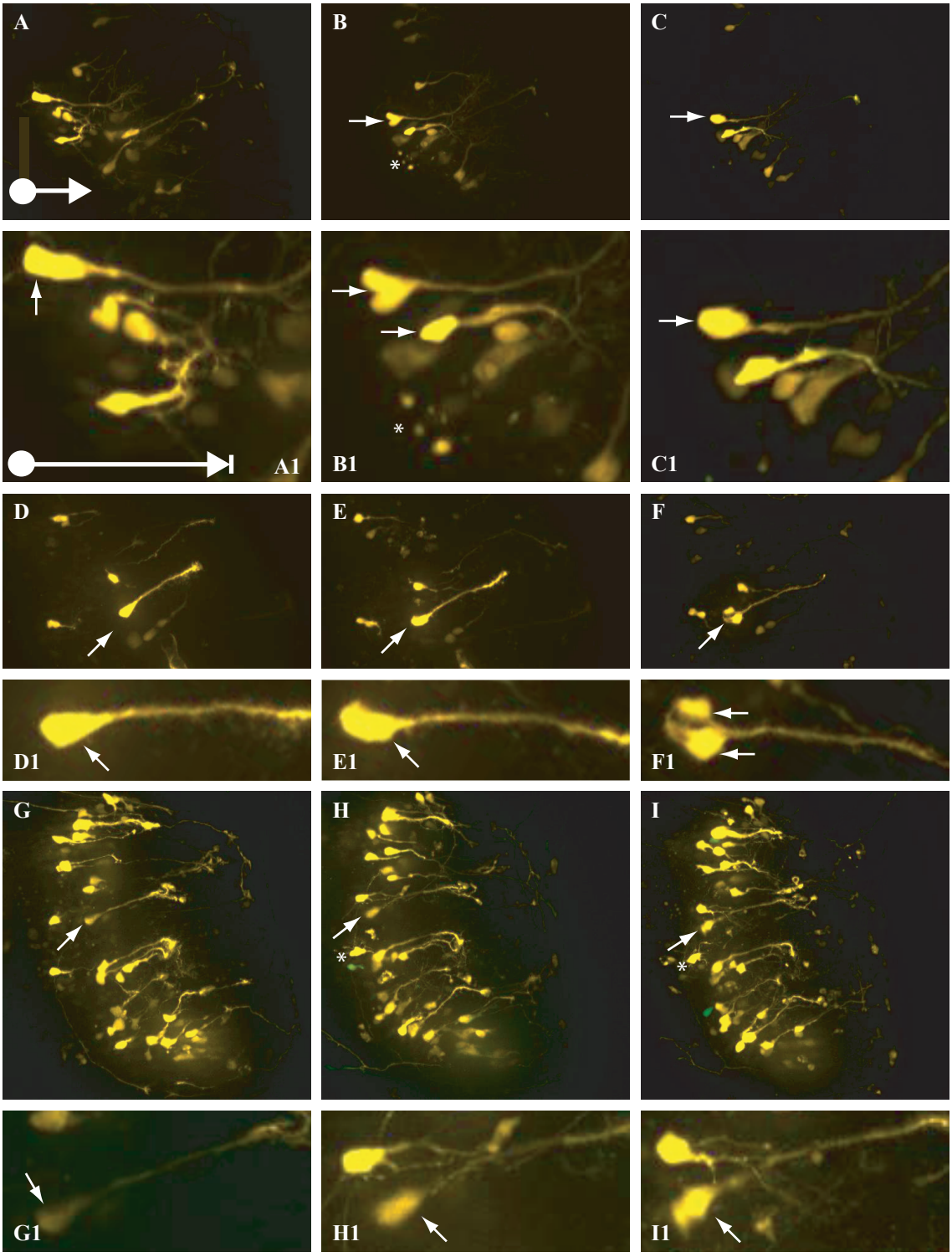
A
B
C
A1
B1
C1
D
E
F
D1
E1
F1
G
H
I
G1
H1
I1

Figure 4.7 | Graphs of percent change of imaging experiments. The y-axis is the normalized percent change of cell number and the x-axis is as indicated on the graphs. **(A)** Graph compares cell-division inhibitor drug treated experiment, DMSO-treated control, and untreated control. Asterisk marks significance of 1-way Anova with p-value of 0.01. **(B)** Graph compares Day1/Day2 changes with Day2/Day3 changes of visual stimulation experiment with untreated controls. A Wilcoxen paired test show significance for visual stimulation experiment between the three days with a p-value of 0.01. **(C)** Graph shows CPG15 morpholino compared with CPG15 control morpholino. There was significant difference in normalized percent change of cell-number between Day1/Day2 but not between Day2/Day3. There was no significant difference in normalized percent change of cell-number between Day2/Day3 but there were significant differences when comparing changes in cell division over all three days. The Mann-Whitney paired test showed p-value <0.01. **(D)** Graph shows Dio3 compared with CPG15 control morpholinos. There were no significant differences between the Dio3 and control set.

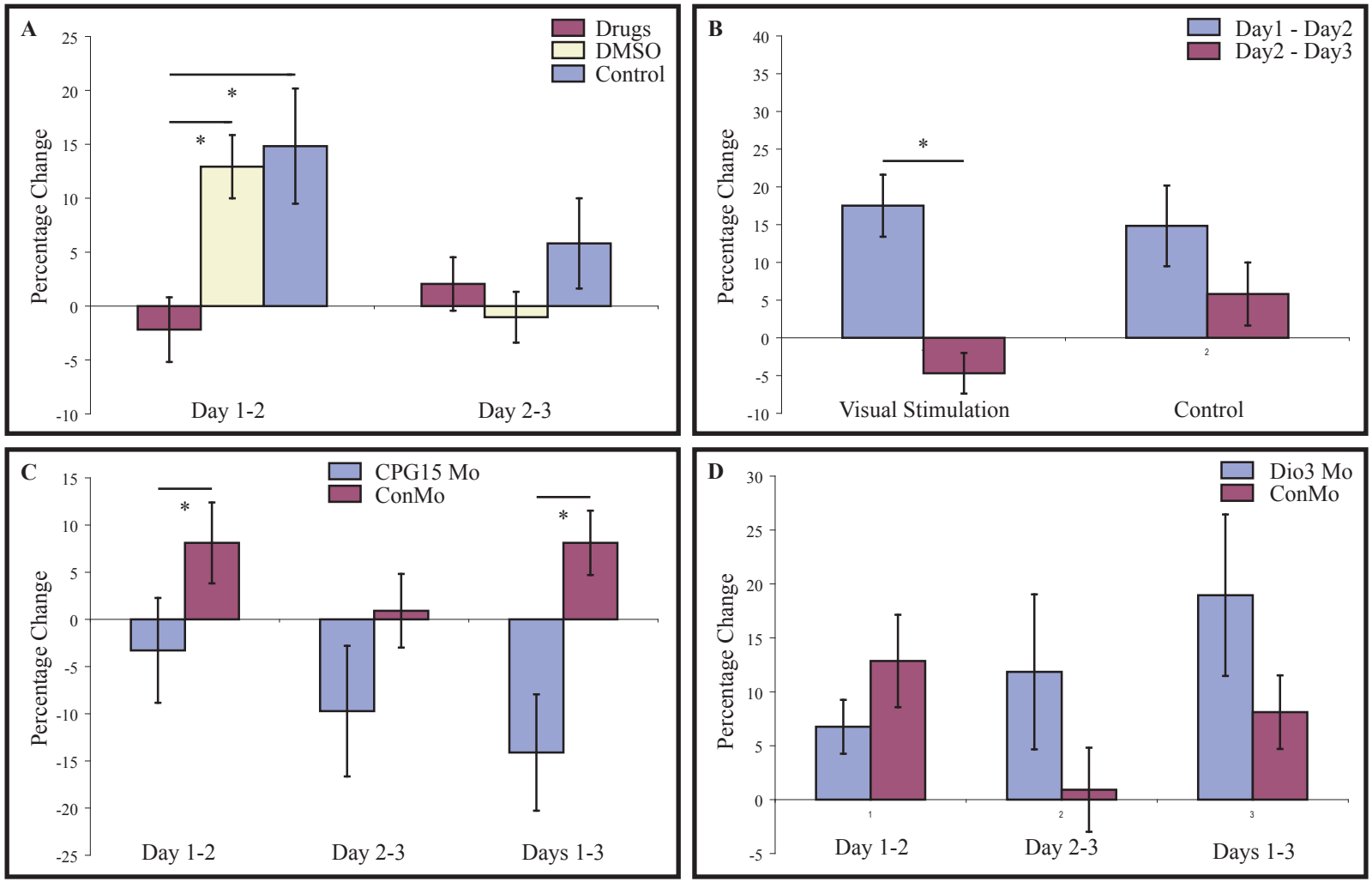
A
Drugs
DMSO
Control
Percentage Change
25
20
15
10
5
0
-5
-10
*
*
Day 1-2
Day 2-3
B
Day1 - Day2
Day2 - Day3
Percentage Change
40
35
30
25
20
15
10
5
0
-5
-10
*
Visual Stimulation
Control
C
CPG15 Mo
ConMo
Percentage Change
15
10
5
0
-5
-10
-15
-20
-25
*
*
Day 1-2
Day 2-3
Days 1-3
D
Dio3 Mo
ConMo
Percentage Change
30
25
20
15
10
5
0
-5
Day 1-2
Day 2-3
Days 1-3

Chapter 5 Discussion

5.1 Sox2/Oct3.mFGF4 reporter labels cells with NPC characteristics

The brain contains a huge variety of cell types; each unique in morphology, connectivity, physiology, and function. To grasp the heterogeneity of the brain, one needs only to glance through the Allen Brain Atlas at http://www.brain-map.org/ (Lein, Hawrylycz et al. 2007). Take Sox2 in the P28 mouse brain as an example; one feature that immediately makes itself known is the scattered locations of this NPC-identifying *in situ* probe. The cerebellum at this stage still has zones of neurogenesis but even in the localized region of interest there are cells that have already stopped expressing Sox2. If one were to randomly mark one of these cells within this region, who is to know if you are looking at a NPC? This demonstrates the value of a cell-type specific reporter: it would be similar to the importance of team jerseys when observing a football game because without it, how is one to know which player belongs to which team in a skirmish? Furthermore, it was of utmost importance to confirm the fidelity of the reporter because conclusions drawn from all subsequent experiments depend on it; all aspects of this thesis confirmed that the Sox2/Oct3.mFGF4 promoter labels NPCs in *X. laevis*.

5.1.1 Immunohistochemistry and microarray show reporter labeled cells PTD1 express NPC markers and pathways

The immunohistochemistry showed that on PTD1, the Sox2 reporter construct was highly co-localized with endogenous Sox2 protein. Because WBE delivers plasmids into cells contacting the ventricle, we tested the likelihood of electroporation of a Sox2+ cell with any plasmid by comparing expression from a CMV promoter-driven plasmid with the reporter expression from the Sox2 reporter plasmid and found that the Sox2 reporter construct resulted in greater selectivity of FP expression within Sox2 immunoreactive cells was markedly higher compared to the CMV reporter. Additionally, the microarray experiments showed that cells harvested PTD1 using the reporter showed higher expression of known NPC markers compared to cells harvested at PTD5. The PreND1vPreND5 raw dataset showed expression of Vimentin, Sox2, Sox3, Sox-D, Sox11, and PCNA. In the ND1vND5 raw dataset, Vimentin, Sox11, and PCNA also appeared to be up-regulated. In contrast, the PreND1vPreND5 raw dataset, NCAM was down-regulated in ND1 cells compared to ND5 cells. All together, the microarray results showed known NPC markers were up-regulated in the Sox2+ reporter labeled cells ND1 (NPC) in comparison to ND5 cells (neurons).

The Ingenuity Pathway Analysis program of both the ND1vND5 and Nd1vSMC raw datasets identified many genes in the cellular growth and proliferation, cell-cycle, and cell death pathways; all pathways known to be active in NPCs. The Ingenuity Pathway Analysis did not specifically highlight pathways known to be characteristic of differentiated neurons; however the database used in the program focused on disease-based pathways, such as cancer and neurodegeneration, which may not have been well represented in our dataset of healthy developing neurons. In addition, lack of annotation in the *X. laevis* genome may have limited our ability to identify additional pathways in Ingenuity.

Ingenuity analysis done of the ND1vND5/ND1vSMC/same filtered dataset showed the 707 genes were involved in pathways functioning in cancer, cell cycle, and cellular growth and proliferation; this means that genes up-regulated in ND1 are genes that are thought to be involved in maintaining stemness. These analyses showed that four independent analyses of ND1 cells, PreND1vPreND5, ND1vND5, ND1vSMC, and Nd1vND5/ND1vSMC, showed ND1 cells labeled by the reporter construct displayed stemness characteristics. In conclusion, all the morphological observations made in the imaging data and markers identified in the immunohistochemistry and microarray strongly suggest that the Sox2/Oct3 plasmid was functioning to label NPCs in the brain of *X. laevis*.

5.1.2 Imaging show the localization and morphology of reporter labeled cells correlated with known NPC characteristics

The imaging experiments with the Sox2/Oct3 reporter construct (JLO#87 & 123) showed that the majority of cells on the PTD1 were localized to the ventricular layer of the tectum; this is analogous to the subventricular-zone in the developing and the adult mammalian brain, where it is a region of active neurogenesis. Many of the cells in contact with the ventricular surface had radial glial morphology with their cell bodies slightly elongated to give the appearance of being packed in like sardines and their basal processes reaching the pial surface. Some cells appear multipolar and do not contact either the ventricular or basal surface of the tectum, similar to basal progenitor cell. Basal progenitors or transient progenitor cells are thought to be a unique characteristic of mammalian cortical development (Gotz and Huttner 2005), but in fact, studies in *Drosophila* (Boone and Doe 2008) and *Xenopus* (Brox, Puelles et al. 2004) show that BPs are not just limited to the cortex indicating that BPs may be more widespread than previously thought. Additionally, the advantage of a long-lived reporter was evident in the PTD5 images where it shows that Sox2/Oct3 reporter expressing cells have differentiated into neurons. I found that the red/green ratios in Kaede-expressing cells which have differentiated into neurons were qualitatively constant, suggesting that the Sox2 reporter construct which depends on endogenous Sox2 and Oct3 to efficiently promote Kaede-green expression was not being promoted due to the lack of Sox2/Oct3 in those cells; neurons are not NPCs, thus are not expressing Sox2 and Oct3. Whereas the red/green ratio in radial glia appeared to decrease as cells continued to synthesize more green Kaede; radial glia are NPCs who are still expressing Sox2 and Oct3, thus they are efficiently promoting Kaede-green expression which results in the change of red/green ratios. Quantitative analyses calculating the exact red/green ratios in cells that appear to be radial glia and in cells that appear to have differentiated have not been performed to validate these observations yet.

5.2 Building a molecular map of the *X. laevis* brain

The mouse nervous system develops *in utero* for 21days, after which, it is still not readily accessible without sacrificing the animal. In contrast, the external development of *X. laevis* embryos facilitates access to the developing nervous system in the intact animal. Furthermore, the CNS develops to become functional over relatively short span of hours and days instead of weeks and months; these reasons alone have made this model system a favorite for embryologist studying nervous system development. The albino *X. laevis*

has the added benefit of the brain being close to the surface and the skin being transparent making *in vivo* time-lapse imaging possible. However, unlike the other model systems such as the mouse, rat, and even the yeast, the *X. laevis* has yet to experience the genetic revolution that has greatly enhanced the understanding of the molecular and biological mechanisms involved in the development of the nervous system. Building a molecular map of the X. laevis brain, i.e. knowing when, where, and what specific genes and pathways are expressed in the cell population of interest will significantly aid in defining their function and furthermore it will help define how it can be manipulated for therapeutic purposes.

Several *X. laevis* laboratories have used microarray to either identify novel genes or profile gene expression in the CNS. Ken Cho's laboratory used microarray to profile neural induction in the animal cap (Peiffer, Bubnoff et al. 2005; Shin, Kitayama et al. 2005); the studies identified several genes not previously linked with neural induction. Another study using *X. laevis* microarray showed that *Xenopus* Fragile-X related gene (xFXR-1) knockdown resulted in the identification of 129 known genes of which 50% were related to muscle and nervous system dysfunction (Huot, Bisson et al. 2005). These studies illustrate that microarray studies in *Xenopus* may shed light on the mechanisms of various nervous system functions. The microarray studies presented here are just a few more steps toward building a molecular atlas of the *X. laevis* CNS especially for NPC studies. By building this map, this work as well as future work on NPCs in *X. laevis* can be placed in context of other works in the field.

5.3 Looking at the *X laevis* NPCs

A favorite quote by Yogi Berra in the Cline laboratory is "You can observe a lot just by watching"; it follows the other popular lab quote of "A picture is worth a thousand words" (Author Unknown). With this in mind, the imaging experiments were used to test the biological output of the candidate genes screened from the microarray experiment. Because the method was an *in vivo* time-lapse imaging protocol, not only is the absolute count of cell proliferation, growth, and differentiation possible, but other observations such the cellular death or division events as it is happening can be made to address questions such as what a cell looks like before, during, and after the event. By watching how cellular events occur, mechanistic hypotheses can be formulated and then tested in the same *in vivo* system that suggested it. For example, if we observe more symmetrical division events relative to asymmetrical division events with the functional knockdown of a candidate gene, we can hypothesize its role in proliferative mechanisms such as those related to maintaining cell polarity, cell cycle, growth hormones, and other signaling pathways mentioned in Table 1.1. Alternatively, if we observe more asymmetrical division events, then we can hypothesize its role in differentiation mechanisms such as expression of pro-neural markers and activation of mitogenic cascades.

5.4 Imagining the future

The major contribution of this work was to establish the albino *Xenopus laevis* as a model system for investigation of the mechanisms involved in regulating neurogenesis. First a reporter construct was made, verified, and used successfully to label NPCs in the

brain of an intact animal. Second, microarray analysis was done to not only identify genes that may regulate neurogenesis but also to use as a comparison to other model systems. Finally, I conducted experiments to establish a baseline for *in vivo* time-lapse imaging of NPCs. A more thorough analysis of datasets already collected during this thesis project is required and follow-up experiments should be done to enhance and further the knowledge gained from this dataset. Additionally, other preliminary studies using a NPC transplantation paradigm was not presented in the body of this work; however, it indicated the clinical applications of this model system as will be described below.

5.4.1 Gal4-UAS system is a versatile expression system in *X. laevis*

These experiments also demonstrate that the Gal4-UAS system functions in the *X. laevis* model system. This system can be used to amplify fluorescent signal from weak promoters and second, it can be used to express multiple genes from the same plasmids as well as from separate plasmids. There are many ideas for the use of this amplification system for NPCs, some of which are mentioned below.

The Musashi promoter is among the plasmids in my library given to me as a gift of Steven Goldman at the University of Rochester. This is a mouse promoter driving humanized GFP. Musashi is a gene that was found in NPC screens of Xenopus NPCs . It is conserved among all vertebrates (Kaneko, Sakakibara et al. 2000) and is expressed in stem cells throughout the body including NPCs (Okano, Kawahara et al. 2005). There was a high likelihood that the mouse promoter could successfully drive protein expression in *X. laevis* because other promoters such as the mouse VGAT promoter has been shown to drive expression in GABAergic neurons (H. He and H Cline, unpublished). When the Musashi1 plasmid is introduced into cells using WBE, there is no visible expression of the plasmid until 3days after electroporation. At the time, this delay in visible fluorescence was not acceptable for the labeled cells may have already exit the cell-cycle by PTD3. By combining the Gal4-UAS system with the current modification to the UAS cassette this promoter may increase the utility of the Musashi1 promoter by amplifying the fluorescent protein expression. In this way, NPCs specific for Musashi1 can be compared to NPCs specific for Sox2/Oct3. It would be interesting to see if the genetic signatures are the same or different by doing the microarray experiment on these two sets. Other possible interesting promoters in my library are the msNestin promoter from Grisha the Enikolopov laboratory and Pax6 promoter from the Robert Grainger laboratory. Neither of these plasmids showed expression PTD1 but it may have just been due to weak promoter activity.

The Gal4-UAS system is also great for expressing multiple GOIs. In the Cline laboratory library of plasmids are three CREB genes: the constituently active CREB (VP16-CREB) and dominant negative CREB (A-CREB) from Charles Vinson laboratory at the NIH and the dominate repressor of CREB (K-CREB) from Anirvan Ghosh laboratory at UCSD. CREB is involved in many pathways both in neuronal plasticity and in NPCs. It has always been an interest of mine to express these genes in NPC to evaluate their role in NPC. With the Gal4-UAS system, these genes can be cloned behind the 14xUASmFGF4 promoter and co-electroporated using WBE with the Gal4 driver

promoted by the Sox2/Oct3 binding sequence and a 14xUAS.mFGF4 color for visualization. It would be prudent for the fluorescent color and the GOI to be on the same plasmid so that one can be assured that a labeled cell is also expressing the GOI. Another GOI that can be tested is CPG15 to complement the findings of the morpholino data. This gene is also easily obtainable for it is in the Cline laboratory plasmid library.

5.4.2 Forever a cloning heart: Other interesting cloning projects

When the reporter design was considered to label NPCs, there was a question as to when an NPC stops being an NPC and becomes a neuron. One of the ways considered to address this question was to use destabilized-GFP. I have in my library of plasmids two forms of destabilized-GFP from Clontech: d1.GFP and d2.GFP. These fluorescent proteins are being driven by the BAC isolated 9kb-P/Sox2, the mFGF4-only, and the Sox2/Oct3 promoters. Preliminary studies with the d1.GFP form of destabilized GFP showed extended expression in *X. laevis* brain (personal communication, Jennifer Bestman). However, none of the six plasmids made with Sox2-specific promoters have been tested. It would be interesting to determine if indeed Sox2, which is a marker of stemness, is turned off using Sox2 promoter constructs. The reason why these plasmids remained in the background was because for my thesis, I needed the continued strong fluorescence in order to be able to harvest cells PTD5 and the use of the Kaede construct to indentify cells present on the first day of imaging partially resolved this question.

Another method that was considered to identify the onset of neuronal differentiation was to use the promoter of Nβ-tubulin, an early neuronal marker. This plasmid was received from Enrique Amaya laboratory at University of Manchester, UK. The design was to insert the Nβ-tubulin promoter on one side of a bi-directional plasmid (BiCs2, JLO#13) to drive one nuclear color such as H2B-eYFP (Fish#147 or JLO#90, also a gift of Enrique Amaya) or any of the NLS-constructs in my library. On the other side of the bi-directional plasmid, insert the Sox2/Oct3 promoter driving a cytosolic FP. In this way, when the Nβ-tubulin promoter turns on, a contrasting nuclear color will be expressed within the NPC that is being observed to indicate a shift in identity. With this elegant design, one can ask many tantalizing questions concerning differentiation events. This design is similar to the BAPTISM construct of (Caron, Prober et al. 2008), where a temporal-specific promoter labeling newly born trigeminal neurons was used to track newly born neurons in the trigeminal ganglion.

5.4.3 Room for more microarrays

Currently the array data from the fifty-five chip experiment remain largely unanalyzed. First, there are many genes to annotate by simply going back to the probe sets and using the sequences to search EST databases and NCBI or EMBL databases for homologous matches with mouse genes. Then, Ingenuity pathway analysis can be done with a larger portion of the raw datasets. Currently only ~12,000 out of the ~34,000 *Xenopus* genes have been annotated with mouse symbols which is less than half of the data. The additional annotation will give a more complete picture of the datasets.

Another analysis that can be done with this current dataset is to perform more comparisons with other NPC microarray datasets. The goal of this type of analysis would

be to further define the *X. laevis* NPCs within the context of NPCs of other model systems. To further take advantage of publically available data, the Allen Brain Atlas can be used to determine where some of the most shared genes are located in embryonic mouse brain to confirm NPC expression of the genes. This, in essence, would be a comprehensive comparative study on NPCs of all types.

Furthermore, the current sets of microarray experiments are ideal in identifying new genes not previously characterized in other NPC studies; however, data mining for candidate NPC markers have not been performed extensively yet. Once novel marker candidates are identified, the Allen Brain Atlas database can be utilized for their mRNA expression. Those marker candidates that are localized to neurogenic regions of the mouse brain can be used to produce antibodies which then can be confirmed in *X. laevis* brains.

In addition to data mining from these datasets, there is also room for more microarray experiments. As mentioned before, with the optimization of all levels of RNA handling, there is a possibility of biological replicates. This contrasts with the technical replicates of the current microarray experiment performed from pooled NPCs from different brains. Biological replicate would consist of 5-50 cells from the same brain; this amount of cells can be picked within 30mins instead of an hour, 30mins that may reduce cell-sorting artifacts. Also, independent confirmation of the current dataset could be made with the new biological replicate dataset further validation both results. Finally, if microarray experiments become a routine part of the Cline laboratory, then morpholinos found to have a significant biological output can be used in further array studies to discover or validate pathways that may be part of that GOI.

5.4.4 Room for more imaging studies

Currently there are unanalyzed imaging data; those data need to be analyzed to test whether GOI affect cell proliferation and differentiation. Analysis of the 3-dimensional data sets should be more sensitive to these types of parameters than analysis of 2D data sets. In addition, it would be valuable to test whether NPCs in different regions of the tectal proliferative zone have different proliferative capacity, as suggested by preliminary experiments by Pranav Sharma. For example NPCs in the caudal-lateral corners of the optic tectum appeared to be more proliferative than the NPCs along the dorsal midline of the tectum. The alternative analysis strategy would to be to divide the tectum or the brain into different regions, such as the rostral and caudal half of tectum. This will not only result in further insight into the NPC proliferative capacity differences in different regions of the brain but it may also be enough to tease out significant results in the morpholino datasets.

Follow-up imaging experiments for the morpholino data analyzed in this thesis have already been suggested as the results were being discussed above; however, the few datasets that have been analyzed gave valuable insight into how to improve the experimental protocol. Many of the GOI chosen for the morpholino screen were predicted to increase proliferation. Because the imaging protocol used visual deprivation as the baseline starting point, it may be that the NPCs are already at their maximal

proliferation rate under these conditions, which could prevent us from detecting significant differences in proliferation with knockdown by morpholinos, which were predicted to increase proliferation. As mentioned before, the visual stimulation protocol described in this thesis may be used to circumvent the maximal proliferation rate dilemma. Another protocol could involve maintaining the animals in normal 12/12 light-dark cycle throughout the imaging protocol. Care would have to be taken as to not photo-activate the Kaede by using a UV filter around the incubator light.

One issue encountered during analysis of the imaging data was the difficulty in discerning two cell bodies on top of each other or right next to each other. Originally, there was a plan to use a 14xUAS.mFGF4-CFP.NLS construct in conjunction with the Kaede; however, this was abandoned because the CFP.NLS expression was so high that it was found in the cytosol as well as the nucleus. My library of plasmids includes several colors of 14xUAS.E1b-H2B.XFP's. These plasmids were not used for this set of experiment because the E1B was considered leaky. However, upon further consideration, this may not be such a critical issue as originally thought since the Kaede construct does not have the E1B and has the mFGF4 minimal promoter. Therefore, if the Sox2/Oct3.mFGF4-Gal4VP16-14xUAS.E1b-H2B.TurboGFP (JLO#107) was transfected along side with 14xUAS.mFGF4-Kaede, then only cells that are expressing Kaede could be accounted for, as was the rule for the analysis protocol described above, and the H2b.TurboGFP can be simply used to discern cell bodies. Green only cells and H2B.TurboGFP-only cells could be omitted from the count.

Finally, an imaging experiment that may further confirm the specificity of the reporter construct for bulk electroporation into *X. laevis* cells is to use morpholinos against Sox2 and Oct3 to functionally knock down these transcription factors in cells electroporated with the Sox2/Oct3.mFGF4 reporter construct. In doing so, the reporter would not be efficiently promoted from the Sox2/Oct3.mFGF4 enhancer element resulting in decreased or no expression. The use of the bidirectional plasmid with a CMV-promoted differently colored fluorescent protein will confirm the plasmids electroporation into a cell.

5.4.5 Clinical applications

Preliminary experiments using a transplantation paradigm showed proof of principle (Figure 5.1). Now that a homogenous pool of NPCs can be successfully isolated, instead of extracting totRNA from them, they could just as easily be transplanted into a stage matched host animals. The possibilities of this type of transplantation experiment are endless. An example would be to WBE morpholino into the host tadpole before transplantation to determine is cell non-autonomous effects are present that may affect transplantation success. The alternate example would be to transplant a morpholino electroporated NPC into a brain to determine cell-autonomous effects of the morpholino. Also, the role of activity in transplantation success can be investigated using this model. In this way, the characteristics that aid in transplanted cell survival, proliferation, and differentiation can be determined and applied to increase the success of transplantation therapies currently being investigated for intractable neurological disorders such as Parkinson's disease.

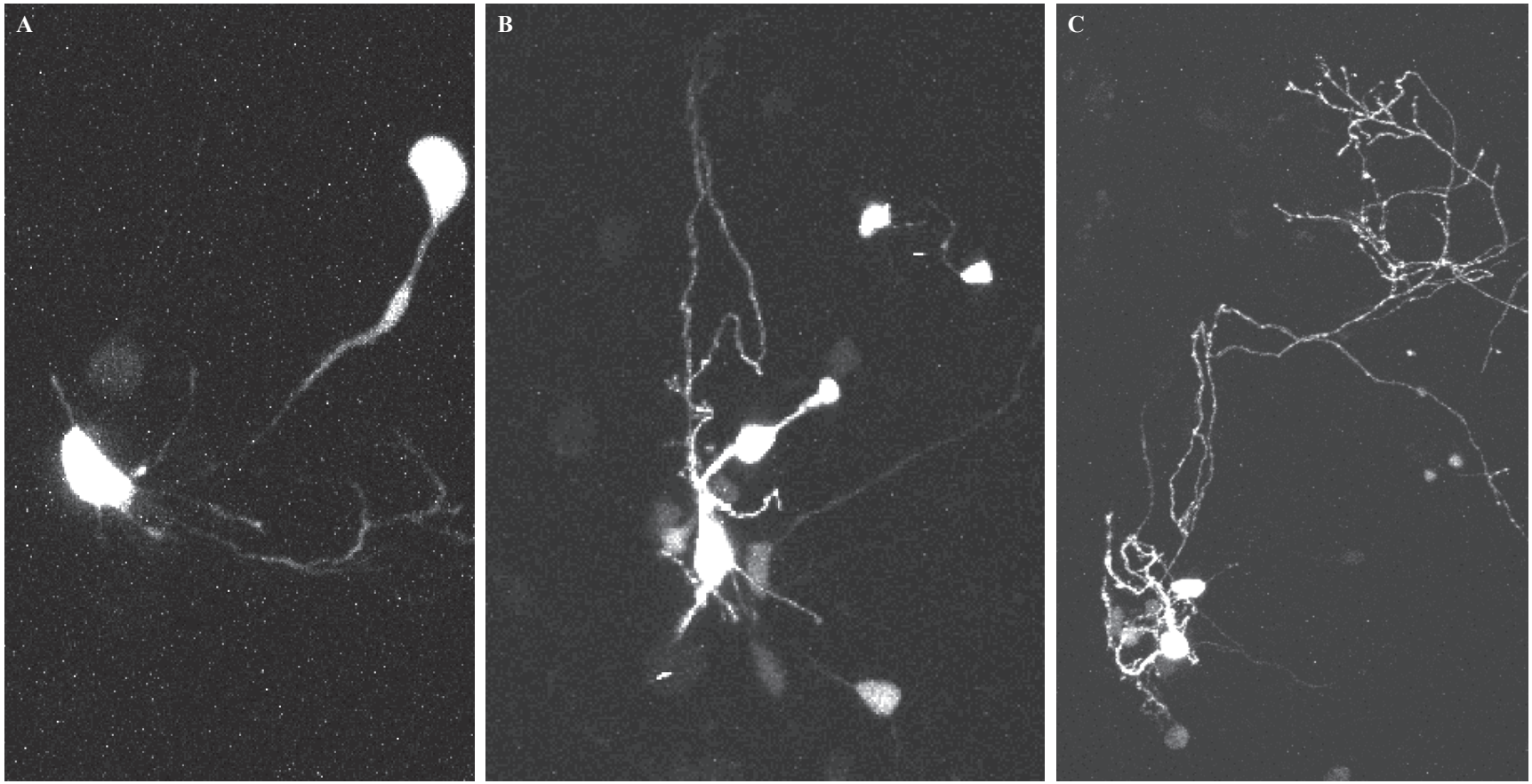

Figure 5.1 | An acute transplantation of dissociated tectal cells into stage matched host animal. This illustrates a preliminary transplantation experiment of stage 46/47 animal host and stage 46/47 donor animal. **(A)** Image shows transplanted cells in the host animal 24hrs after transplantation. **(B)** Image shows transplanted cells 48hrs after transplantation. Notice the elongation and elaboration of processes. **(C)** Image shows transplanted cells 5days after transplation.

Bibliography

Aaku-Saraste, E., A. Hellwig, et al. (1996). "Loss of Occludin and Functional Tight Junctions, but Not ZO-1, during Neural Tube Closure--Remodeling of the Neuroepithelium Prior to Neurogenesis." Developmental Biology **180**(2): 664-679.

Aaku-Saraste, E., B. Oback, et al. (1997). "Neuroepithelial cells downregulate their plasma membrane polarity prior to neural tube closure and neurogenesis." Mech. Dev. **69**: 71.

Abramova, N., C. Charniga, et al. (2005). "Stage-specific changes in gene expression in acutely isolated mouse CNS progenitor cells." Developmental Biology **283**(2): 269-281.

Agathocleous, M., I. Iordanova, et al. (2009). "A directional Wnt/beta-catenin-Sox2-proneural pathway regulates the transition from proliferation to differentiation in the Xenopus retina." Development **136**(19): 3289-3299.

Agrawal, S. M., L. Lau, et al. (2008). "MMPs in the central nervous system: Where the good guys go bad." Seminars in Cell & Developmental Biology **19**(1): 42-51.

Ahn, J. I., K. H. Lee, et al. (2004). "Temporal expression changes during differentiation of neural stem cells derived from mouse embryonic stem cell." Journal of Cellular Biochemistry **93**(3): 563-578.

Aigner, S. and F. H. Gage (2005). "A Small Gem with Great Powers: Geminin Keeps Neural Progenitors Thriving." Developmental Cell **9**(2): 171-172.

Aizenman, C. D. and H. T. Cline (2007). "Enhanced Visual Activity In Vivo Forms Nascent Synapses in the Developing Retinotectal Projection." J Neurophysiol **97**(4): 2949-2957.

Ajamian, F., T. Suuronen, et al. (2003). "Upregulation of class II histone deacetylases mRNA during neural differentiation of cultured rat hippocampal progenitor cells." Neuroscience Letters **346**(1-2): 57-60.

Akchiche, N., C. Bossenmeyer, et al. (2009). "Differentiation and neural integration of hippocampal neuronal progenitors: Signaling pathways sequentially involved." Hippocampus **9999**(9999): NA.

Altman, J. and G. D. Das (1965). "Autoradiographic and histological evidence of postnatal hippocampal neurogenesis in rats." J. Comp. Neurol. **124**(3): 319-335.

Amaya, E. and K. Kroll (1999). "A method for generating transgenic frog embryos." Methods in Molecular Biology **97**: 393-414.

Ambrosetti, D. C., C. Basilico, et al. (1997). "Synergistic activation of the fibroblast growth factor 4 enhancer by Sox2 and Oct-3 depends on protein-protein interactions facilitated by a specific spatial arrangement of factor binding sites." Mol. Cell. Biol. **17**(11): 6321-6329.

Ambrosetti, D. C., H. R. Scholer, et al. (2000). "Modulation of the Activity of Multiple Transcriptional Activation Domains by the DNA Binding Domains Mediates the Synergistic Action of Sox2 and Oct-3 on the Fibroblast Growth Factor-4 Enhancer." J. Biol. Chem. **275**(30): 23387-23397.

Antanitus, D. S., B. H. Choi, et al. (1976). "The demonstration of glial fibrillary acidic protein in the cerebrum of the human fetus by indirect immunofluorescence." Brain Research **103**(3): 613-616.

Anthony, T. E., C. Klein, et al. (2004). "Radial glia serve as neuronal progenitors in all regions of the central nervous system." Neuron **41**: 881.

Attardo, A., F. Calegari, et al. (2008). "Live Imaging at the Onset of Cortical Neurogenesis Reveals Differential Appearance of the Neuronal Phenotype in Apical versus Basal Progenitor Progeny." PLoS ONE **3**(6): e2388.

Azuma, K., T. Urano, et al. (2009). "Association of Estrogen Receptor-alpha and Histone Deacetylase 6 Causes Rapid Deacetylation of Tubulin in Breast Cancer Cells." Cancer Res **69**(7): 2935-2940.

Ballas, N., C. Grunseich, et al. (2005). "REST and Its Corepressors Mediate Plasticity of Neuronal Gene Chromatin throughout Neurogenesis." Cell **121**(4): 645-657.

Ballas, N. and G. Mandel (2005). "The many faces of REST oversee epigenetic programming of neuronal genes." Current Opinion in Neurobiology **15**(5): 500-506.

Barraud, P., L. Thompson, et al. (2005). "Isolation and characterization of neural precursor cells from the Sox1-GFP reporter mouse." European Journal of Neuroscience **22**(7): 1555-1569.

Barres, B. A., B. E. Silverstein, et al. (1988). "Immunological, morphological, and electrophysiological variation among retinal ganglion cells purified by panning." Neuron **1**(9): 791-803.

Barthel, L. K. and P. A. Raymond (1990). "Improved method for obtaining 3-microns cryosections for immunocytochemistry." J. Histochem. Cytochem. **38**(9): 1383-1388.

Bauer, H. C., H. Tempfer, et al. (2006). "Neuronal stem cells in adults." Experimental Gerontology **41**(2): 111-116.

Bertrand, N., D. S. Castro, et al. (2002). "Proneural genes and the specification of neural cell types." Nat Rev Neurosci **3**(7): 517-530.

Bestman, J. E. and H. T. Cline (2008). "The RNA binding protein CPEB regulates dendrite morphogenesis and neuronal circuit assembly in vivo." Proceedings of the National Academy of Sciences **105**(51): 20494-20499.

Bestman, J. E., R. C. Ewald, et al. (2006). "In vivo single-cell electroporation for transfer of DNA and macromolecules." Nat. Protocols **1**(3): 1267-1272.

Bhattacharyya, A., E. McMillan, et al. (2008). "Normal Neurogenesis but Abnormal Gene Expression in Human Fragile X Cortical Progenitor Cells." Stem Cells and Development **17**(1): 107-118.

Bonfanti, L. (2006). "PSA-NCAM in mammalian structural plasticity and neurogenesis." Progress in Neurobiology **80**(3): 129-164.

Boone, J. Q. and C. Q. Doe (2008). "Identification of Drosophila type II neuroblast lineages containing transit amplifying ganglion mother cells." Dev Neurobiol **68**(9): 1185-95.

Boulder, C. (1970). "Embryonic vertebrate central nervous system: revised terminology." Anat. Rec. **166**: 257.

Brox, A., L. Puelles, et al. (2004). "Expression of the genes Emx1, Tbr1, and Eomes (Tbr2) in the telencephalon of Xenopus laevis confirms the existence of a ventral

pallial division in all tetrapods." The Journal of Comparative Neurology **474**(4): 562-577.
Bruel-Jungerman, E., S. Laroche, et al. (2005). "New neurons in the dentate gyrus are involved in the expression of enhanced long-term memory following environmental enrichment." European Journal of Neuroscience **21**(2): 513-521.
Buchwalter, G., C. Gross, et al. (2004). "Ets ternary complex transcription factors." Gene **324**: 1-14.
Buck, S. B., J. Bradford, et al. (2008). "Detection of S-phase cell cycle progression using 4-ethynyl-2'-deoxyuridin incorporation with click chemisty, an alternative to using 5-bromo-2'-deoxyuridine antibodies." BioTechniques **44**(7): 927-929.
Bursztajn, S., W. A. Falls, et al. (2007). "Cell proliferation in the brains of NMDAR NR1 transgenic mice." Brain Research **1172**: 10-20.
Bylund, M., E. Andersson, et al. (2003). "Vertebrate neurogenesis is counteracted by Sox1-3 activity." Nature Neuroscience **6**(11): 1162-1168.
Cao, Y. and C. Dulac (2001). "Profiling brain transcription: neurons learn a lesson from yeast." Current Opinion in Neurobiology **11**(5): 615-620.
Capela, A. and S. Temple (2002). "LeX/ssea-1 is expressed by adult mouse CNS stem cells, identifying them as nonependymal." Neuron **35**: 865.
Capela, A. and S. Temple (2006). "LeX is expressed by principle progenitor cells in the embryonic nervous system, is secreted into their environment and binds Wnt-1." Dev Biol **291**: 300.
Cappelletti, G., M. Galbiati, et al. (2007). "Neuritin (cpg15) enhances the differentiating effect of NGF on neuronal PC12 cells." Journal of Neuroscience Research **85**(12): 2702-2713.
Caron, S. J. C., D. Prober, et al. (2008). "In vivo birthdating by BAPTISM reveals that trigeminal sensory neuron diversity depends on early neurogenesis." Development **135**(19): 3259-3269.
Casper, K. B. and K. D. McCarthy (2006). "GFAP-positive progenitor cells produce neurons and oligodendrocytes throughout the CNS." Mol. Cell Neurosci. **31**: 676.
Castrén, M., T. Tervonen, et al. (2005). "Altered differentiation of neural stem cells in fragile X syndrome." Proceedings of the National Academy of Sciences of the United States of America **102**(49): 17834-17839.
Castro-Caldas, M., A. Neves-Carvalho, et al. (2009). "GSTpi expression in MPTP-induced dopaminergic neurodegeneration of C57BL/6 mouse midbrain and striatum." J Mol Neurosci **38**(2): 114-27.
Chambaut-Guérin, A.-M., S. Hérigault, et al. (2000). "Induction of Matrix Metalloproteinase MMP-9 (92-kDa Gelatinase) by Retinoic Acid in Human Neuroblastoma SKNBE Cells." Journal of Neurochemistry **74**(2): 508-517.
Chenn, A. and S. K. McConnell (1995). "Cleavage orientation and the asymmetric inheritance of Notch1 immunoreactivity in mammalian neurogenesis." Cell **82**: 631.
Chenn, A. and C. A. Walsh (2003). "Increased Neuronal Production, Enlarged Forebrains and Cytoarchitectural Distortions in beta-Catenin Overexpressing Transgenic Mice." Cereb. Cortex **13**(6): 599-606.
Chin, J. H., H. Shiwaku, et al. (2009). "Neural stem cells express Oct-3/4." Biochemical and Biophysical Research Communications **In Press, Corrected Proof**.

Chiu, S. L., C. M. Chen, et al. (2008). "Insulin Receptor Signaling Regulates Synapse Number, Dendritic Plasticity, and Circuit Function In Vivo " Neuron **58**(5): 708-719.

Chumley, M. J., T. Catchpole, et al. (2007). "EphB Receptors Regulate Stem/Progenitor Cell Proliferation, Migration, and Polarity during Hippocampal Neurogenesis." J. Neurosci. **27**(49): 13481-13490.

Clarke, S. R., A. K. Shetty, et al. (1994). "Reactive astrocytes express the embryonic intermediate neurofilament nestin." Neuroreport **5**: 1885-1888.

Clement-Ziza, M., D. Gentien, et al. (2009). "Evaluation of methods for amplification of picogram amounts of total RNA for whole genome expression profiling." BMC Genomics **10**(1): 246.

Copeland, N. G., N. A. Jenkins, et al. (2001). "Recombineering: a powerful new tool for mouse functional genomics." Nat Rev Genet **2**(10): 769-779.

Corti, S., M. Nizzardo, et al. (2007). "Isolation and characterization of murine neural stem/progenitor cells based on Prominin-1 expression." Experimental Neurology **205**(2): 547-562.

Cox, M. L., C. L. Schray, et al. (2006). "Assessment of fixatives, fixation, and tissue processing on morphology and RNA integrity." Experimental and Molecular Pathology **80**(2): 183-191.

Craig, C. G., V. Tropepe, et al. (1996). "In vivo growth factor expansion of endogenous subependymal neural precursor cell populations in the adult mouse brain." J. Neurosci. **16**(8): 2649-2658.

Cremisi, F., A. Philpott, et al. (2003). "Cell cycle and cell fate interactions in neural development." Current Opinion in Neurobiology **13**(1): 26-33.

D'Amour, K. A. and F. H. Gage (2003). "Genetic and functional differences between multipotent neural and pluripotent embryonic stem cells." Proceedings of the National Academy of Sciences of the United States of America **100**(Suppl 1): 11866-11872.

Dahmane, N., P. Sanchez, et al. (2001). "The Sonic Hedgehog-Gli pathway regulates dorsal brain growth and tumorigenesis." Development **128**(24): 5201-5212.

Denver, R. J., F. Hu, et al. (2009). "Thyroid hormone receptor subtype specificity for hormone-dependent neurogenesis in Xenopus laevis." Developmental Biology **326**(1): 155-168.

Díaz, E. (2009). "From microarrays to mechanisms of brain development and function." Biochemical and Biophysical Research Communications **385**(2): 129-131.

Dittrich, P. S., S. P. Schäfer, et al. (2005). "Characterization of the Photoconversion on Reaction of the Fluorescent Protein Kaede on the Single-Molecule Level." Biophysical Journal **89**(5): 3446-3455.

Dong, W., R. H. Lee, et al. (2009). "Visual Avoidance in Xenopus Tadpoles Is Correlated With the Maturation of Visual Responses in the Optic Tectum." J Neurophysiol **101**(2): 803-815.

Doyle, J. P., J. D. Dougherty, et al. (2008). "Application of a Translational Profiling Approach for the Comparative Analysis of CNS Cell Types " Cell **135**(4): 749-762.

Dworkin, S., J. Malaterre, et al. (2009). "cAMP Response Element Binding Protein Is Required for Mouse Neural Progenitor Cell Survival and Expansion." Stem Cells **27**(6): 1347-1357.

Easterday, M. C., J. D. Dougherty, et al. (2003). "Neural progenitor genes: Germinal zone expression and analysis of genetic overlap in stem cell populations." Developmental Biology **264**(2): 309-322.

Eberwine, J., H. Yeh, et al. (1992). "Analysis of gene expression in single live neurons." Proceedings of the National Academy of Sciences of the United States of America **89**(7): 3010-3014.

Egger, B., J. Chell, et al. (2008). "Insights into neural stem cell biology from flies." Philos Tran R Soc Lond B Biol Sci **363**(1489): 39-56.

Eisch, A. J., H. A. Cameron, et al. (2008). "Adult Neurogenesis, Mental Health, and Mental Illness: Hope or Hype?" J. Neurosci. **28**(46): 11785-11791.

Ekonomou, A., I. Kazanis, et al. (2005). "Neuronal migration and ventral subtype identity in the telencephalon depend on SOX1." PLoS Biology **3**(6): e186.

Encinas, J. M., A. Vaahtokari, et al. (2006). "Fluoxetine targets early progenitor cells in the adult brain." **103**(21): 8233-8238.

Engert, F., H. W. Tao, et al. (2002). "Moving visual stimuli rapidly induce direction sensitivity of developing tectal neurons." Nature **419**(6906): 470-475.

Englund, C., A. Fink, et al. (2005). "Pax6, Tbr2, and Tbr1 Are Expressed Sequentially by Radial Glia, Intermediate Progenitor Cells, and Postmitotic Neurons in Developing Neocortex." J. Neurosci. **25**(1): 247-251.

Eriksson, P. S., E. Perfilieva, et al. (1998). "Neurogenesis in the adult human hippocampus." Nat. Med. **4**(11): 1313-1317.

Estivill-Torrus, G., H. Pearson, et al. (2002). "Pax6 is required to regulate the cell cycle and the rate of progression from symmetrical to asymmetrical division in mammalian cortical progenitors." Development **129**(2): 455-466.

Fabel, K. and G. Kempermann (2008). "Physical Activity and the Regulation of Neurogenesis in the Adult and Aging Brain." NeuroMolecular Medicine **10**(2): 59-66.

Falk, J., J. Drinjakovic, et al. (2007). "Electroporation of cDNA/Morpholinos to targeted areas of embryonic CNS in Xenopus." BMC Developmental Biology **7**(1): 107.

Farkas, L. M. and W. B. Huttner (2008). "The cell biology of neural stem and progenitor cells and its significance for their proliferation versus differentiation during mammalian brain development." Current Opinion in Cell Biology **20**(6): 707-715.

Favaro, R., M. Valotta, et al. (2009). "Hippocampal development and neural stem cell maintenance require Sox2-dependent regulation of Shh." Nature Neuroscience.

Feng, L., M. E. Hatten, et al. (1994). "Brain lipid-binding protein (BLBP): a novel signaling system in the developing mammalian CNS." Neuron **12**: 895.

Fodor, S., J. Read, et al. (1991). "Light-directed, spatially addressable parallel chemical synthesis." Science **251**(4995): 767-73.

Fujita, S. (1962). "Kinetics of cellular proliferation." Exp. Cell Res. **28**: 52.

Fukai, J., H. Yokote, et al. (2008). "EphA4 promotes cell proliferation and migration through a novel EphA4-FGFR1 signaling pathway in the human glioma U251 cell line." Molecular Cancer Therapeutics **7**(9): 2768-2778.

Gandhi, R., K. C. Luk, et al. (2008). "Group I mGluR5 metabotropic glutamate receptors regulate proliferation of neuronal progenitors in specific forebrain developmental domains." Journal of Neurochemistry **104**(1): 155-172.

Garcia, A. D., N. B. Doan, et al. (2004). "GFAP-expressing progenitors are the principal source of constitutive neurogenesis in adult mouse forebrain." Nat. Neurosci. **7**: 1233.

Ge, S., D. A. Pradhan, et al. (2007). "GABA sets the tempo for activity-dependent adult neurogenesis." Trends in Neurosciences **30**(1): 1-8.

Gogolla, N., I. Galimberti, et al. (2006). "Preparation of organotypic hippocampal slice cultures for long-term live imaging." Nat. Protocols **1**(3): 1165-1171.

Goldman, S. A. and F. Nottebohm (1983). "Neuronal production, migration, and differentiation in a vocal control nucleus of the adult female cannary brain." Proceedings of the National Academy of Sciences of the United States of America **80**(8): 2390-2394.

Gotz, M., E. Hartfuss, et al. (2002). "Radial glial cells as neuronal precursors: a new perspective on the correlation of morphology and lineage restriction in the developing cerebral cortex of mice." Brain Res. Bull. **57**: 777.

Gotz, M. and W. B. Huttner (2005). "The cell biology of neurogenesis." Nat Rev Mol Cell Biol **6**(10): 777-788.

Graham, V., J. Khudyakov, et al. (2003). "SOX2 Functions to Maintain Neural Progenitor Identity." Neuron **39**(5): 749-765.

Groisman, I., M. Ivshina, et al. (2006). "Control of cellular senescence by CPEB." Genes & Development **20**(19): 2701-2712.

Haas, K., K. Jensen, et al. (2002). "Targeted electroporation in Xenopus tadpoles in vivo-from single cells to the entire brain." Differentiation **70**(4-5): 148-154.

Haas, K., W. C. Sin, et al. (2001). "Single-Cell Electroporationfor Gene Transfer In Vivo." Neuron **29**(3): 583-591.

Haglid, K., A. Hamberger, et al. (1976). "Cellular and subcellular distribution of the S-100 protein in rabbit and rat central nervous system." J Neurosci Res **2**(3): 175-91.

Hayes, N. L. and R. S. Nowakowski (2000). "Exploiting the dynamics of S-phase tracers in developing brain: interkinetic nuclear migration for cells entering versus leaving the S-phase." Dev. Neurosci. **22**: 44.

Heiman, M., A. Schaefer, et al. (2008). "Translational Profiling Approach for the Molecular Characterization of CNS Cell Types." Cell **135**(4): 738-748.

Hemmati-Brivanlou, A. and D. Melton (1997). "Vertebrate Neural Induction." Annual Review of Neuroscience **20**(1): 43-60.

Hirsch, N., L. B. Zimmerman, et al. (2002). "Xenopus tropicalis transgenic lines and their use in the study of embryonic induction." Developmental Dynamics **225**(4): 522-535.

Holt, C. (1983). "The topography of the initial retinotectal projection." Prog Brain Res **58**: 339-45.

Hongo, S., T. Watanabe, et al. (2006). "Ndrg4 enhances NGF-induced ERK activation uncoupled with Elk-1 activation." Journal of Cellular Biochemistry **98**(1): 185-193.

Hsieh, J., K. Nakashima, et al. (2004). "Histone deacetylase inhibition-mediated neuronal differentiation of multipotent adult neural progenitor cells." Proceedings of the National Academy of Sciences of the United States of America **101**(47): 16659-16664.

Huberman, A. D., M. B. Feller, et al. (2008). "Mechanisms Underlying Development of Visual Maps and Receptive Fields." Annual Review of Neuroscience **31**(1): 479-509.

Huot, M. E., N. Bisson, et al. (2005). "The RNA-binding Protein Fragile X-related 1 Regulates Somite Formation in Xenopus laevis." Mol. Biol. Cell **16**(9): 4350-4361.

Huttner, W. B. and Y. Kosodo (2005). "Symmetric versus asymmetric cell division during neurogenesis in the developing vertebrate central nervous system." Current Opinion in Cell Biology **17**(6): 648-657.

Ikeda, W., H. Nakanishi, et al. (1999). "Afadin: A Key Molecule Essential for Structural Organization of Cell–Cell Junctions of Polarized Epithelia during Embryogenesis." J. Cell Biol. **146**(5): 1117-1132.

Irizarry, R., S. Ooi, et al. (2003). "Use of mixture models in a microarray-based screening procedure for detecting differentially represented yeast mutants." Stat Appl Genet Mol Biol **2**.

Itsykson, P., N. Ilouz, et al. (2005). "Derivation of neural precursors from human embryonic stem cells in the presence of noggin." Mol Cell Neurosci **30**: 24.

Jagasia, R., K. Steib, et al. (2009). "GABA-cAMP Response Element-Binding Protein Signaling Regulates Maturation and Survival of Newly Generated Neurons in the Adult Hippocampus." J. Neurosci. **29**(25): 7966-7977.

Joester, A. and A. Faissner (2001). "The structure and function of tenascins in the nervous system." Matrix Biology **20**(1): 13-22.

Jung, C. G., H. Hida, et al. (2004). "Pleiotrophin mRNA is highly expressed in neural stem (progenitor) cells of mouse ventral mesencephalon and the product promotes production of dopaminergic neurons from embryonic stem cell-derived nestin-positive cells." FASEB J.: 03-0927fje.

Kamemura, K., A. Ito, et al. (2008). "Effects of downregulated HDAC6 expression on the proliferation of lung cancer cells." Biochemical and Biophysical Research Communications **374**(1): 84-89.

Kaneko, Y., S. Sakakibara, et al. (2000). "Musashi1: An Evolutionally Conserved Marker for CNS Progenitor Cells Including Neural Stem Cells." Developmental Neuroscience **22**(1-2): 139-153.

Kaneko, Y., S. Sakakibara, et al. (2000). "Musashi1: an evolutionally conserved marker for CNS progenitor cells including neural stem cells." Dev Neurosci **22**(1-2): 139-53.

Karsten, S. L., V. M. D. Van Deerlin, et al. (2002). "An evaluation of tyramide signal amplification and archived fixed and frozen tissue in microarray gene expression analysis." Nucl. Acids Res. **30**(2): e4-.

Katoh, M. and M. Katoh (2005). "Comparative genomics on mammalian Fgf3-Fgf4 locus." Internation Journal of Oncology **27**(1): 281-5.

Katoh, Y. and M. Katoh (2005). "Comparative genomics on Sox2 orthologs." Oncology Report **14**(3): 898-800.

Kawaguchi, A., T. Ikawa, et al. (2008). "Single-cell gene profiling defines differential progenitor subclasses in mammalian neurogenesis." Development **135**(18): 3113-3124.

Kempermann, G., H. van Praag, et al. (2000). "Activity-dependent regulation of neuronal plasticity and self repair." Prog Brain Res **127**: 35048.

Kishi, M., K. Mizuseki, et al. (2000). "Requirement of Sox2-mediated signaling for differentiation of early Xenopus neuroectoderm." Development **127**(4): 791-800.

Knoblich, J. A. (2001). "Asymmetric cell division during animal development." Nat Rev Mol Cell Biol **2**(1): 11-20.

Knoblich, J. A. (2008). "Mechanisma of asymmetric stem cell division." Cell **132**(4): 583-97.

Komitova, M. and P. S. Eriksson (2004). "Sox-2 is expressed by neural progenitors and astroglia in the adult rat brain." Neuroscience Letters **369**(1): 24-27.

Kornack, D. R. and P. Rakic (1999). "Continuation of neurogenesis in the hippocampus of the adult macaque monkey." PNAS **96**(10): 5768-5773.

Kosaka, N., M. Kodama, et al. (2006). "FGF-4 regulates neural progenitor cell proliferation and neuronal differentiation." FASEB J. **20**(9): 1484-1485.

Kosodo, Y., K. Roper, et al. (2004). "Asymmetric distribution of the apical plasma membrane during neurogenic divisions of mammalian neuroepithelial cells." EMBO J **23**(11): 2314-2324.

Kosodo, Y., K. Toida, et al. (2008). "Cytokinesis of neuroepithelial cells can divide their basal process before anaphase." EMBO J **27**(23): 3151-3163.

Köster, R. and S. Fraser (2004). "Time-lapse microscopy of brain development." Methods Cell Biology **76**: 207-35.

Köster, R. W. and S. E. Fraser (2001). "Tracing Transgene Expression in Living Zebrafish Embryos." Developmental Biology **233**(2): 329-346.

Kriegstein, A. and A. Alvarez-Buylla (2009). "The Glial Nature of Embryonic and Adult Neural Stem Cells." Annual Review of Neuroscience **32**(1): 149-184.

Kriegstein, A. R. and M. Götz (2003). "Radial glia diversity: A matter of cell fate." Glia **43**(1): 37-43.

Kuhn, H. G., J. Winkler, et al. (1997). "Epidermal Growth Factor and Fibroblast Growth Factor-2 Have Different Effects on Neural Progenitors in the Adult Rat Brain." J. Neurosci. **17**(15): 5820-5829.

Kulesh, D., D. Clive, et al. (1987). "Identification of interferon-modulated proliferation-related cDNA sequences." Proc Natl Acad Sci U S A **84**(23): 8453-7.

Kuruba, R., B. Hattiangady, et al. (2009). "Hippocampal neurogenesis and neural stem cells in temporal lobe epilepsy." Epilepsy & Behavior **14**(1, Supplement 1): 65-73.

Lashkari, D. A., J. L. DeRisi, et al. (1997). "Yeast microarrays for genome wide parallel genetic and gene expression analysis." Proceedings of the National Academy of Sciences of the United States of America **94**(24): 13057-13062.

Lasky, J. L. and H. Wu (2005). "Notch Signaling, Brain Development, and Human Disease." Pediatric Research **57**(5 Part 2): 104R-109R.

Lee, A. S. (2007). "GRP78 Induction in Cancer: Therapeutic and Prognostic Implications." Cancer Res **67**(8): 3496-3499.

Lee, W. C. A. and E. Nedivi (2002). "Extended Plasticity of Visual Cortex in Dark-Reared Animals May Result from Prolonged Expression of cpg15-Like Genes." J. Neurosci. **22**(5): 1807-1815.

Lehre, K. P., L. M. Levy, et al. (1995). "Differential expression of two glial glutamate transporters in the rat brain: quantitative and immunocytochemical observations." J. Neurosci. **15**(3): 1835-1853.

Lein, E. S., M. J. Hawrylycz, et al. (2007). "Genome-wide atlas of gene expression in the adult mouse brain." Nature **445**(7124): 168-176.

Lemkine, G. F., A. Raji, et al. (2005). "Adult neural stem cell cycling in vivo requires thyroid hormone and its alpha receptor." FASEB J.: 04-2916fje.

Lendahl, U., L. B. Zimmerman, et al. (1990). "CNS stem cells express a new class of intermediate filament protein." Cell **60**(4): 585-595.

Levitt, P. and P. Rakic (1980). "Immunoperoxidase localization of glial fibrillary acidic protein in radial glial cells and astrocytes of the developing rhesus monkey brain." J. Comp. Neurol. **193**: 815.

Li, F., Z. Chong, et al. (2005). "Vital elements of the Wnt-Frizzled signaling pathway in the nervous system." Current Neurovasc. Res. **2**(4): 331-40.

Lindsten, T., J. A. Golden, et al. (2003). "The Proapoptotic Activities of Bax and Bak Limit the Size of the Neural Stem Cell Pool." J. Neurosci. **23**(35): 11112-11119.

Lindvall, O. (2003). "Stem cells for cell therapy in Parkinson's disease." Pharmacological Research **47**(4): 279-287.

Lledo, P. M., A. Saghatelyan, et al. (2004). "Inhibitory Interneurons in the Olfactory Bulb: From Development to Function." Neuroscientist **10**(4): 292-303.

LoTurco, J. J., D. F. Owens, et al. (1995). "GABA and glutamate depolarize cortical progenitor cells and inhibit DNA synthesis." Neuron **15**(6): 1287-1298.

Luo, Z. and D. H. Geschwind (2001). "Microarray Applications in Neuroscience." Neurobiology of Disease **8**(2): 183-193.

Ma, D. K., W. R. Kim, et al. (2009). "Activity-dependent Extrinsic Regulation of Adult Olfactory Bulb and Hippocampal Neurogenesis." Annals of the New York Academy of Sciences **1170**(International Symposium on Olfaction and Taste): 664-673.

Machold, R., S. Hayashi, et al. (2003). "Sonic Hedgehog Is Required for Progenitor Cell Maintenance in Telencephalic Stem Cell Niches." Neuron **39**(6): 937-950.

Maniccia, A., C. Lewis, et al. (2009). "Mitochondrial localization, ELK-1 transcriptional regulation and growth inhibitory functions of BRCA1, BRCA1a, and BRCA1b proteins." J Cell Physiology **219**(3): 634-41.

Mannello, F., G. A. M. Tonti, et al. (2006). "Role and Function of Matrix Metalloproteinases in the Differentiation and Biological Characterization of Mesenchymal Stem Cells." Stem Cells **24**(3): 475-481.

Marshall, C. A., B. G. Novitch, et al. (2005). "Olig2 directs astrocyte and oligodendrocyte formation in postnatal subventricular zone cells." J. Neurosci. **25**: 7289.

Martinez-Cerdeno, V., S. C. Noctor, et al. (2006). "The role of intermediate progenitor cells in the evolutionary expansion of the cerebral cortex." Cereb. Cortex **16**: i152.

Martinou, J. C., M. Dubois-Dauphin, et al. (1994). "Overexpression of BCL-2 in transgenic mice protects neurons from naturally occurring cell death and experimental ischemia." Neuron **13**(4): 1017-1030.
Mignone, J. L., V. Kukekov, et al. (2004). "Neural stem and progenitor cells in nestin-GFP transgenic mice." The Journal of Comparative Neurology **469**(3): 311-324.
Mirescu, C. and E. Gould (2006). "Stress and adult neurogenesis." Hippocampus **16**(3): 233-238.
Misson, J. P., M. A. Edwards, et al. (1988). "Mitotic cycling of radial glial cells of the fetal murine cerebral wall: a combined autoradiographic and immunohistochemical study." Brain Res. **466**: 183.
Miyagi, S., M. Nishimoto, et al. (2006). "The Sox2 regulatory region 2 functions as a neural stem cell-specific enhancer in the telencephalon." Journal of Biological Chemistry **281**(19): 13374-81.
Miyata, T., A. Kawaguchi, et al. (2001). "Asymmetric Inheritance of Radial Glial Fibers by Cortical Neurons " Nueron **31**(5): 727-742.
Miyata, T., A. Kawaguchi, et al. (2004). "Asymmetric production of surface-dividing and non-surface-dividing cortical progenitor cells." Development **131**: 3133.
Mizrahi, A., J. Lu, et al. (2006). "In vivo imaging of juxtaglomerular neuron turnover in the mouse olfactory bulb." PNAS **103**(6): 1912-1917.
Mizuno, H., T. K. Mal, et al. (2003). "Photo-Induced Peptide Cleavage in the Green-to-Red Conversion of a Fluorescent Protein." Molecular Cell **12**(4): 1051-1058.
Mizuseki, K., M. Kishi, et al. (1998). "Xenopus Zic-related-1 and Sox-2, two factors induced by chordin, have distinct activities in the initiation of neural induction." Development **125**(4): 579-587.
Muotri, A. R., V. T. Chu, et al. (2005). "Somatic mosaicism in neuronal precursor cells mediated by L1 retrotransposition." Nature **435**(7044): 903-910.
Nakamichi, N., T. Takarada, et al. (2009). "Neurogenesis mediated by gamma-aminobutyric acid and glutamate signaling." J Pharmacol Sci **110**(2): 133-49.
Naoyuki, M., H. Syu-Ichi, et al. (2002). "Association of ASIP/mPAR-3 with adherens junctions of mouse neuroepithelial cells." Developmental Dynamics **225**(1): 61-69.
Nedivi, E., A. Javaherian, et al. (2001). "Developmental regulation of CPG15 expression in Xenopus." Journal of Comparative Neurology **435**(4): 464-73.
Nieto, M., E. S. Monuki, et al. (2004). "Expression of Cux-1 and Cux-2 in the subventricular zone and upper layers II-V of the cerebral cortex." J. Comp. Neurol. **479**: 168.
Nieuwkoop and Faber (1994). Normal Table of Xenopus laevis. New York, Garland Publishing.
Noctor, S. C., A. C. Flint, et al. (2001). "Neurons derived from radial glial cells establish radial units in neocortex." Nature **409**: 714.
Noctor, S. C., V. Martinez-Cerdeno, et al. (2004). "Cortical neurons arise in symmetric and asymmetric division zones and migrate through specific phases." Nat. Neurosci. **7**: 136.
Noctor, S. C., V. Martinez-Cerdeno, et al. (2007). "Contribution of intermediate progenitor cells to cortical histogenesis." Arch. Neurol. **64**: 639.

Noctor, S. C., V. Martínez-Cerdeño, et al. (2008). "Distinct behaviors of neural stem and progenitor cells underlie cortical neurogenesis." The Journal of Comparative Neurology **508**(1): 28-44.

Novack, D. and S. Korsmeyer (1994). "Bcl-2 protein expression during murine development." American Journal of Pathology **145**(1): 61-73.

Nygaard, V. and E. Hovig (2006). "Options available for profiling small samples: a review of sample amplification technology when combined with microarray profiling." Nucl. Acids Res. **34**(3): 996-1014.

O'Rourke, N. A. and S. E. Fraser (1990). "Dynamic changes in optic fiber terminal arbors lead to retinotopic map formation: An in vivo confocal microscopic study." Neuron **5**(2): 159-171.

Ogino, H., W. B. McConnell, et al. (2006). "Highly efficient transgenesis in Xenopus tropicalis using I-SceI meganuclease." Mechanisms of Development **123**(2): 103-113.

Ohkubo, Y., A. O. Uchida, et al. (2004). "Fibroblast Growth Factor Receptor 1 Is Required for the Proliferation of Hippocampal Progenitor Cells and for Hippocampal Growth in Mouse." J. Neurosci. **24**(27): 6057-6069.

Okabe, S., K. Forsberg-Nilsson, et al. (1996). "Development of neuronal precursor cells and functional postmitotic neurons from embryonic stem cells in vitro." Mechanisms of Development **59**(1): 89-102.

Okano, H., H. Kawahara, et al. (2005). "Function of RNA-binding protein Musashi-1 in stem cells." Experimental Cell Research **306**(2): 349-356.

Okuda, T., K. Tagawa, et al. (2004). "Oct-3/4 repression accelerates differentiation of neural progenitor cells in vitro and in vivo." Molecular Brain Research **132**(1): 18-30.

Olson, A. K., B. D. Eadie, et al. (2006). "Environmental enrichment and voluntary exercise massively increase neurogenesis in the adult hippocampus via dissociable pathways." Hippocampus **16**(3): 250-260.

Oredsson, S. M. (2003). "Polyamine dependence of normal cell-cycle progression." Biochem. Soc. Trans. **31**(2): 366-370.

Palluault, F., C. Slomianny, et al. (1992). "High osmotic pressure enables fine ultrastructural and cytochemical studies on Pneumocystic carinii." Parasitology research **78**(5): 437-444.

Parent, J. M. and G. G. Murphy (2008). "Mechanisms and functional significance of aberrant seizure-induced hippocampal neurogenesis." Epilepsia **49**(s5): 19-25.

Parker, M. A., J. K. Anderson, et al. (2005). "Expression profile of an operationally-defined neural stem cell clone." Experimental Neurology **194**(2): 320-332.

Paupard, M.-C., A. Miller, et al. (2001). "Immuno-EM Localization of GFP-tagged Yolk Proteins in C. elegans Using Microwave Fixation." J. Histochem. Cytochem. **49**(8): 949-956.

Pecorari, L., O. Marin, et al. (2009). "Elongation Factor 1 alpha interacts with phospho-Akt in breast cancer cells and regulates their proliferation, survival and motility." Molecular Cancer **8**(1): 58.

Peh, G. S. L., R. J. Lang, et al. (2009). "CD133 Expression by Neural Progenitors Derived from Human Embryonic Stem Cells and Its Use for Their Prospective Isolation." Stem Cells and Development **18**(2): 269-282.

Peiffer, D. A., A. V. Bubnoff, et al. (2005). "A Xenopus DNA microarray approach to identify novel direct BMP target genes involved in early embryonic development." Developmental Dynamics **232**(2): 445-456.

Pereira, A. C., D. E. Huddleston, et al. (2007). "An in vivo correlate of exercise-induced neurogenesis in the adult dentate gyrus." Proceedings of the National Academy of Sciences **104**(13): 5638-5643.

Peunova, N., V. Scheinker, et al. (2001). "Nitric Oxide Is an Essential Negative Regulator of Cell Proliferation in Xenopus Brain." J. Neurosci. **21**(22): 8809-8818.

Platel, J., B. Lacar, et al. (2007). "GABA and glutamate signaling: homeostatic control of adult forebrain neurogenesis." Journal of molecular histology **38**(4).

Pontious, A., T. Kowalczyk, et al. (2008). "Role of intermediate progenitor cells in cerebral cortex development." Dev. Neurosci. **30**: 24.

Porter, B. E. (2008). "Neurogenesis and epilepsy in the developing brain." Epilepsia **49**(s5): 50-54.

Pratt, K. G., W. Dong, et al. (2008). "Development and spike timing-dependent plasticity of recurrent excitation in the Xenopus optic tectum." Nat Neurosci **11**(4): 467-475.

Prickaerts, J., G. Koopmans, et al. (2004). "Learning and adult neurogenesis: Survival with or without proliferation?" Neurobiology of Learning and Memory **81**(1): 1-11.

Pruszak, J., K.-C. Sonntag, et al. (2007). "Markers and Methods for Cell Sorting of Human Embryonic Stem Cell-Derived Neural Cell Populations." Stem Cells **25**(9): 2257-2268.

Putz, U., C. Harwell, et al. (2005). "Soluble CPG15 expressed during early development rescues cortical progenitors from apoptosis." Nature Neuroscience **8**(3): 322-31.

Raballo, R., J. Rhee, et al. (2000). "Basic Fibroblast Growth Factor (Fgf2) Is Necessary for Cell Proliferation and Neurogenesis in the Developing Cerebral Cortex." J. Neurosci. **20**(13): 5012-5023.

Raineteau, O., L. Rietschin, et al. (2004). "Neurogenesis in hippocampal slice cultures." Molecular and Cellular Neuroscience **26**(2): 241-250.

Rajagopal, J., T. J. Carroll, et al. (2008). "Wnt7b stimulates embryonic lung growth by coordinately increasing the replication of epithelium and mesenchyme." Development **135**(9): 1625-1634.

Rao, M., Ed. (2006). Neural Development and Stem Cells. Totowa, New Jersey, Humana Press Inc.

Reynolds, B. and S. Weiss (1992). "Generation of neurons and astrocytes from isolated cells of the adult mammalian central nervous system." Science **255**(5052): 1707-10.

Riou, J., M. Delarue, et al. (1998). "Role of fibroblast growth factor during early midbrain development in Xenopus." Mech Dev **78**(1-2): 3-15.

Rodda, D. J., J.-L. Chew, et al. (2005). "Transcriptional Regulation of Nanog by OCT4 and SOX2." Journal of Biological Chemistry **280**(26): 24731-24737.

Rosene, D. L., N. J. Roy, et al. (1986). "A cryoprotection method that facilitates cutting frozen sections of whole monkey brains for histological and histochemical

processing without freezing artifact." J. Histochem. Cytochem. **34**(10): 1301-1315.
Ryu, S. and W. Driever (2006). "Minichromosome Maintenance Proteins as Markers for Proliferation Zones During Embryogenesis." Cell Cycle **5**(11): 1140-1142.
Sadikot, A. F., A. M. Burhan, et al. (1998). "NMDA receptor antagonists influence early development of GABAergic interneurons in the mammalian striatum." Developmental Brain Research **105**(1): 35-42.
Sakaguchi, D. S. and R. K. Murphey (1985). "Map formation in the developing Xenopus retinotectal system: an examination of ganglion cell terminal arborizations." J. Neurosci. **5**(12): 3228-3245.
Sasai, Y. (2001). "Roles of Sox factors in neural determination: conserved signaling in evolution?" Int J Dev Biol **45**(1): 321-6.
Sasai, Y. and E. M. De Robertis (1997). "Ectodermal Patterning in Vertebrate Embryos." Developmental Biology **182**(1): 5-20.
Sauer, F. C. (1935). "Mitosis in the neural tube." J. Comp. Neurol. **62**: 377.
Sauer, M. E. and B. E. Walker (1959). "Radioautographic study of interkinetic nuclear migration in the neural tube." Proc. Soc. Exp. Biol. Med. **101**: 557.
Schena, M., D. Shalon, et al. (1995). "Quantitative Monitoring of Gene Expression Patterns with a Complementary DNA Microarray." Science **270**(5235): 467-470.
Scholzen, T. and J. Gerdes (2000). "The Ki-67 protein: From the known and the unknown." Journal of Cellular Physiology **182**(3): 311-322.
Scicchitano, M. S., D. A. Dalmas, et al. (2006). "Preliminary Comparison of Quantity, Quality, and Microarray Performance of RNA Extracted From Formalin-fixed, Paraffin-embedded, and Unfixed Frozen Tissue Samples." J. Histochem. Cytochem. **54**(11): 1229-1237.
Sejersen, T. and U. Lendahl (1993). "Transient expression of the intermediate filament nestin during skeletal muscle development." J Cell Sci **106**(4): 1291-1300.
Serafini, T. (1999). "Of neurons and gene chips: Commentary." Current Opinion in Neurobiology **9**(5): 641-644.
Sgambato, V., P. Vanhoutte, et al. (1998). "In Vivo Expression and Regulation of Elk-1, a Target of the Extracellular-Regulated Kinase Signaling Pathway, in the Adult Rat Brain." J. Neurosci. **18**(1): 214-226.
Shi, Y., G. Sun, et al. (2008). "Neural stem cell self-renewal." Critical reviews in oncology/hematology **65**(1): 43-53.
Shibata, T., K. Yamada, et al. (1997). "Glutamate Transporter GLAST Is Expressed in the Radial Glia-Astrocyte Lineage of Developing Mouse Spinal Cord." J. Neurosci. **17**(23): 9212-9219.
Shin, Y., A. Kitayama, et al. (2005). "Identification of neural genes using <I>Xenopus</I> DNA microarrays." Developmental Dynamics **232**(2): 432-444.
Sibilia, M., J. P. Steinbach, et al. (1998). "A strain-independent postnatal neurodegeneration in mice lacking the EGF receptor." EMBO J **17**(3): 719-731.
Sidman, R. L., I. L. Miale, et al. (1959). "Cell proliferation and migration in the primitive ependymal zone: an autoradiographic study of histogenesis in the nervous system." Exp. Neurol. **1**: 322.

Silva, R. N., D. A. Ribeiro, et al. (2007). "Placental glutathione S-transferase correlates with cellular proliferation during rat tongue carcinogenesis induced by 4-nitroquinoline 1-oxide." Experimental and Toxicologic Pathology **59**(1): 61-68.

Sin, W. C., K. Haas, et al. (2002). "Dendrite growth increased by visual activity requires NMDA receptor and Rho GTPases." Nature **419**(6906): 475-480.

Smart, I. H. (1973). "Proliferative characteristics of the ependymal layer during the early development of the mouse neocortex: a pilot study based on recording the number, location and plane of cleavage of mitotic figures." J. Anat. **116**: 67.

Snir, M., R. Ofir, et al. (2006). "Xenopus laevis POU91 protein, an Oct3/4 homologue, regulates competence transitions from mesoderm to neural cell fates." EMBO J **25**(15): 3664-3674.

Sohail, A. (2009). "The culture of neural stem cells." Journal of Cellular Biochemistry **106**(1): 1-6.

Srivastava, A. S., S. Shenouda, et al. (2006). "Transplanted Embryonic Stem Cells Successfully Survive, Proliferate, and Migrate to Damaged Regions of the Mouse Brain." Stem Cells **24**(7): 1689-1694.

Stears, R. L., R. C. Getts, et al. (2000). "A novel, sensitive detection system for high-density microarrays using dendrimer technology." Physiol. Genomics **3**(2): 93-99.

Stoykova, A., M. Gotz, et al. (1997). "Pax6-dependent regulation of adhesive patterning, R-cadherin expression and boundary formation in developing forebrain." Development **124**: 3765.

Straznicky, K. and R. Gaze (1972). "The development of the tectum in Xenopus laevis: an autoradiographic study." Journal of Embryology and Experimental Morphology **28**(1): 87-115.

Tabuchi, K. and W. M. Kirsch (1975). "Immunocytochemical localization of S-100 protein in neurons and glia of hamster cerebellum." Brain Research **92**(1): 175-180.

Tadahiro, F., W. Zhen, et al. (2008). "cpg15 and cpg15-2 constitute a family of activity-regulated ligands expressed differentially in the nervous system to promote neurite growth and neuronal survival." The Journal of Comparative Neurology **507**(5): 1831-1845.

Takahashi, T., J. P. Misson, et al. (1990). "Glial process elongation and branching in the developing murine neocortex: a qualitative and quantitative immunohistochemical analysis." J. Comp. Neurol. **302**: 15.

Takashi, N., M. Hideki, et al. (2007). "Postnatal neurogenesis in hippocampal slice cultures: Early in vitro labeling of neural precursor cells leads to efficient neuronal production." Journal of Neuroscience Research **85**(8): 1704-1712.

Tao, H. W. and M. M. Poo (2005). "Activity-Dependent Matching of Excitatory and Inhibitory Inputs during Refinement of Visual Receptive Fields." Neuron **45**(6): 829-836.

Tarabykin, V., A. Stoykova, et al. (2001). "Cortical upper layer neurons derive from the subventricular zone as indicated by Svet1 gene expression." Development **128**: 1983.

Taupin, P. (2007). "BrdU immunohistochemistry for studying adult neurogenesis: Paradigms, pitfalls, limitations, and validation." Brain Research Reviews **53**(1): 198-214.

Toledo, E. M., M. Colombres, et al. (2008). "Wnt signaling in neuroprotection and stem cell differentiation." Progress in Neurobiology **86**(3): 281-296.

Tonchev, A. B., T. Yamashima, et al. (2006). "Transcription factor protein expression patterns by neural or neuronal progenitor cells of adult monkey subventricular zone." Neuroscience **139**(4): 1355-1367.

Tropepe, V., C. G. Craig, et al. (1997). "Transforming Growth Factor-alpha Null and Senescent Mice Show Decreased Neural Progenitor Cell Proliferation in the Forebrain Subependyma." J. Neurosci. **17**(20): 7850-7859.

Turrin, N. P. and S. Rivest (2006). "Tumor Necrosis Factor-alpha But Not Interleukin 1-beta Mediates Neuroprotection in Response to Acute Nitric Oxide Excitotoxicity." J. Neurosci. **26**(1): 143-151.

Uchida, N., D. W. Buck, et al. (2000). "Direct isolation of human central nervous system stem cells." Proc Natl Acad Sci USA **97**: 14720.

Vaillant, C., M. Didier-Bazes, et al. (1999). "Spatiotemporal Expression Patterns of Metalloproteinases and Their Inhibitors in the Postnatal Developing Rat Cerebellum." J. Neurosci. **19**(12): 4994-5004.

van Praag, H., G. Kempermann, et al. (1999). "Running increases cell proliferation and neurogenesis in the adult mouse dentate gyrus." Nature Neuroscience **2**(3): 266-70.

Vega, C. and D. Peterson (2005). "Stem cell proliferative history in tissue revealed by temporal halogenated thymidine analog discrimination." Nature Methods **2**(3): 167-9.

Viti, J., A. Gulacsi, et al. (2003). "Wnt Regulation of Progenitor Maturation in the Cortex Depends on Shh or Fibroblast Growth Factor 2." J. Neurosci. **23**(13): 5919-5927.

von Holst, A. (2008). "Tenascin C in stem cell niches: redundant, permissive or instructive?" Cells Tissues Organs **188**(1-2): 170-7.

Wang, L., S. Andersson, et al. (2003). "Estrogen receptor ER-beta knockout mice reveal a role for ER-beta in migration of cortical neurons in the developing brain." Proceedings of the National Academy of Sciences of the United States of America **100**(2): 703-708.

Wang, T. W., G. P. Stromberg, et al. (2006). "Sox3 expression identifies neural progenitors in persistent neonatal and adult mouse forebrain germinative zones." The Journal of Comparative Neurology **497**(1): 88-100.

Warren, N., D. Caric, et al. (1999). "The Transcription Factor, Pax6, is Required for Cell Proliferation and Differentiation in the Developing Cerebral Cortex." Cereb. Cortex **9**(6): 627-635.

Wegner, M. and C. C. Stolt (2005). "From stem cells to neurons and glia: a Soxist's view of neural development." Trends in Neurosciences **28**(11): 583-588.

Wei, L. C., M. Shi, et al. (2002). "Nestin-containing cells express glial fibrillary acidic protein in the proliferative regions of central nervous system of postnatal developing and adult mice." Developmental Brain Research **139**(1): 9-17.

Weigmann, A., D. Corbeil, et al. (1997). "Prominin, a novel microvilli-specific polytopic membrane protein of the apical surface of epithelial cells, is targeted to plasmalemmal protrusions of non-epithelialâ€‰cells." Proceedings of the National Academy of Sciences of the United States of America **94**(23): 12425-12430.

Wiebe, M. S., P. J. Wilder, et al. (2000). "Isolation, characterization, and differential expression of the murine Sox-2 promoter." Gene **246**(1-2): 383-393.

Wu, G. Y. and H. T. Cline (2003). "Time-lapse in vivo imaging of the morphological development of Xenopus optic tectal interneurons." The Journal of Comparative Neurology **459**(4): 392-406.

Yang, J., J. Oza, et al. (2008). "Neural differentiation and the attenuated heat shock response." Brain Research **1203**: 39-50.

Yoneda, Y. and K. Ogita (1991). "Neurochemical aspects of the N-methyl-d-aspartate receptor complex." Neuroscience Research **10**(1): 1-33.

Yoon, K. and N. Gaiano (2005). "Notch signaling in the mammalian central nervous system: insights from mouse mutants." Nature Neuroscience **8**(6): 709-15.

Yoon, K., S. Nery, et al. (2004). "Fibroblast Growth Factor Receptor Signaling Promotes Radial Glial Identity and Interacts with Notch1 Signaling in Telencephalic Progenitors." J. Neurosci. **24**(43): 9497-9506.

Zappone, M. V., R. Galli, et al. (2000). "Sox2 regulatory sequences direct expression of a (beta)-geo transgene to telencephalic neural stem cells and precursors of the mouse embryo, revealing regionalization of gene expression in CNS stem cells." Development **127**(11): 2367-2382.

Zechner, D., Y. Fujita, et al. (2003). "Beta-Catenin signals regulate cell growth and the balance between progenitor cell expansion and differentiation in the nervous system." Developmental Biology **258**(2): 406-418.

Zeng, X., J. Cai, et al. (2004). "Dopaminergic differentiation of human embryonic stem cells." Stem Cells **22**: 925.

Zhadanov, A. B., D. W. Provance Jr, et al. (1999). "Absence of the tight junctional protein AF-6 disrupts epithelial cell-cell junctions and cell polarity during mouse development." Current Biology **9**(16): 880-888, S1-S2.

Zhao, M., D. Li, et al. (2007). "Fibroblast Growth Factor Receptor-1 is Required for Long-Term Potentiation, Memory Consolidation, and Neurogenesis." Biological Psychiatry **62**(5): 381-390.

Zhong, W. and W. Chia (2008). "Neurogenesis and asymmetric cell division." Current Opinion in Neurobiology **18**(1): 4-11.

Zimmer, C., M. C. Tiveron, et al. (2004). "Dynamics of Cux2 expression suggests that an early pool of SVZ precursors is fated to become upper cortical layer neurons." Cereb. Cortex **14**: 1408.